#399

COMPOSITE INTERPLANETARY

FIELD AND PLASMA TAPE
SM-41A
SM-41B SPHE-00762

FLUX-ADDED COMPOSITE OMNITAPE
SM-41E SPHE 00765

Table of Contents

---

1. INTRODUCTION:

The documentation for this data set was originally on paper, kept in NSSDC's Data Set Catalogs (DSCs). The paper documentation in the Data Set Catalogs have been made into digital images, and then collected into a single PDF file for each Data Set Catalog. The inventory information in these DSCs is current as of July 1, 2004. This inventory information is now no longer maintained in the DSCs, but is now managed in the inventory part of the NSSDC information system. The information existing in the DSCs is now not needed for locating the data files, but we did not remove that inventory information.

The offline tape datasets have now been migrated from the original magnetic tape to Archival Information Packages (AIP's).

A prior restoration may have been done on data sets, if a requestor of this data set has questions; they should send an inquiry to the request office to see if additional information exists.

2. ERRATA/CHANGE LOG:

NOTE: Changes are made in a text box, and will show up that way when displayed on screen with a PDF reader.

When printing, special settings may be required to make the text box appear on the printed output.

Version	Date	Person	Page	Description of Change
01				
02				

3 LINKS TO RELEVANT INFORMATION IN THE ONLINE NSSDC INFORMATION SYSTEM:

http://nssdc.gsfc.nasa.gov/nmc/

[NOTE: This link will take you to the main page of the NSSDC Master Catalog. There you will be able to perform searches to find additional information]

4. CATALOG MATERIALS:

a. Associated Documents To find associated documents you will need to know the document ID number and then click here. http://nssdcftp.gsfc.nasa.gov/miscellaneous/documents/

b. Core Catalog Materials

Composite Interplanetary

Field and Plasma Tape

SM-41A

SM-41B SPHE-00762

These data sets consist of one tape each. The tapes are 9-track, 6250 BPI, binary and contain one file of data. The tapes were created on an IBM 360 computer. Each data set is a different format of the Interplanetary Field and Plasma data. Excerpts of the supporting documents** identified by Joe King, have been included for distribution to requesters. The complete document is available upon request.

The D and C numbers, along with the time spans are as follows:

Data Set ID	Format	D#	C#	Time Span
SM-41A	36-word	D-29951	C-19228	11/02/63 - 01/12/76
SM-41B*	37-word	D-33319	C-20312	11/02/63 - 02/08/93

* Part of this data set is also available thru NODIS

** Selected text pages from supporting documents are:

77-04 pages 1-33 plus the scatterplots 1-27
79-08 pages 1-3
86-04 pages 1-30
89-17 2 introduction pages

SM-41E SPHE-00765

FLUX-ADDED COMPOSITE OMNITAPE

These tapes contain hourly IMF data (in GSE and GSM components), interplanetary plasma parameters, and geomagnetic and solar activity indices, and energetic proton fluxes. Missing parameter values are filled with zeroes. The tapes are single file, unlabeled, 9 track available in IBM or VAX binary, ASCII or EBCDIC formats. A discussion of the construction of the original OMNI tape data set can be found in the Interplanetary Medium Data Book series. The "flux added OMNI tape" data set was first created in 1992 by appending to the OMNI tape original records proton fluxes from the IMP-7 and -8 CPME instrument (PI: S. M. Krimigis) as provided by T. P. Armstrong.

Format	Data Control
Binary	DCB=(RECFM=FB,LRECL=176,BLKSIZE=16896,DEN=4)
ASCII	DCB=(RECFM=FB,LRECL=231,BLKSIZE=22176,DEN=4)

WORD	ASCII	IBM BINARY	MEANING	UNITS/COMMENTS
1	I1	I*4	FLAG	=1: IMF and Plasma data, same spacecraft =2: IMF and Plasma data, different spacecraft =3: No Plasma data =4: No IMF data =5: No IMF or Plasma data
2	I2	I*4	Year	63,64,65,.....
3	I3	I*4	Decimal Day	January 1 = Day 1
4	I2	I*4	Decimal Hour	(0,1,.....23)
5	I4	I*4	Bartels Rotation Number	
6	I2	I*4	ID for IMF spacecraft	See table
7	I2	I*4	ID for SW Plasma spacecraft	See Table
8	I4	I*4	# of points in IMF averages	
9	I4	I*4	# of points in Plasma averages	

COMPOSITE OMNITAPE

This tape contains hourly IMF data (in GSE and GSM components), interplanetary plasma parameters, and geomagnetic and sunspot indices. The tape is single file, unlabelled, 9 track, created in binary on the IBM 360/75 computer.

DCB=(RECFM=VBS,LRECL=148,BLKSIZE=28420,DEN=3)

WORD	TYPE	MEANING	UNITS/COMMENTS
1	I*4	Flag	=1: IMF and Plasma data, same SC =2: IMF and Plasma data, diff SC =3: No Plasma data =4: No IMF data =5: No IMF or Plasma data
2	I*4	Year	63,64,65.....
3	I*4	Decimal Day	Jan 1 = Day 0
4	I*4	Decimal Hour	(0,1,.....23)
5	I*4	Bartels Rotation Number	
6	I*4	ID for IMF SC	See table
7	I*4	ID for SW Plasma SC	See table
8	I*4	# of fine time scale PTS in IMF Avgs	
9	I*4	# of fine time scale PTS in Plasma Avgs	
10	R*4	Field Magnitude Avg, $\lvert\overline{B}\rvert$	$\frac{1}{N}\sum \lvert B\rvert$, gammas
11	R*4	Magnitude of Average Field vector, F	$\left[\overline{B}_x^2+\overline{B}_y^2+\overline{B}_z^2\right]^{1/2}$
12	R*4	Lat. Angle of AV. Field VR	Deg (GSE Coords)
13	R*4	Long. Angle of AV. Field VR	Deg (GSE Coords)
14	R*4	$\overline{B}_x$,GSE	Gammas
15	R*4	$\overline{B}_y$,GSE	Gammas

WORD	TYPE	MEANING	UNITS/COMMENTS
16	R*4	$\overline{B}_z$, GSE	Gammas
17	R*4	$\overline{B}_y$, GSM	Gammas
18	R*4	$\overline{B}_z$, GSM	Gammas
19	R*4	$\sigma_{\overline{\lvert B \rvert}}$	RMS Standard deviation in avg Magnitude (wd. 10), gammas
20	R*4	$\sigma_{\overline{B}}$	RMS Standard deviation in field vector, in gammas (see footnote)
21	R*4	$\sigma_{\overline{B}_x}$	RMS standard deviation in GSE X comp. av, gammas
22	R*4	$\sigma_{\overline{B}_y}$	RMS standard deviation in GSE Y comp. av, gammas
23	R*4	$\sigma_{\overline{B}_z}$	RMS standard deviation in GSE Z comp. av, gammas
24	R*4	Plasma temperature	^oK
25	R*4	Ion density	cm^{-3}
26	R*4	Bulk speed	km/sec
27	R*4	Bulk flow longitude angle	Degrees, GSE coords, >0 for flow from west of sun
28	R*4	Bulk flow latitude angle	Degrees, GSE coords, >0 for flow from south of sun
29	R*4	$\sigma_{\overline{T}}$	^oK
30	R*4	$\sigma_{\overline{N}}$	cm^{-3}
31	R*4	$\sigma_{\overline{V}}$	km/sec
32	R*4	$\sigma_{\overline{\phi}_V}$	deg
33	R*4	$\sigma_{\overline{\theta}_V}$	deg
34	I*4	K_p	from ESRO Tape
35	I*4	C_9	see trans, AGU,
36	I*4	R	Sunspot # 49, 463, 1968

but see note below

The $\sigma_{\overline{B}_A}$ values were not provided with the HEOS IMF data; for such records, words 21-23 contain $\sigma_{\overline{|B|}}$ (repeat of word 19) and, in degrees, $\sigma_{\overline{\theta}_B}$ and $\sigma_{\overline{\phi}_B}$, respectively.

The following spacecraft identifiers have been used

Spacecraft Name	Spacecraft ID
IMP 1 (Expl 18)	18
IMP 3 (Expl 28)	28
IMP 4 (Expl 34)	34
IMP 5 (Expl 41)	41
IMP 6 (Expl 43)	43
IMP 7 (Expl 47)	47
IMP 8 (Expl 50)	50
AIMP 1 (Expl 33)	33
AIMP 2 (Expl 35)	35
HEOS 1 and HEOS 2	1
VELA 3	3
OGO 5	5
Merged LASL VELA speeds (64-3/71)	99
Merged LASL IMP T,N,V (3/71-12/74)	98

Footnote: $\sigma_{\underline{B}}$ is $(\sigma_{B_x}^2+\sigma_{B_y}^2+\sigma_{B_z}^2)^{\frac{1}{2}}$ for IMP records, and is $(\sigma_{|B|}^2+|\bar{B}|^2-F^2)^{\frac{1}{2}}$ for HEOS records.

SM-41B

COMPOSITE OMNITAPE

These tapes contain hourly IMF data (in GSE and GSM components), interplanetary plasma parameters, and geomagnetic and sunspot indices. Missing parameter values are filled with zeroes. The tapes are single file, unlabelled, 9 track available in IBM or VAX binary, ASCII or EBCDIC formats. A discussion of the construction of this data set can be found in the Interplanetary Medium Data Book series.

Format	Data Control
Binary	DCB=(RECFM=FB,LRECL=148,BLKSIZE=28416,DEN=4)
ASCII	DCB=(RECFM=FB,LRECL=182,BLKSIZE=29120,DEN=4)

WORD	ASCII	IBM BINARY	MEANING	UNITS/COMMENTS
1	I1	I*4	FLAG	=1: IMF and Plasma data, same spacecraft =2: IMF and Plasma data, different spacecraft =3: No Plasma data =4: No IMF data =5: No IMF or Plasma data
2	I2	I*4	Year	63,64,65,.....
3	I3	I*4	Decimal Day	January 1 = Day 1
4	I2	I*4	Decimal Hour	(0,1,.....23)
5	I4	I*4	Bartels Rotation Number	
6	I2	I*4	ID for IMF Spacecraft	See table
7	I2	I*4	ID for SW Plasma spacecraft	See table
8	I4	I*4	# of points in IMF averages	
9	I4	I*4	# of points in Plasma averages	

WORD	ASCII	IBM BINARY	MEANING	UNITS/COMMENTS
10	F6.2	R*4	Field Magnitude Average, $\lvert\tilde{B}\rvert$	$\frac{1}{N}\sum_i \lvert B\rvert_i$, gammas
11	F6.2	R*4	Magnitude of average field vector, F	$[\bar{B}_x^{\,2} + \bar{B}_y^{\,2} + \bar{B}_z^{\,2}]^{1/2}$
12	F6.2	R*4	Latitudinal angle (θ_B) of Average field vector	Degrees (GSE coordinates)
13	F6.2	R*4	Longitudinal angle (ϕ_B) of Average field vector	Degrees (GSE coordinates)
14	F6.2	R*4	B_x, GSE	Gammas
15	F6.2	R*4	B_y, GSE	Gammas
16	F6.2	R*4	B_z, GSE	Gammas
17	F6.2	R*4	B_y, GSM	Gammas
18	F6.2	R*4	B_z, GSM	Gammas
19	F6.2	R*4	$\sigma_{\lvert B\rvert}$	RMS Standard deviation in average magnitude (word 10), Gammas
20	F6.2	R*4	$\sigma_{\underset{\sim}{B}}$	RMS Standard deviation in field vector, in Gammas**
21	F6.2	R*4	σ_{B_x}	RMS Standard deviation in GSE X component average, Gammas†
22	F6.2	R*4	σ_{B_y}	RMS Standard deviation in GSE Y component average, Gammas†
23	F6.2	R*4	σ_{B_z}	RMS Standard deviation in GSE Z component average, Gammas†

---

†The σ_{B_i} values were not provided with HEOS IMF data; for such records, words 21-23 contain $\sigma_{\lvert B\rvert}$ (repeat of word 19) and, in degrees, σ_{θ_B} and σ_{ϕ_B}, respectively.

** $\sigma_{\underset{\sim}{B}}$ is $[(\sigma_{B_x})^2 + (\sigma_{B_y})^2 + (\sigma_{B_z})^2]^{1/2}$ for IMP records, and is $[(\sigma_{\lvert B\rvert})^2 + \lvert\tilde{B}\rvert^2 - F^2]^{1/2}$ for HEOS records.

WORD	ASCII	IBM BINARY	MEANING	UNITS/COMMENTS
24	F8.0	R*4	Plasma temperature (T)	°K
25	F5.1	R*4	Ion Density (N)	cm^{-3}
26	F6.1	R*4	Bulk speed (V)	km/sec
27	F6.1	R*4	Bulk flow longitude angle (ϕ_V)	Degrees, GSE coordinates, >0 for flow from west of sun
28	F6.1	R*4	Bulk flow latitude angle (θ_V)	Degrees, GSE coordinates, >0 for flow from south of sun * see discussion below
29	F8.0	R*4	σ_T	°K
30	F5.1	R*4	σ_N	cm^{-3}
31	F6.1	R*4	σ_V	km/sec
32	F6.1	R*4	σ_{ϕ_v}	degrees
33	F6.1	R*4	σ_{θ_v}	degrees
34§	I2	I*4	K_p	(e.g. 3+ = 33, 6- = 57, 4 = 40)
35§	I1	I*4	C9	Geomagnetic activity index (0 to 9)
36§	I4	I*4	R	Sunspot #
37	I5	I*4	DST Index	NT

§ From ESRO tape. See Trans. AGU, 49, 463, 1968.

*** Owing to differential gain shifts of the two collector plates of the IMP-8 MIT Faraday cup, an error occurred in the derivation of the solar wind flow latitude direction. This error was not discovered until much erroneous data had been distributed. In December, 1988, flow latitude values from IMP-8 on the NSSDC OMNI tape and online version thereof were adjusted for this effect by the subtraction of 2.0 for the years 1973-1977, and by the subtraction of 5.0 for all subsequent years.

The following spacecraft identifiers have been used:

Spacecraft Name	Spacecraft ID
IMP 1 (Expl 18)	18
IMP 3 (Expl 28)	28
IMP 4 (Expl 34)	34
IMP 5 (Expl 41)	41
IMP 6 (Expl 43)	43
IMP 7 (Expl 47)	47
IMP 8 (Expl 50)	50
AIMP 1 (Expl 33)	33
AIMP 2 (Expl 35)	35
HEOS 1 and HEOS 2	1
VELA 3	3
OGO 5	5
Merged LANL VELA speeds (7/64-3/71)	99
Merged LANL IMP T,N,V (Including all IMP 8 LANL plasma)	98
ISEE 1	11
ISEE 2	12
ISEE 3	13
PROGNOZ 10	10

COMPOSITE INTERPLANETARY

FIELD AND PLASMA TAPE

SM-41E

THIS DATA SET CONSISTS OF ONE TAPE. THE TAPE IS 9-TRACK, 6250 BPI, BINARY AND CONTAINS ONE FILE OF DATA. THE TAPE WAS CREATED ON AN VAX COMPUTER. THIS DATA SET IS THE 44-WORD VERSION OF THE INTERPLANETARY FIELD AND PLASMA DATA. EXCERPTS OF THE SUPPORTING DOCUMENTS**, AS IDENTIFIED BY JOE KING, HAVE BEEN INCLUDED FOR DISTRIBUTION TO REQUESTERS. THE COMPLETE DOCUMENT IS AVAILABLE UPON REQUEST. THE D AND C NUMBERS, ALONG WITH THE TIME SPAN FOLLOWS:

FORMAT	D#	C#	TIME SPAN
44-WORD	D-085880	C-029048	11/02/63 - 11/16/96

* PART OF THIS DATA SET IS ALSO AVAILABLE THRU NODIS

**SELECTED TEXT PAGES FORM SUPPORTING DOCUMENTS ARE:

77-04 PAGES 1-33 PLUS THE SCATTERPLOTS 1-27
79-08 PAGES 1-3
86-04 PAGES 1-30
89-17 2 INTRODUCTION PAGES

WORD	ASCII	IBM BINARY	MEANING	UNITS/COMMENTS
10	F6.2	R*4	Field Magnitude Average, $\lvert\tilde{B}\rvert$	$\frac{1}{N}\sum_i \lvert B\rvert_i$, gammas
11	F6.2	R*4	Magnitude of average field vector, F	$[\bar{B}_x^2 + \bar{B}_y^2 + \bar{B}_x^2]^{1/2}$
12	F6.2	R*4	Latitudinal angle (θ_B) of Average field vector	Degrees (GSE coordinates)
13	F6.2	R*4	Longitudinal angle (ϕ_B) of Average field vector	Degrees (GSE coordinates)
14	F6.2	R*4	B_X, GSE	Gammas
15	F6.2	R*4	B_Y, GSE	Gammas
16	F6.2	R*4	B_Z, GSE	Gammas
17	F6.2	R*4	B_Y, GSM	Gammas
18	F6.2	R*4	B_Z, GSM	Gammas
19	F6.2	R*4	$\sigma_{\lvert B\rvert}$	RMS Standard deviation in average magnitude (word 10), Gammas
20	F6.2	R*4	$\sigma_{\tilde{B}}$	RMS Standard deviation in field vector, in Gammas**
21	F6.2	R*4	σ_{B_x}	RMS Standard deviation in GSE X component average, Gammas†
22	F6.2	R*4	σ_{B_y}	RMS Standard deviation in GSE Y component average, Gammas†
23	F6.2	R*4	σ_{B_z}	RMS Standard deviation in GSE Z component average, Gammas†

† The σ_{B_i} values were not provided with HEOS IMF data; for such records, words 21-23 contain $\sigma_{\lvert B\rvert}$ (repeat of word 19) and, in degrees, σ_{θ_B} and σ_{ϕ_B}, respectively.

** $\sigma_{\tilde{B}}$ is $[(\sigma_{B_x})^2 + (\sigma_{B_y})^2 + (\sigma_{B_z})^2]^{1/2}$ for IMP records, and is $[(\sigma_{\lvert B\rvert})^2 + \lvert\tilde{B}\rvert^2 - F^2]^{1/2}$ for HEOS records.

The following spacecraft identifiers have been used:

Spacecraft Name	Spacecraft ID
IMP 1 (Expl 18)	18
IMP 3 (Expl 28)	28
IMP 4 (Expl 34)	34
IMP 5 (Expl 41)	41
IMP 6 (Expl 43)	43
IMP 7 (Expl 47)	47
IMP 8 (Expl 50)	50
AIMP 1 (Expl 33)	33
AIMP 2 (Expl 35)	35
HEOS 1 and HEOS 2	1
VELA 3	3
OGO 5	5
Merged LANL VELA speeds (7/64 - 3/71)	99
Merged LANL IMP T, N, V (Including all IMP 8 LANL plasma)	98
ISEE 1	11
ISEE 2	12
ISEE 3	13
PROGNOZ 10	10

*** Owing to differential gain shifts of the two collector plates of the IMP-8 MIT Faraday cup, an error occurred in the derivation of the solar wind flow latitude direction. This error was not discovered until much erroneous data had been distributed. In December, 1988, flow latitude values from IMP-8 on the NSSDC OMNI tape and online version thereof were adjusted for this effect by the subtraction of 2.0 for the years 1973-1977, and by the subtraction of 5.0 for all subsequent years.

WORD	ASCII	IBM BINARY	MEANING	UNITS/COMMENTS
24	F8.0	R*4	Plasma temperature (T)	°K
25	F5.1	R*4	Ion Density (N)	cm^{-3}
26	F6.1	R*4	Bulk speed (V)	km/sec
27	F6.1	R*4	Bulk flow longitude angle (ϕ_V)	Degrees, ~~GSE coordinates~~, >0 for flow from west of sun
28	F6.1	R*4	Bulk flow ~~longitude~~ latitude angle (θ_V)	Degrees, ~~GSE coordinates~~, >0 for flow from south of sun * see discussion below
29	F8.0	R*4	σ_T	°K
30	F5.1	R*4	σ_N	cm^{-3}
31	F6.1	R*4	σ_V	km/sec
32	F6.1	R*4	σ_{ϕ_V}	degrees
33	F6.1	R*4	σ_{θ_V}	degrees
34§	I2	I*4	K_p	(e.g. 3+ = 33, 6- = 57, 4 = 40)
35§	I1	I*4	C9	Geomagnetic activity index (0 to 9)
36§	I4	I*4	R	Sunspot #
37	I5	I*4	DST Index	
38	F8.2	R*4	Proton flux	>1 Mev
39	F8.2	R*4	Proton flux	>2 Mev
40	F8.2	R*4	Proton flux	>4 Mev
41	F8.2	R*4	Proton flux	>10 Mev
42	F8.2	R*4	Proton flux	>30 Mev
43	F8.2	R*4	Proton flux	>60 Mev
44	I1	I4	*Flag	0,1,2,3,4,5,6

§ From ESRO tape. See Trans. AGU, 49, 463, 1968.

* If the flag is 0 there are not Proton flux data, or all the Proton flux data are dominated by magnetospheric event.
If the flag is 1 then the >1, >2, >4, >10, >30 Mev channels were judged to have magnetospheric "contamination".
If the flag is 2 then the >1, >2, >3, >4 Mev channels were judged to have magnetospheric "contamination".
If the flag is 3 then the >1, >2, >3 Mev channels were judged to have magnetospheric "contamination".
If the flag is 4 then the >1, >2, Mev channels were judged to have magnetospheric "contamination".
If the flag is 5 then the >1, Mev channels was judged to have magnetospheric "contamination".
If the flag is 6 then no channel was judged to have magnetospheric "contamination".

WORD	ASCII	IBM BINARY	MEANING	UNITS/COMMENTS	
24	F8.0	R*4	Plasma temperature (T)	°K	
25	F5.1	R*4	Ion Density (N)	cm^{-3}	
26	F6.1	R*4	Bulk speed (V)	km/sec	
27	F6.1	R*4	Bulk flow longitude angle (ϕ_V)	Degrees, GSE coordinates, >0 for flow from west of sun	
28	F6.1	R*4	Bulk flow latitude angle (θ_V)	Degrees, GSE coordinates, >0 for flow from south of sun * see discussion below	
29	F8.0	R*4	σ_T	°K	
30	F5.1	R*4	σ_N	cm^{-3}	
31	F6.1	R*4	σ_V	km/sec	
32	F6.1	R*4	σ_{ϕ_v}	degrees	
33	F6.1	R*4	σ_{θ_v}	degrees	
34§	I2	I*4	K_p	(e.g. 3+ = 33, 6- = 57, 4 = 40)	
35§	I1	I*4	C9	Geomagnetic activity index (0 to 9)	
36§	I4	I*4	R	Sunspot #	
37	I5	I*4	DST Index	NT	
38	F8.2	R*4	Proton flux	(cmsq sec sr)$^{-1}$	>1 Mev
39	F8.2	R*4	Proton flux	(cmsq sec sr)$^{-1}$	>2 Mev
40	F8.2	R*4	Proton flux	(cmsq sec sr)$^{-1}$	>4 Mev
41	F8.2	R*4	Proton flux	(cmsq sec sr)$^{-1}$	>10 Mev
42	F8.2	R*4	Proton flux	(cmsq sec sr)$^{-1}$	>30 Mev
43	F8.2	R*4	Proton flux	(cmsq sec sr)$^{-1}$	>60 Mev
44	I1	I4	*Flag		0,1,2,3,4,5,6

§ From ESRO tape. See Trans. AGU, 49, 463, 1968.

* If the flag is 0 there are not Proton flux data, or all the Proton flux data are dominated by magnetospheric event.
If the flag is 1 then the >1, >2, >4, >10, >30 Mev channels were judged to have magnetospheric "contamination".
If the flag is 2 then the >1, >2, >3, >4 Mev channels were judged to have magnetospheric "contamination".
If the flag is 3 then the >1, >2, >3 Mev channels were judged to have magnetospheric "contamination".
If the flag is 4 then the >1, >2, Mev channels were judged to have magnetospheric "contamination".
If the flag is 5 then the >1, Mev channels was judged to have magnetospheric "contamination".
If the flag is 6 then no channel was judged to have magnetospheric "contamination."

From: NCF::KING 16-SEP-1994 07:33:42.73
To: POST
CC:
Subj: mod to yesterday's version

From: NCF::KING 16-SEP-1994 07:32:36.32
To: JAMES
CC: KING
Subj: further mods

Nate, MIT has requested further mods to the text you added yesterday. I have incorporated most of their suggestions in the revised text below. Could you please replace yesterday's text with today's (below, as is). Thanks
Joe

From: SMTP%"kip@space.mit.edu" 15-SEP-1994 15:24:10.09
To: KING
CC:
Subj: Al's comments

Date: Thu, 15 Sep 94 15:24:25 EDT
From: Karolen I. Paularena <kip@space.mit.edu>
To: KING@NSSDCA.GSFC.NASA.GOV
Subject: Al's comments
Cc: kip

Joe, I'm sorry to do this to you... but Al wanted several changes, and I think it's important that he be happy with what you've done. I hope you agree (and aren't upset that I asked him!). At any rate, here's what he's requested as changes to what you sent. Please let me know what you decide. - Karolen

[suggested deletions from ajl] and replacement wording

Note that, as discussed in the paper data books, cross-normalization of parameters obtained from different sources has been done to yield more multi-source uniformity and to allow comparison of parameters. For data later than 1971, only plasma density and temperature values have been normalized. No implication about which data set is "correct" is implied; the historical choice was to normalize to the IMP8/LANL data. For the post-1971 period the normalization equations used were (from Table 9 of Data Book Supplement 3, NSSDC 86-04):

For IMP8/LANL, no normalization.

For IMP8/MIT, $(\log N)_{norm} = .12 + 0.89*(\log N)_{obsvd}$
$(\log T)_{norm} = -.62 + 1.11*(\log T)_{obsvd}$

For ISEE3, $(\log N)_{norm} = .20 + 0.83*(\log N)_{obsvd}$
$(\log T)_{norm} = -.55 + 1.07*(\log T)_{obsvd}$

For ISEE1, $(\log N)_{norm} = .18 + 0.85*(\log N)_{obsvd}$
$(\log T)_{norm} = (\log T)_{obsvd}$

From: NCF::KING 15-SEP-1994 08:36:02.09
To: POST
CC: KING
Subj: OMNIformat

Ralph, could you pick up item 2 below, and add it to the paper OMNI format statement we send out with copies of the OMNItape. Thanks. Joe

From: NCF::KING 15-SEP-1994 08:34:37.98
To: JAMES
CC: KING
Subj: OMNIfile text mods

Nate, I'd like you to help me update some of the OMNIfile text.

1. In the introductory paragraph, after the sentence "most data are discussed in NSSDC's Interplanetary Medium Data Books" add a new sentence "See file documentation below for cross-normalization information." If this causes our one screenful of introductory text to overflow to a 2nd screen , pls get back to me.

2. After the list of s/c ID's in the format statement, add the following:

Note that, as discussed in the paper data books, some cross-normalization of parameters across the various data sources has been effected to give more multi-source uniformity. For data later than 1971, only plasma density and temperature values have been normalized. A certain historic arbitrariness has been maintained in which data sets were normalized to which other data sets. The normalization equations used, for the post-1971 period, were (from Table 9 of Data Book Supplement 3, NSSDC 86-04):

For IMP8/LANL, no normalization.

For IMP8/MIT, (log N)norm = .12 + 0.89*(log N)obsvd
(log T)norm =-.62 + 1.11*(log T)obsvd

For ISEE3, (log N)norm = .20 + 0.83*(log N)obsvd
(log T)norm =-.55 + 1.07*(log T)obsvd

For ISEE1, (log N)norm = .18 + 0.85*(log N)obsvd
(log T)norm = (log T)obsvd

NSSDC
WDC-A-R&S

79-08

National Space Science Data Center/
World Data Center A For Rockets and Satellites

Interplanetary Medium Data Book - Supplement 1

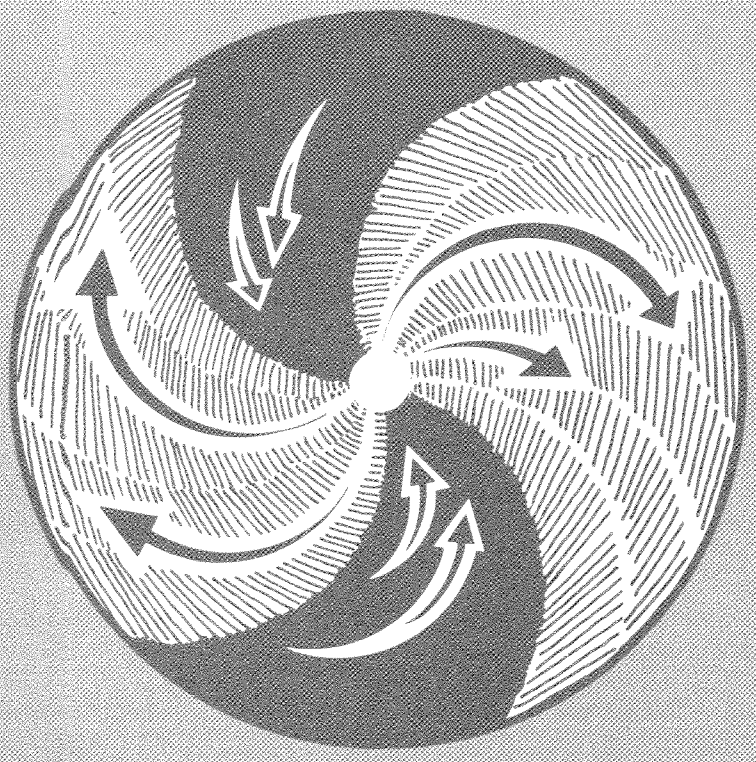

December 1979

NSSDC/WDC-A-R&S 79-08

Interplanetary Medium Data Book Supplement 1
1975-1978

by

Joseph H. King
Laboratory for Extraterrestrial Physics

December 1979

National Space Science Data Center
National Aeronautics and Space Administration
Goddard Space Flight Center
Greenbelt, Maryland 20771

TABLE OF CONTENTS

Introduction

The *Interplanetary Medium Data Book* (NSSDC/WDC-A-R&S 77-04, 1977) contains plots and listings of hourly averaged interplanetary field and plasma parameters covering the period November 27, 1963 through December 30, 1975. Since the issuance of that *Data Book*, additional data have become available which fill some 1975 data gaps and which extend the data coverage well into 1978. This document contains all the presently available data for the years 1975-1978, and represents the first supplement to the *Interplanetary Medium Data Book*. A second supplement is likely to fill 1978 gaps and to extend coverage into the early 1980's.

The Magnetic Field Data

All the newly available interplanetary magnetic field (IMF) data have come from the IMP 8 triaxial fluxgate magnetometer experiment of N. F. Ness and R. P. Lepping of Goddard Space Flight Center. This experiment, from which 1973-1975 data were published in the earlier *Data Book*, is discussed in some detail in that *Data Book*. The IMF data in this *Supplement* extend through May 21, 1978. Later data will be available in the next supplement. Note that some of the early 1975 IMF data contained in this *Supplement* are from the HEOS 1 experiment of P. C. Hedgecock, and were published in the earlier *Data Book*.

The Plasma Data

This *Supplement* contains derived plasma parameters from the IMP 7 and IMP 8 instruments of both the Los Alamos Scientific Laboratory (LASL; S. J. Bame, principal investigator) and the Massachusetts Institute of Technology (MIT; H. S. Bridge, principal investigator). Discussions of the LASL electrostatic analyzers and the MIT Faraday cups are found in the earlier *Data Book*.

For this *Supplement*, the LASL data were available for the years 1975 and 1976 in the form of a tape of hourly averaged proton density, flow speed, and temperature values. The interplanetary data from the IMP 7 and IMP 8 spacecraft were merged at LASL before submission to NSSDC. Note that whereas 1-hour averages are now available for 1975-1976, the LASL data of the earlier *Data Book* were 3-hour averaged parameters.

The MIT data were submitted to the National Space Science Data Center (NSSDC) on separate IMP 7 and IMP 8 magnetic tapes which cover the periods September 27, 1972, to September 26, 1978, and October 1, 1973, to December 1, 1978, respectively. The IMP 8 parameters, all 1-hour averages, consist of proton density, flow speed, temperature, flow latitude and longitude angles, and the standard deviations in these averages. Due mainly to noise in the IMP 7 spacecraft-to-ground telemetry stream, only flow speed could be recovered from IMP 7 data with high reliability, and it is only IMP 7 flow speed that is presented in this *Supplement*.

The MIT IMP 7 and IMP 8 flow speeds (V_7 and V_8) agree with each other to within 2 percent, as evidenced by the results of a regression analysis applied to 1,771 pairs of simultaneous IMP 7 and IMP 8 interplanetary speed values measured in 1977-1978. This analysis, in which the sum of perpendicular distances between data points and regression line is minimized (see discussion in earlier *Data Book*), yielded

$$V_8 = 0.996\ V_7 + 6.77 \text{ km/s}.$$

In the earlier *Data Book*, MIT density (N) and temperature (T) data were normalized to LASL data using the results of regression analysis, viz.

$$\log N_{LASL} = 0.89 \log N_{MIT} + 0.121$$

$$\log T_{LASL} = 1.1 \log T_{MIT} - 0.62$$

Regressions of logarithms were performed because both density and temperature exhibited distributions which were more "log-normal" than normal. The corresponding relation for flow speed was

$$V_{LASL} = 0.99 V_{MIT} + 6.2$$

Owing to the closeness of this last relation to $V_{LASL} = V_{MIT}$, the MIT flow speeds were not normalized. The preceding three relations were based on 5,297 hours between October 1973 and December 1974 in which simultaneous 1-hour MIT and 3-hour LASL parameters were available.

We have performed similar regression analyses for 1975 and 1976, and we present the results in the following table.

$$P_{LASL} = a\, P_{MIT} + b$$

	P = Log N		Log T		V		
Time Period	a	b	a	b	a	b	Number of Points
10/73-12/74	.89	.12	1.11	-.62	.99	6.2	5,297
01/75-12/75	.91	.10	1.13	-.74	1.00	-2.4	4,016
01/76-12/76	.91	.09	1.12	-.69	1.01	-4.4	4,332

A most significant result is the near constancy of the relations between the LASL and MIT data. This suggests that characteristics of individual sensors probably do not change significantly with time, and that the use of the differing instrumentations and data analysis procedures lead to real and persistent differences in the final derived parameters (density and temperature). Our approach of normalizing MIT data to LASL data is not to be construed as imputing "error" more to the MIT data than to the LASL data; indeed, we are not able to judge this matter. We originally normalized MIT IMP 8 data to the composite LASL IMP 6/7/8 data set simply because the latter data set consisted of data from three spacecraft. For consistency with the previous approach, we shall continue to normalize MIT density and temperature data to LASL data. Further, in view of the near constancy of the MIT/LASL regression relations, as evidenced by the table, we shall normalize the 1975-1978 MIT density and temperature data using the relations that were previously utilized for the 1973-1974 MIT IMP 8 data, and we shall continue to leave the MIT speed values unnormalized.

Given the availability of plasma data from more than one source for a given hour, the priority for selecting data was first MIT IMP 8, then LASL IMP 7/8, then MIT IMP 7. The MIT IMP 8 data were chosen first because: (1) although the set of listed and plotted parameters are available in either of the

first two source data sets, there are additional MIT parameters which are put on the magnetic tape from which this *Supplement* is generated and which is itself available to scientists upon request; and (2) MIT data were preferred to LASL data in the earlier *Data Book* owing to the better time resolution of the former.

Data Presentation

This *Data Book Supplement* consists of graphical and tabular presentations of some of the parameters of the composite data set. There are two plots for each solar rotation in which any plasma or field data were obtained. On facing pages, for convenience in lining up features in the data, are found a plot of plasma data (proton temperature, density, and bulk speed) and a plot of field data (average magnitude, geocentric solar magnetospheric (GSM) B_Z component, and geocentric solar ecliptic (GSE) latitude and longitude angles of the average field vector). Note that on those rare occasions when the parameter values exceed the allowed range, a heavy mark is placed near the edge of the plot. For such cases, the reader is advised to consult the data listings for appropriate numerical values.

Following the plots are found listings of selected hourly parameters, including proton temperature (in units of 1000°K), density (cm^{-3}), bulk speed (km/s), and the IMF parameters: average magnitude, GSM cartesian components, latitude and longitude angles of the vector made up of the average GSE field components, and the vector standard deviation (see earlier *Data Book* for discussion).

Identifiers of both the plasma and IMF data sources are also listed (H = MIT IMP 7, J = MIT or GSFC IMP 8, L = LASL IMP 7/8, X = HEOS).

Note that the data are listed in 1-day blocks and that days with no field or plasma data are omitted from the listings.

Additional Data Availability

The magnetic tape, which contains 1963-1978 data and from which this *Data Book Supplement* was generated, is very similar in format to that used for, and discussed in detail in, the earlier *Data Book*. The present tape has been improved by virtue of the addition of later data and of the geomagnetic DST index.

Copies of this tape (with a detailed format), as well as copies of the *Interplanetary Medium Data Book* and of this *Supplement*, are available by request to:

National Space Science Data Center
Code 601.4
NASA/Goddard Space Flight Center
Greenbelt, Maryland 20771

NSSDC NATIONAL SPACE SCIENCE DATA CENTER

WORLD DATA CENTER A for ROCKETS AND SATELLITES 86-04

Interplanetary Medium Data Book – Supplement 3, 1977–1985

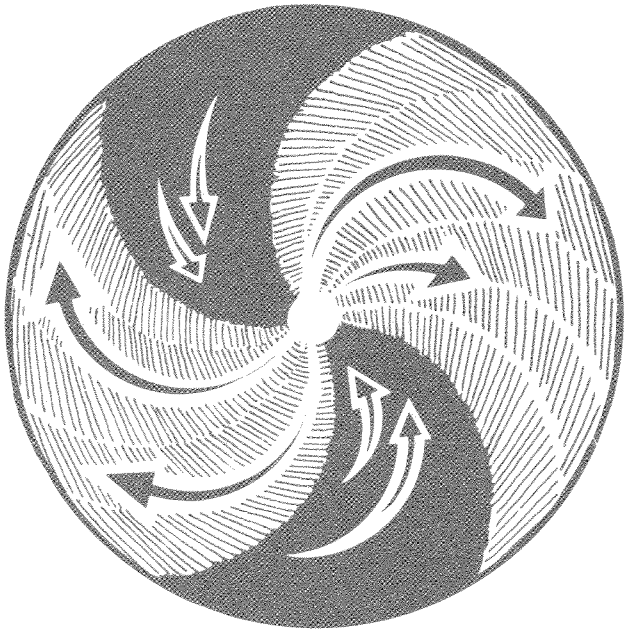

April 1986

NASA

National Aeronautics and Space Administration

Goddard Space Flight Center

NSSDC/WDC-A-R&S 86-04

Interplanetary Medium Data Book - Supplement 3

1977 - 1985

By

David A. Couzens

and

Joseph H. King

April 1986

National Space Science Data Center (NSSDC)/
World Data Center A for Rockets and Satellites (WDC-A-R&S)
National Aeronautics and Space Administration
Goddard Space Flight Center
Greenbelt, Maryland 20771

ACKNOWLEDGMENTS

The continuation of this Data Book series would be impossible if not for the sustained efforts of the GSFC, MIT, LANL and JPL groups in carefully analyzing and reducing their data and in making these data available to the NSSDC and hence to the solar terrestrial physics community.

Much of the computer programming for this supplement was performed by Howard A. Leckner. His thoroughness and perseverance are greatly appreciated.

TABLE OF CONTENTS

LIST OF TABLES

LIST OF FIGURES

INTERPLANETARY MEDIUM DATA BOOK - SUPPLEMENT 3

1977 - 1985

ABSTRACT

The updating of the hourly resolution near-Earth solar wind data compilation is discussed. Data plots and listings are then presented. In the text, the time shifting of ISEE 3 magnetic field and plasma data, using corotation delay is explained in detail. Normalizations of IMP(MIT), ISEE 3, and ISEE 1 temperatures and densities to equivalent IMP(LANL) values are also discussed. The levels of arbitrariness in combining data sets, and of random differences between data sets, are elucidated.

Introduction

In previous issues of this series, hourly averaged interplanetary magnetic field and plasma parameters have been listed and plotted. These parameters have come from a number of spacecraft in the near-Earth solar wind. Data for 1963-1975 were contained in the *Interplanetary Medium Data Book* (NSSDC/WDC-A-R&S 77-04, 1977), data for 1975-1978 were published in the *Interplanetary Medium Data Book - Supplement 1* (NSSDC/WDC-A-R&S 79-08, 1979) and data for 1978-1982 were published in the *Interplanetary Medium Data Book - Supplement 2* (NSSDC/WDC-A-R&S 83-01, 1983). This third supplement represents an extension of the earlier compilations to 1985. Supplement 3 supersedes Supplement 2 in terms of both the data and the discussion. It begins in 1977 in order to incorporate ISEE 1 data, and corrects previously announced errors published in Supplement 2 which affected values of B_y (GSM) and B_z (GSM) in 1980 to 1982 and some B_y (GSE) values in mid-1980. Because of its size, this supplement has been published in two volumes. The first volume (Supplement 3) contains descriptive information and 27-day plots of various parameters. Listings of selected parameters are contained in Supplement 3A. Copies of all the books in this series, as well as the parent OMNI tape from which the listings and plots are generated, are available from the National Space Science Data Center (NSSDC). These data (from 1976 onward) are also accessible online through the NSSDC VAX. Access procedures are described subsequently.

Data Sources for this Supplement

Data for this supplement come from the IMP 8, ISEE 3 and ISEE 1 spacecraft. IMP 8 was launched on October 26, 1973, and is in a low eccentricity, ~30Re x 40 Re, 12.5-day geocentric orbit. IMP 8 is in the solar wind for a duration of 6 to 8 days per orbit. ISEE 3 was launched on August 12, 1978. Until mid-1982 it orbited the Earth-sun libration point approximately 240 Earth radii sunward of the earth, ranging up to 100 Re from the Earth-sun line. ISEE 3 was then redirected into the Earth's geotail. It sampled the solar wind for a large portion of 1982 and for portions of 1983. Launched on October 22, 1977, ISEE 1 has a highly elliptical orbit with an apogee of 23 Re and a period of about 57 hours. Usually ISEE 1 only enters the solar wind from August through December where it can spend up to 30 or more hours of each orbit in the interplanetary medium. As of early 1986, IMP 8 and ISEE 1 continue to provide near-Earth data.

The six data sets folded into this compilation are identified in Table 1. Some of the plasma data attributed to Los Alamos IMP 8 actually were provided as a mix of Los Alamos IMP 6, IMP 7 and IMP 8 data. All ISEE 1 and IMP 8 plasma parameters are based on ion measurements. ISEE 3 plasma parameters are based on ion measurements through day 48, 1980 (at which time the ion portion of the instrument failed), and electron measurements after this time. When both ISEE 3 and IMP 8 (field or plasma) data were available for a given hour, the IMP data were used in this compilation due to IMP's greater proximity to the Earth. When both MIT and LANL IMP 8 plasma data were available, the MIT data were chosen for historical reasons. ISEE 3 plasma data were chosen preferentially to ISEE 1 plasma data because of the availability of additional statistical and flow direction parameters.

TABLE 1. Data Sources for this Supplement

Spacecraft		Principal Investigator	Time Span (YR/DOY)
Magnetic Fields	IMP 8	N. F. Ness (GSFC)	73/302 --- 85/091
	ISEE 3	E. J. Smith (JPL)	78/225 --- 83/365
Plasma	IMP 8	H. S. Bridge (MIT)	73/334 --- 85/107
	IMP 8	S. J. Bame (LANL)	71/076 --- 84/357
	ISEE 3	S. J. Bame (LANL)	78/228 --- 82/279
	ISEE 1	S. J. Bame (LANL)	77/303 --- 79/365

* Key scientists associated with the reduction of these data include R. P. Lepping, B. T. Tsurutani, J. D. Sullivan, A. J. Lazarus, J. A. Gosling, W. C. Feldman, and R. D. Zwickl.

Systematic and Random Differences Between Data Sets

The principal task in interspersing data from different sources is to make the data sets as compatible as possible. Thus, a data compilation is desired in which small amplitude, long term changes, and larger amplitude, short term changes may be studied with relatively high confidence levels. Absolute values of parameters, and small amplitude, hourly changes are less accurately determined, especially when more than one data source is involved.

There may be random differences and systematic differences between data sets. Systematic differences result from calibration errors in one or both data sets. In this context, "calibration" implies the whole process of transforming the electrical output of a sensor or sensors measuring some physical parameter to a declaration of what the physical parameter value is.

Random differences occur at least in part because two instruments may be measuring at different times or places, in the presence of temporal evolution or spatial gradients in the parameter being measured. In the case of hourly averages, differing parts of an hour may have been measured by two experiments. Random differences may also arise from the use of the differing instrumentation and data analysis technique, which has been discussed by Neugebauer (*Sp. Sci. Rev.*, 33, 127, 1982).

When a regression analysis is performed between two data sets of "simultaneously measured" parameter values, the deviation of the regression line from Y = X gives a measure of the systematic difference between data sets, and the scatter of data points about the regression line gives a measure of the random difference. For the case of ISEE 3, data must first be time shifted to expected Earth arrival times. If this is not done, the random differences found by regressing IMP 8 and ISEE 3 parameters are not irreducible. This is because the ISEE 3 to IMP 8 transit time is comparable to the hourly time resolution used in this compilation.

For those parameters for which systematic differences are comparable to or greater than the random differences, a cross-normalization of data sets is performed. It has been found that only density and temperature need to be

cross-normalized. That is, IMF parameters and flow speed had systematic differences significantly less than random differences. The decisions as to which data set to normalize to which other data set involved a certain arbitrariness, which was discussed in the original Data Book and Supplement 1.

Time Shifting of ISEE 3 Data

Either or both of two approaches to time-shifting ISEE 3 fine scale data may be expected to yield statistically irreducible random errors. (There are random differences between two sets of observations and random errors between either set of observations and the "true" values.) These approaches are corotation and convection. Consider initially the first of these. The corotation delay equation is:

$$\tau = \frac{X}{V}\left\{\frac{1+\frac{V}{R\Omega}\frac{Y}{X}}{1-\frac{Ve}{R\Omega}}\right\}$$

In this equation, τ is the time shift, X and Y are the ecliptic plane projections of the geocentric ISEE 3 position vector along and across the Earth-sun line, V is the measured solar wind speed (assumed radial), $R\Omega$ is the equivalent speed of solar rotation at 1 AU (~428 km/s), and Ve is the orbital speed of the Earth (~30km/s).

Use of the corotation delay equation would be completely correct if the constant-phase surfaces of all solar wind variations were normal to the ecliptic plane and aligned with the ideal spiral interplanetary magnetic field (IMF) direction, and if solar wind variations had no temporal evolution on the ISEE-to-Earth transit time scale nor spatial gradients transverse to the Earth-sun line on scales less than ~100 Re. None of these required conditions is satisfied by all solar wind variations. Thus, random errors are an inevitable part of the inference of near-Earth solar wind parameter values from ISEE 3 data and the corotation delay equation.

A study of these errors was begun by comparing "simultaneous" 5-min-averaged ISEE 3 and IMP 8 field and plasma data. Simultaneity here implies that the IMP 8 time is within 2.5 min of the corotation-shifted ISEE 3 time. In this analysis, the X and Y of the corotation delay equation relate to the ISEE-IMP separation vector rather than to the geocentric ISEE position vector.

Figure 1 shows a scatter plot of simultaneous, 5-min averaged ISEE 3 and IMP 8 measurements of the Z(GSE) component of the IMF. These data were taken between day 36 and 66 of 1979, when ISEE 3 was within 50 R_e of the Earth-sun line. There are 1867 data points included. The regression line determined by minimizing the sum of squares of perpendicular distances between data points and regression line is shown on the figure. That the regression line is not Y = X relates to systematic differences and will be addressed in the next section. Of principal interest here is the scatter of points about the regression line. The rms perpendicular distance between data points and regression line (labelled RMS PERP DIST OF PTS ABT LINE on the plot and called the "scatter function" for convenience in the following) is 1.35 nanoTeslas (nT). This means that for a given ISEE 3 5-min observation of B_z, IMP 8 would

PARAMETER : BZ - GSE
TIME SPAN IS: 79036 TO 79066
NO. OF PTS: 1867
SHIFT TYPE: COROTATION
AVERAGES: IMP 0.76 ±5.05
: ISE 0.77 ±5.18

BZ-IMP = 0.01(±0.03) + 0.97(±0.01) × BZ-ISEE

RMS PERP DIST OF PTS ABT LINE: 1.35

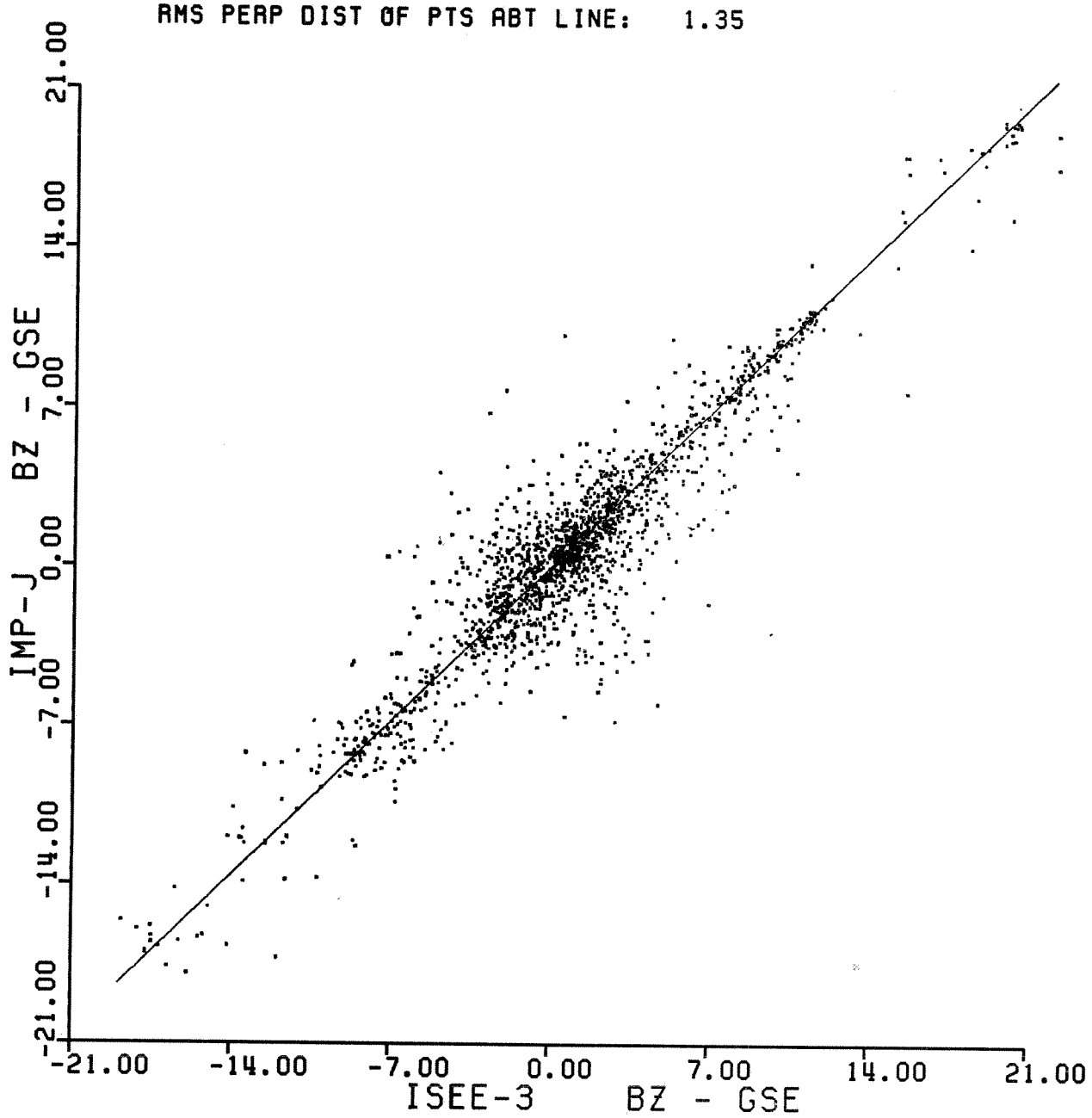

Figure 1. Scatter plot and best fit regression line for IMP 8 and ISEE 3 B_Z 5-min values, Feb. 6 - Mar. 7, 1979

measure, over the five corresponding corotation-shifted minutes, a value of B_z in the range given by the ISEE 3 value, plus or minus $\sqrt{2}$ * 1.35 nT, with a probability of ~68%. (The $\sqrt{2}$ factor enters because 1.35 nT is a distance normal to the regression line, while for the present purpose we need an equivalent distance parallel to the ordinate. Regression line slopes are close enough to unity that $\sqrt{2}$ is an adequate approximation throughout.)

Using 5-min data, regression lines and scatter functions have been determined for each of seven interplanetary parameters, for each of eight (magnetic field) or thirteen (plasma) time periods, for each of three approaches to time-shifting ISEE 3 data. (Time periods after day 48, 1980, were treated separately since 5-min resolution plasma data were not available. The method used to time shift these later time periods is explained toward the end of this section.) The parameters analyzed are field Cartesian components (B_x, B_y, B_z), field magnitude (B_m), flow speed (V), proton density (N), and temperature (T). Because N and T are distributed more logarithmically than linearly, log N and log T were used in the regression analysis.

The time periods for which analyses were performed were defined by the ISEE 3 orbital phase: Y(ISEE) < -50 R_e; -50 R_e < Y(ISEE) < 50 R_e; 50 R_e < Y(ISEE). Most intervals so defined had durations between 30 and 60 days, and contained between 1000 and 3000 ISEE/IMP 5-min data points. Note that because IMP 8 covers the range -40 R_e < Y < 40 R_e during each 12.5 day orbit, there is some overlap of Y(ISEE)-Y(IMP) between $|Y(ISEE)|$ < 50 R_e and $|Y(ISEE)|$ > 50 R_e periods.

The three time shifts used for ISEE data were corotation (delay equation given above), convection [delay = (X(ISEE)-X(IMP))/V], and no shift. Convection is expected to yield smaller random errors than corotation if the constant-phase surfaces of interplanetary variations are more nearly normal to a heliocentric radius vector than they are aligned with the ideal spiral IMF direction, by a statistically significant amount. The no-shift case was included to estimate the level of reduction of the random differences produced by time-shifting ISEE data.

Figure 2 summarizes the scatter function information for all physical parameters and time periods, for the case of corotation-shifting of the ISEE 3 data. Note that scatter functions separately computed for individual Cartesian components of the IMF have been averaged. Note also that scatter functions computed for $|Y(ISEE)|$ < 50 R_e and $|Y(ISEE)|$ > 50 R_e intervals are distinguished. Lines have been drawn connecting the $|Y(ISEE)|$ < 50 R_e intervals.

Several points may be noted in Figure 2. First, there is variability from one interval to the next. For the IMF components, the scatter functions are larger for the $|Y(ISEE)|$ > 50 R_e intervals than for the $|Y(ISEE)|$ < 50 R_e intervals. This is less clearly true for the field magnitude, and is not true for the plasma parameters. These statements are also true when convective shifting of ISEE data is considered. This behavior is consistent with the transverse scale of plasma parameter variations being greater than 50 to 100 R_e, and with the scale for field component (or direction) variations being comparable to or less than 50 to 100 R_e. Field magnitude variation scales seem to be intermediate.

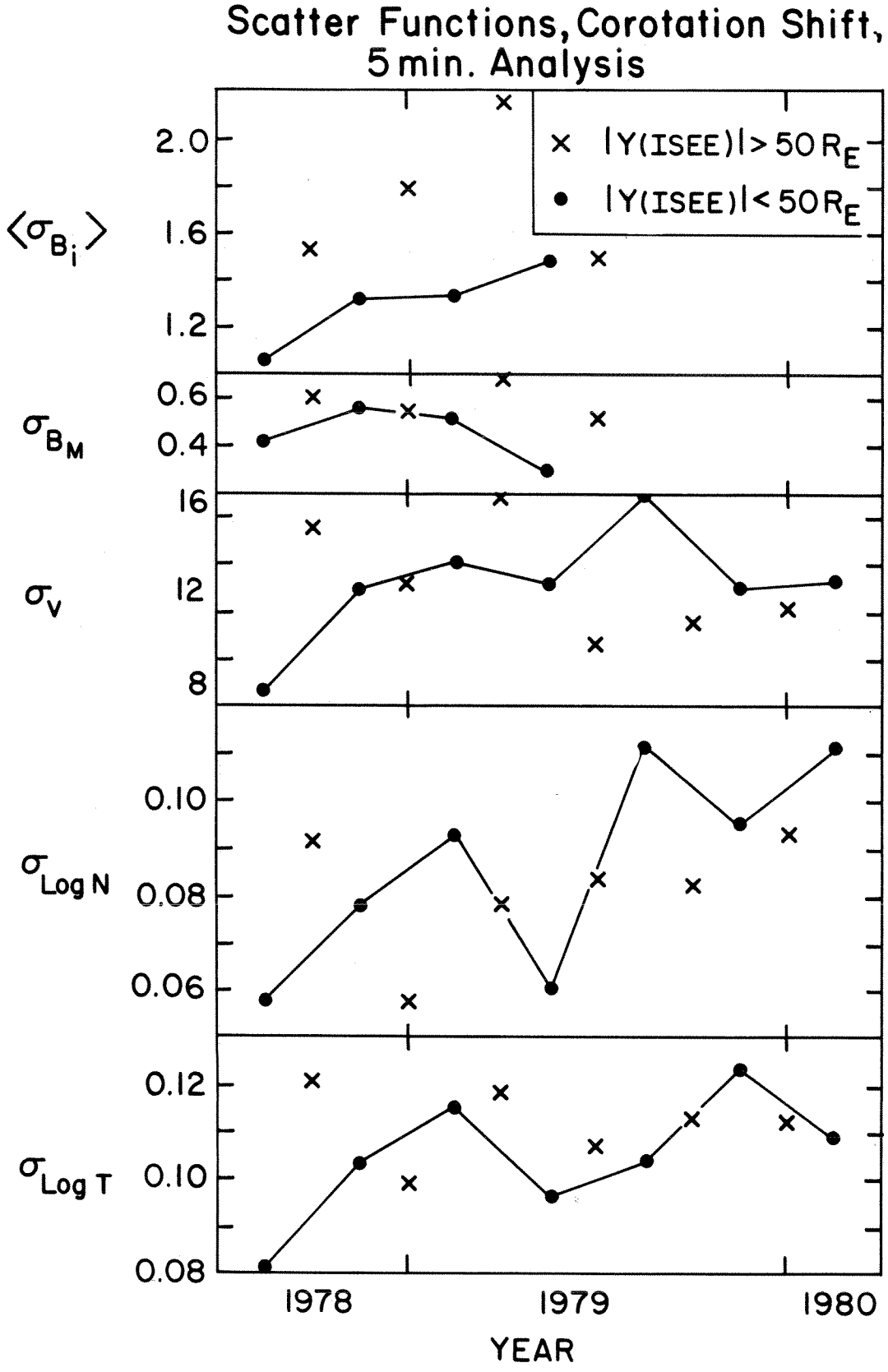

Figure 2. Scatter functions, corotation shift, 5-min analysis

Note that the scatter functions for field magnitude are significantly smaller than scatter functions for field components. This is consistent with a preponderance of constant-field-intensity Alfvenic fluctuations in the solar wind.

As averaged over all time periods, the mean scatter functions for the five panels of Figure 2 are 1.52 nT, 0.51 nT, 12.4 km/s, 0.084, and 0.108. Recall the above discussion of Figure 1 concerning the relation of these values to the inference of near-Earth parameter values from ISEE observations. Note that the last two of these five mean scatter functions correspond to one-sigma uncertainties in near-Earth density and temperatures values of 30% and 40%, given ISEE 3 observations.

Next we compare these results, based on corotation shifting, with the results of convective shifting and no shifting. Figure 3 (left and center panels) contains histograms of ratios of scatter functions for these latter analyses to those illustrated in Figure 2. Note that $|Y(ISEE)| < 50\ R_e$ and $|Y(ISEE)| > 50\ R_e$ cases are again distinguished.

From the convection-to-corotation histogram, it is apparent that very similar scatter functions are obtained with corotation and convection. Very seldom do the convection and corotation scatter functions differ by more than 10% for a given physical parameter and time period. When all time periods and parameters are considered, it is found that the convective scatter function exceeds the corotation scatter function in 55% of the cases (39 out of 71). Even for the $|Y(ISEE)| > 50\ R_e$ cases when the corotation and convection analyses might be expected to exhibit the greatest differences (owing to the greater delay differences), there is no statistically significant difference between the corotation and convection cases. From this it may be concluded that the distribution of constant-phase surfaces of interplanetary variations is peaked neither along the ideal IMF spiral direction nor perpendicular to a heliocentric radius vector. Our choice of time shifting by corotation rather than by convection is seen to be a basically arbitrary choice.

Given this statistical equivalence of convective and corotational time shifting of ISEE 3 data, it may be asked whether these shifts give a statistically significant improvement (reduction of random differences, or scatter functions) relative to not shifting ISEE data at all. From the no-shift to corotation-shift histogram of Figure 3 (center panel), it is clear that time shifting does indeed make a difference. The extent of the difference depends on both the physical parameter and on $|Y(ISEE)|$.

Time shifting reduces the random differences by anywhere between 0% and 40% for plasma parameters, and up to a factor of 2 for field parameters. The greater improvement in field parameters results from these parameters' smaller scale lengths. That is, a greater portion of the random differences between (no-shift) simultaneous ISEE 3 and IMP 8 field parameters results from the temporal-spatial displacement of these spacecraft than is the case for plasma parameters, and this displacement is at least partially compensated for by the time-shifting.

Time shifting also reduces the scatter functions by a greater amount for the $|Y(ISEE)| < 50\ R_e$ intervals than for the $|Y(ISEE)| > 50\ R_e$ intervals; this effect is more pronounced for the field parameters than for the plasma data.

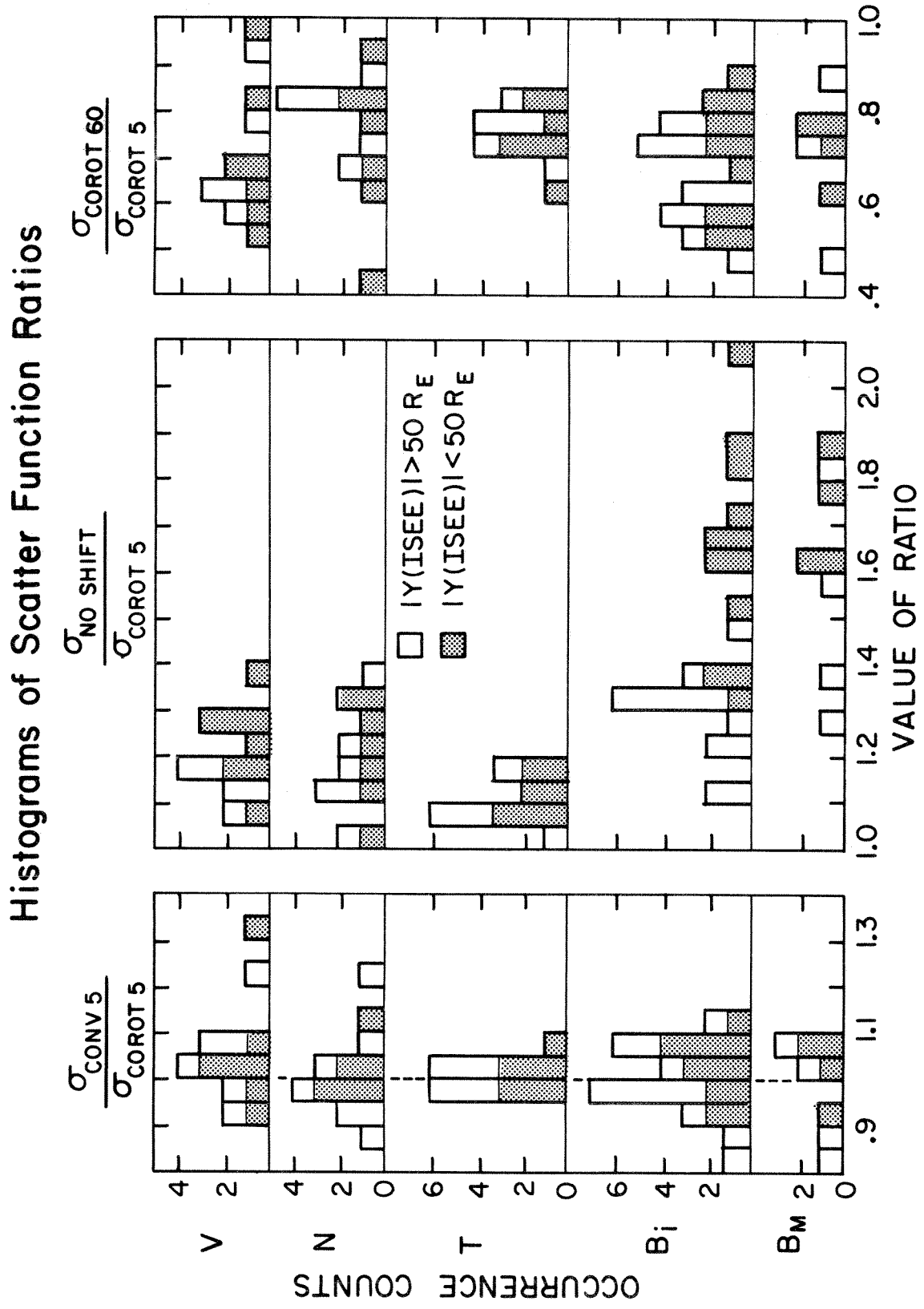

Figure 3. Histograms of scatter function ratios

This is an effect of transverse spatial gradients in interplanetary variations and the existence of a distribution of constant-phase orientations. These become increasingly significant as |Y(ISEE)| increases, and they are handled only imperfectly with a simple time shift which assumes a uniform constant-phase orientation.

All the foregoing discussion has concerned 5-min resolution analysis. It is expected that coarser time resolution would yield smaller random differences, since finer scale structures which probably contribute significantly to the 5-min-resolution random differences would be averaged out. This expectation is realized.

ISEE 3 hourly averages, constructed from corotation-shifted 5-min averages, have been compared to corresponding IMP 8 hourly averages. The scatter functions determined in this analysis have been compared to those obtained in the 5-min resolution analysis. Ratios of hour-based scatter functions to 5-min-based scatter functions are also shown in Figure 3 (right panel). The process of taking hourly averages of 5-min averages reduces the random difference between data sets by up to a factor of 2. There is no major dependence on which physical parameter is involved, nor on |Y(ISEE)|. There is a weak suggestion that the reduction in scatter function is slightly greater for flow speed and for field components than for the other parameters.

In Figure 4 are presented the scatter function values themselves, as obtained from the hourly resolution analysis. The format and scaling are the same as for Figure 2, although the scales have been translated to account for the smaller hourly based scatter functions. There were typically between 300 and 600 pairs of "corotation-simultaneous" ISEE and IMP hourly averages in each time period.

Again, variability is observed from one interval to the next, although for most parameters the amplitude of the variability is reduced relative to Figure 2. Again, scatter functions for field components are smaller at $|Y(ISEE)| < 50\ R_e$ than at $|Y(ISEE)| > 50\ R_e$; this |Y(ISEE)| dependence is less apparent for field magnitude and is not apparent for plasma parameters.

As discussed in the next section, a single cross-normalization will be applied to each parameter for all time. It is of interest to determine random differences between ISEE and IMP for each parameter over the full span of the simultaneously available data. Figures 5-11 contain scatter plots, regression lines and scatter functions for all seven physical parameters, based on all available "corotation-simultaneous" hourly averages.

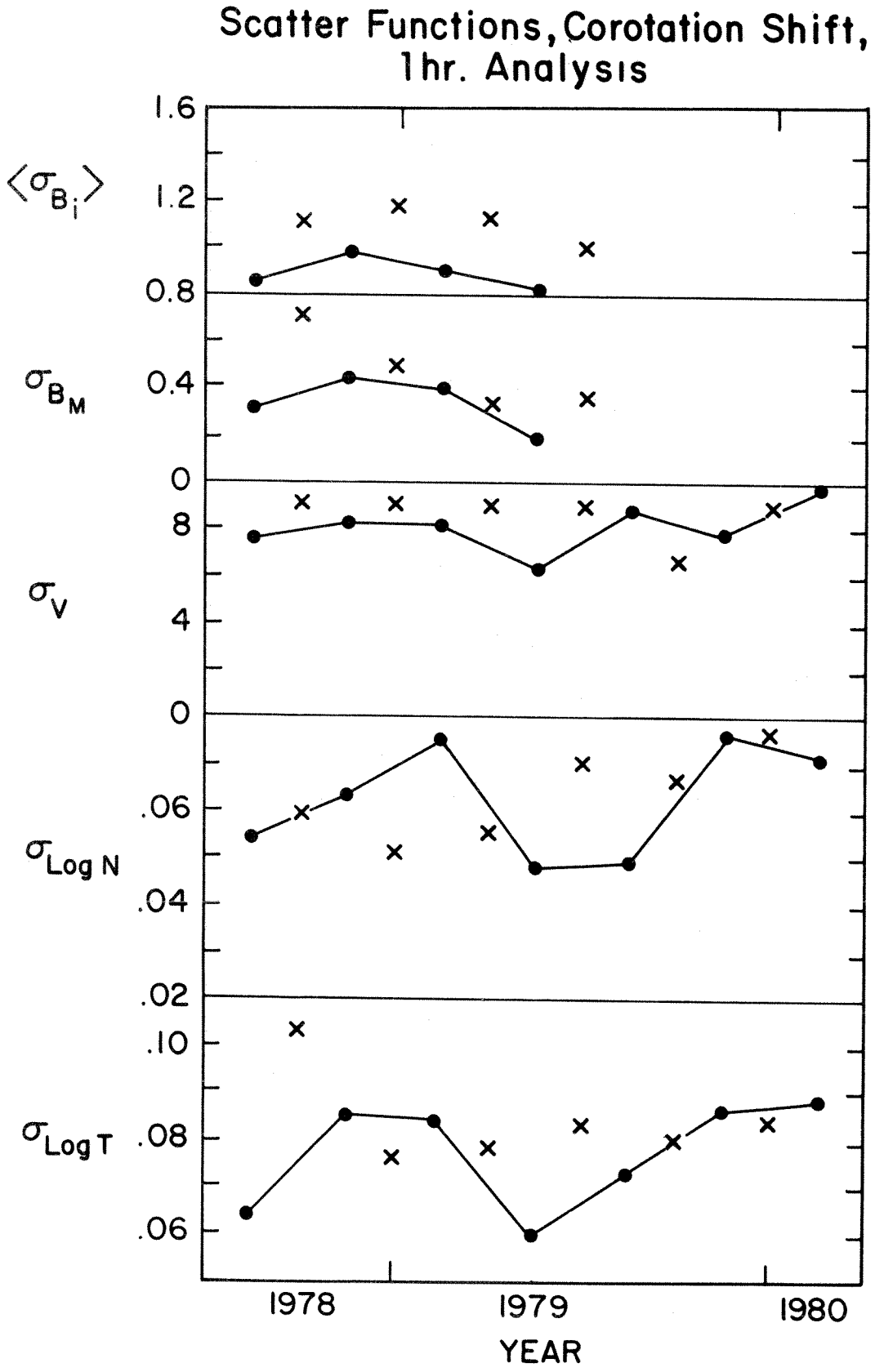

Figure 4. Scatter functions, corotation shift, 1-hr. analysis

PARAMETER : BX - GSE
TIME SPAN IS: 78224 TO 79178
NO. OF PTS: 3400
SHIFT TYPE: COROTATION
AVERAGES: IMP 0.24 ±4.14
: ISE 0.20 ±4.22

BX-IMP = 0.04(±0.02) + 0.98(±0.01) * BX-ISEE

RMS PERP DIST OF PTS ABT LINE: 0.97

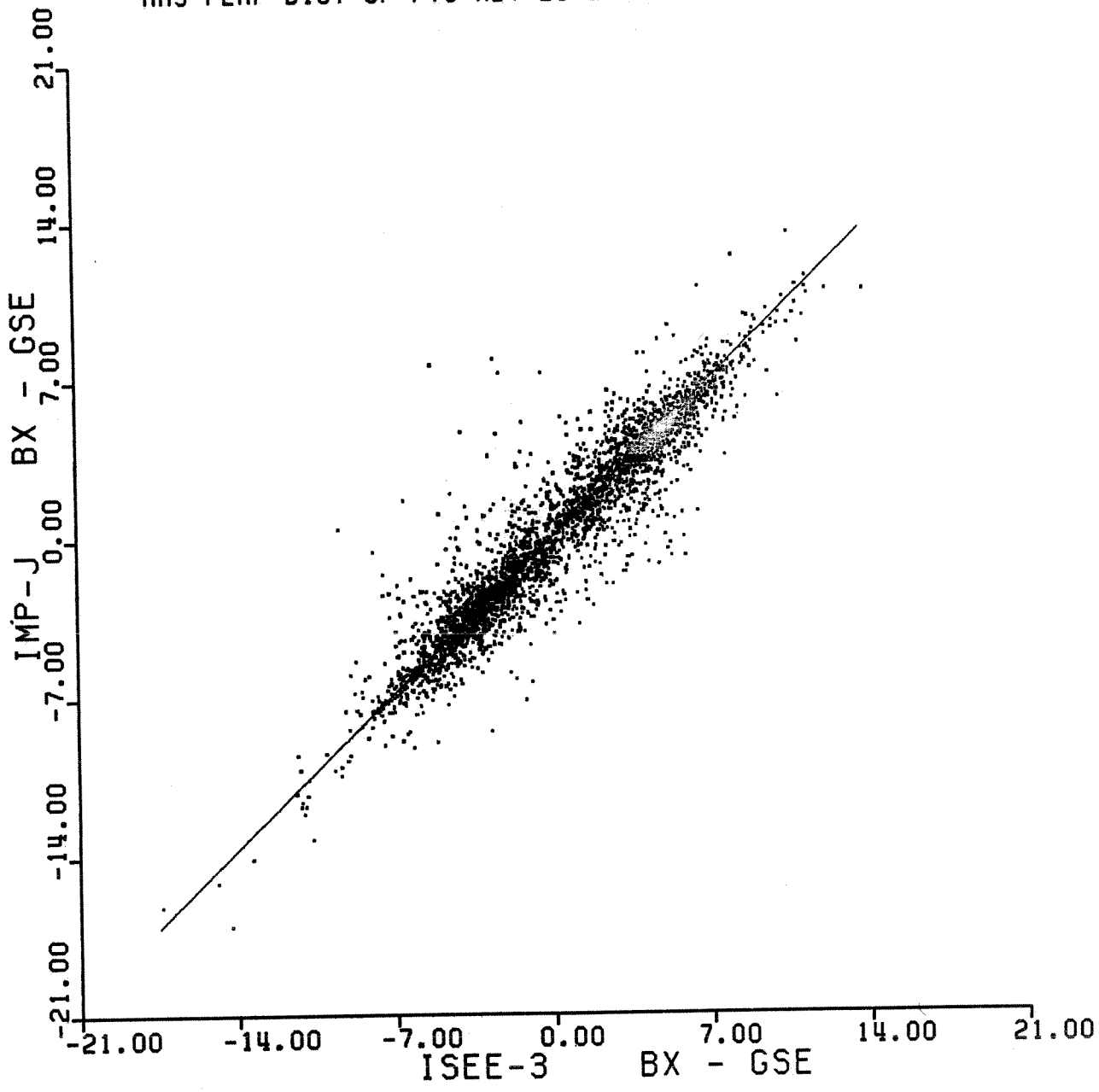

Figure 5. Scatter plot and best fit regression line for IMP 8 and ISEE 3 B_X hourly averages, Aug. 78 - June 79

PARAMETER : BY - GSE
TIME SPAN IS: 78224 TO 79178
NO. OF PTS: 3400
SHIFT TYPE: COROTATION
AVERAGES: IMP -0.15 ±4.73
: ISE -0.15 ±4.87

BY-IMP = -0.00(±0.02) + 0.97(±0.01) × BY-ISEE

RMS PERP DIST OF PTS ABT LINE: 1.01

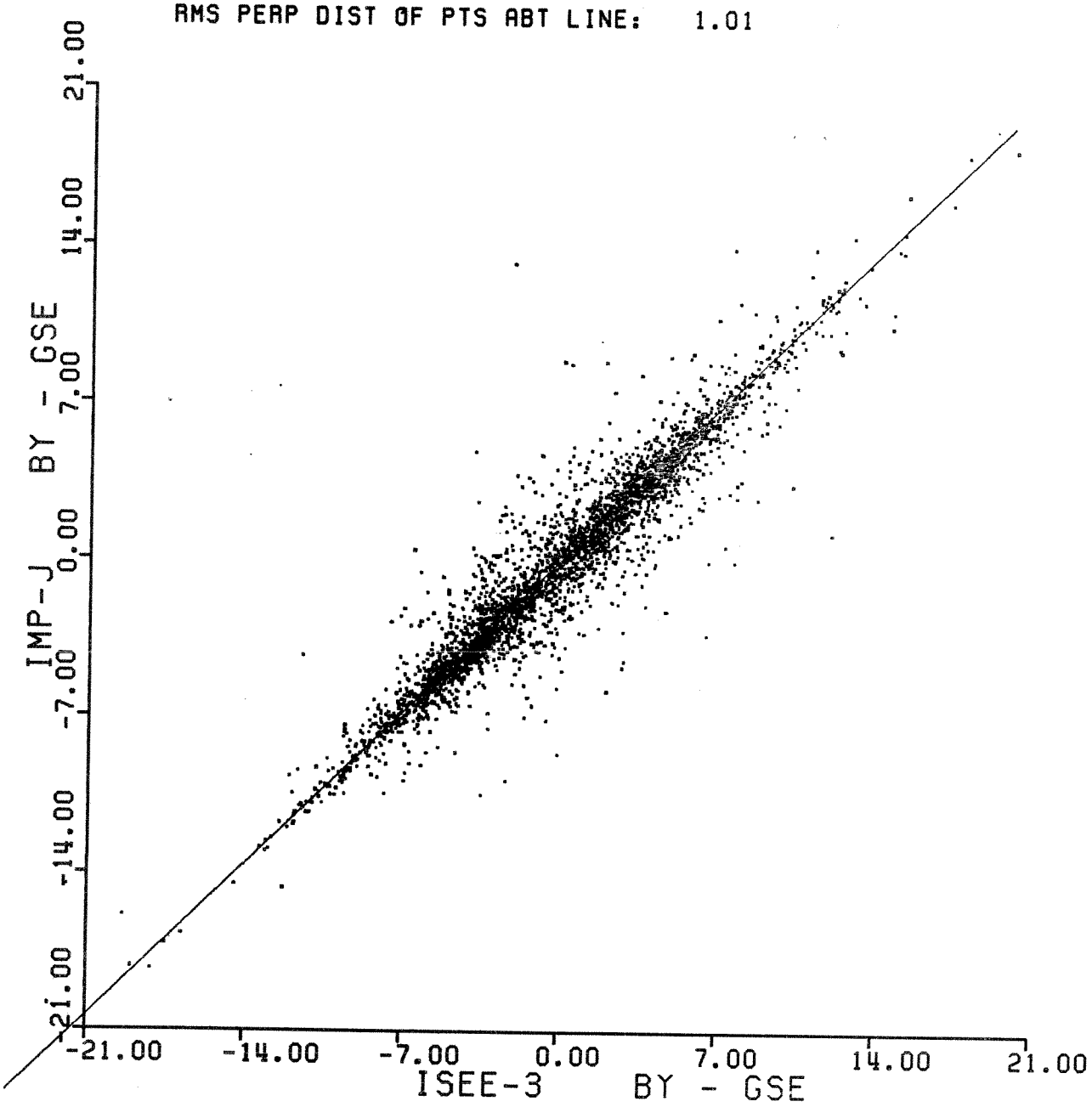

Figure 6. Scatter plot and best fit regression line for IMP 8 and ISEE 3 B_y hourly averages, Aug. 78 - June 79

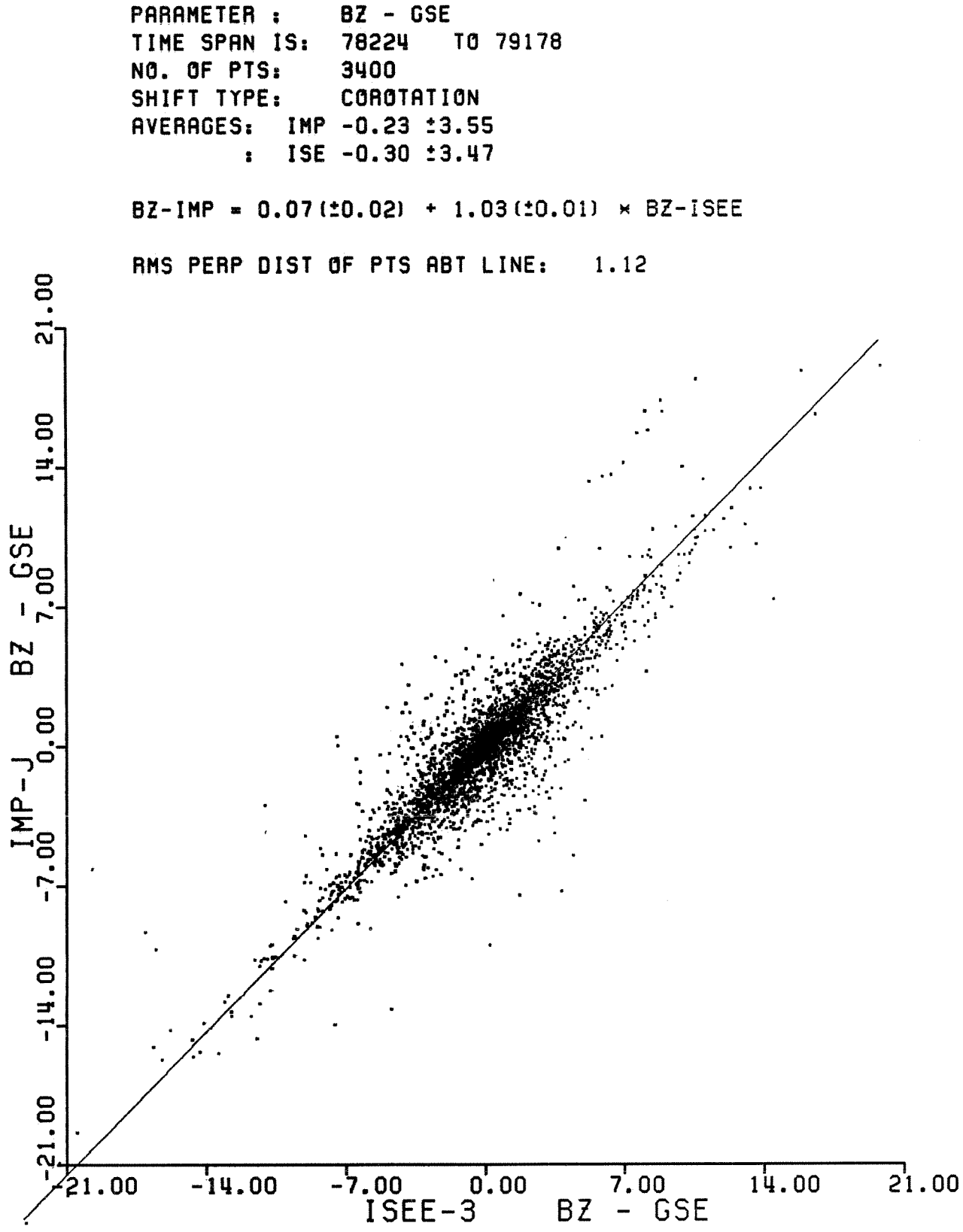

Figure 7. Scatter plot and best fit regression line for IMP 8 and ISEE 3 B_z hourly averages, Aug. 78 - June 79

PARAMETER : B-MAGNITUDE
TIME SPAN IS: 78224 TO 79178
NO. OF PTS: 3400
SHIFT TYPE: COROTATION
AVERAGES: IMP 7.30 ±3.08
: ISE 7.42 ±3.08

MAG-IMP = -0.13(±0.01) + 1.00(±0.00) × MAG-ISEE

RMS PERP DIST OF PTS ABT LINE: 0.48

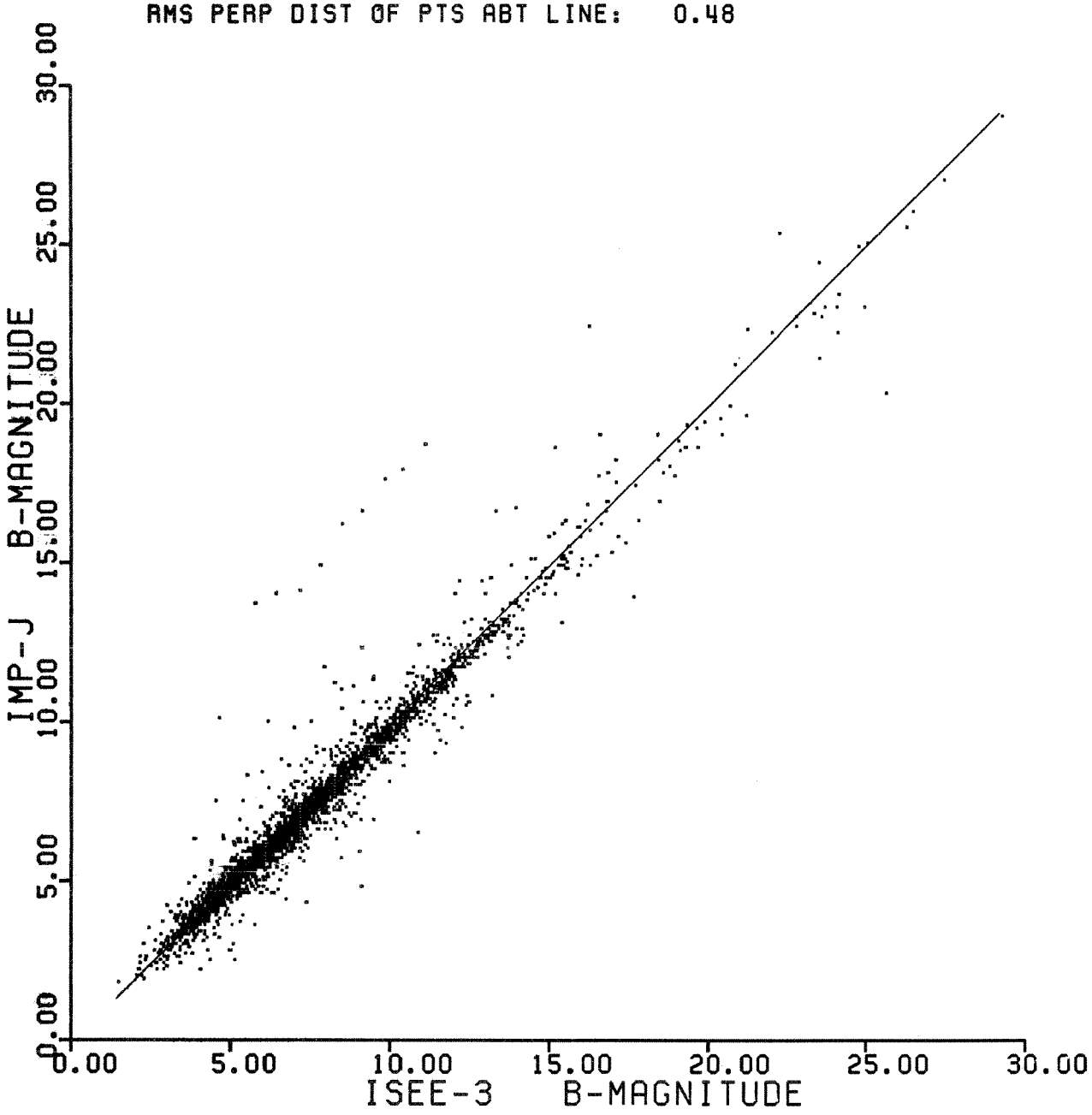

Figure 8. Scatter plot and best fit regression line for IMP 8 and ISEE 3 hourly averaged field magnitudes, Aug. 78 - June 79

PARAMETER : SPEED
TIME SPAN IS: 78228 TO 80049
NO. OF PTS: 5000
SHIFT TYPE: COROTATION
AVERAGES: IMP 417 ±81
: ISE 410 ±81

V-IMP = 5.97(±0.05) + 1.00(±0.00) × V-ISEE

RMS PERP DIST OF PTS ABT LINE: 8.44

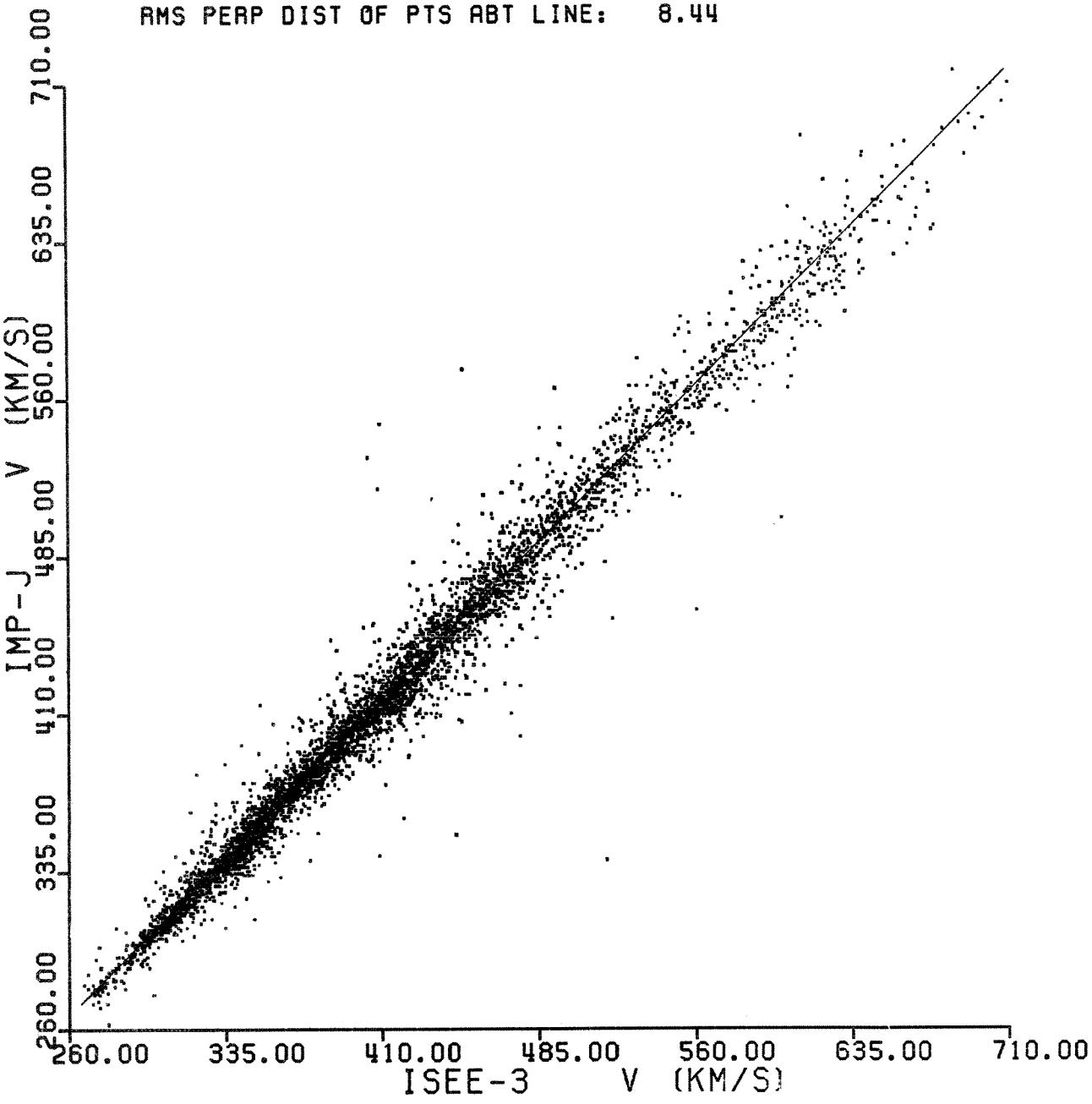

Figure 9. Scatter plot and best fit regression line for IMP 8 and ISEE 3 hourly averaged speeds, Aug. 78 - Feb. 80

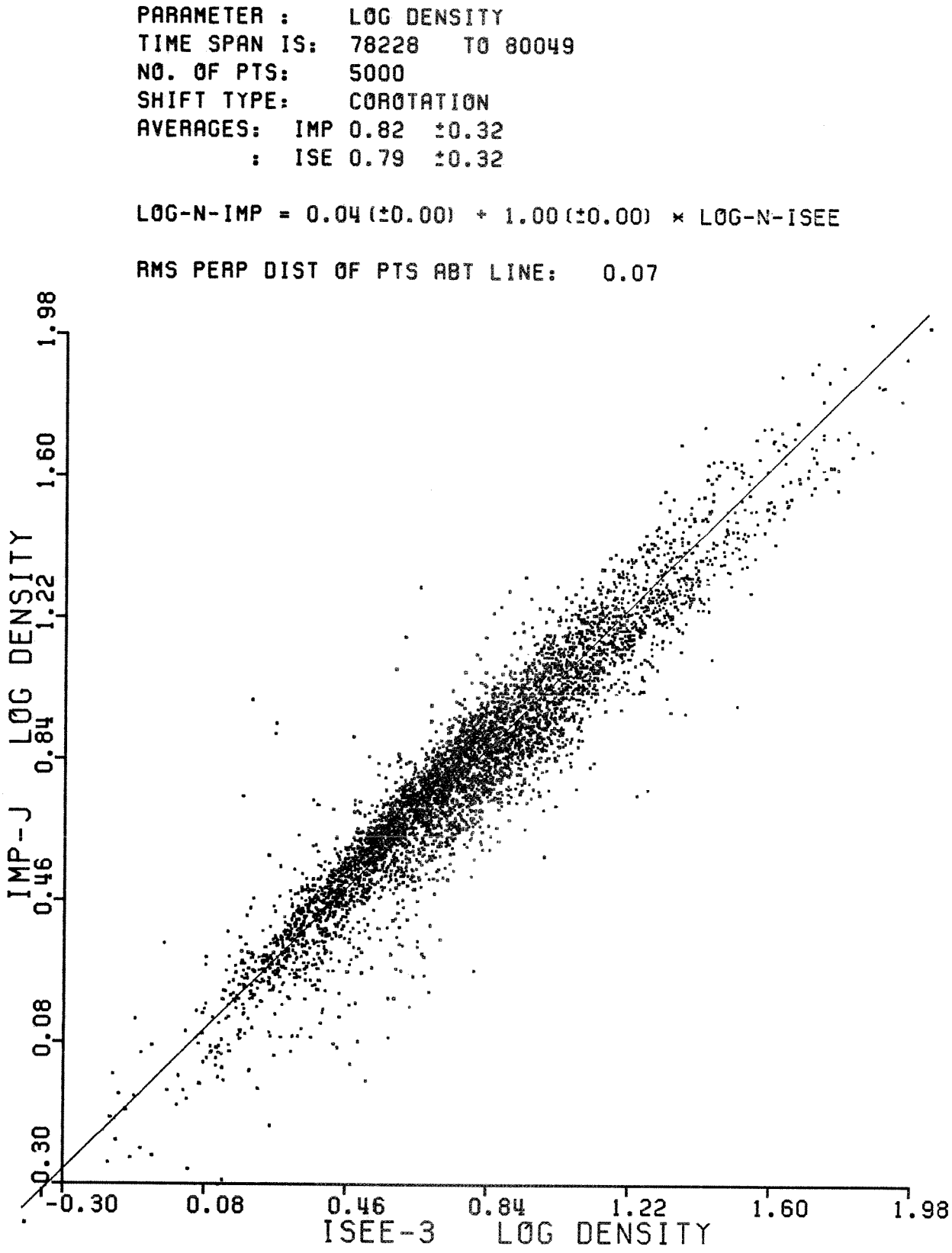

Figure 10. Scatter plot and best fit regression line for IMP 8 and ISEE 3 logarithms of hourly averaged densities, Aug. 78 - Feb. 80

PARAMETER : LOG TEMP
TIME SPAN IS: 78228 TO 80049
NO. OF PTS: 5000
SHIFT TYPE: COROTATION
AVERAGES: IMP 4.95 ±0.30
: ISE 4.90 ±0.29

LOG-T-IMP = -0.08(±0.01) + 1.03(±0.01) × LOG-T-ISEE

RMS PERP DIST OF PTS ABT LINE: 0.09

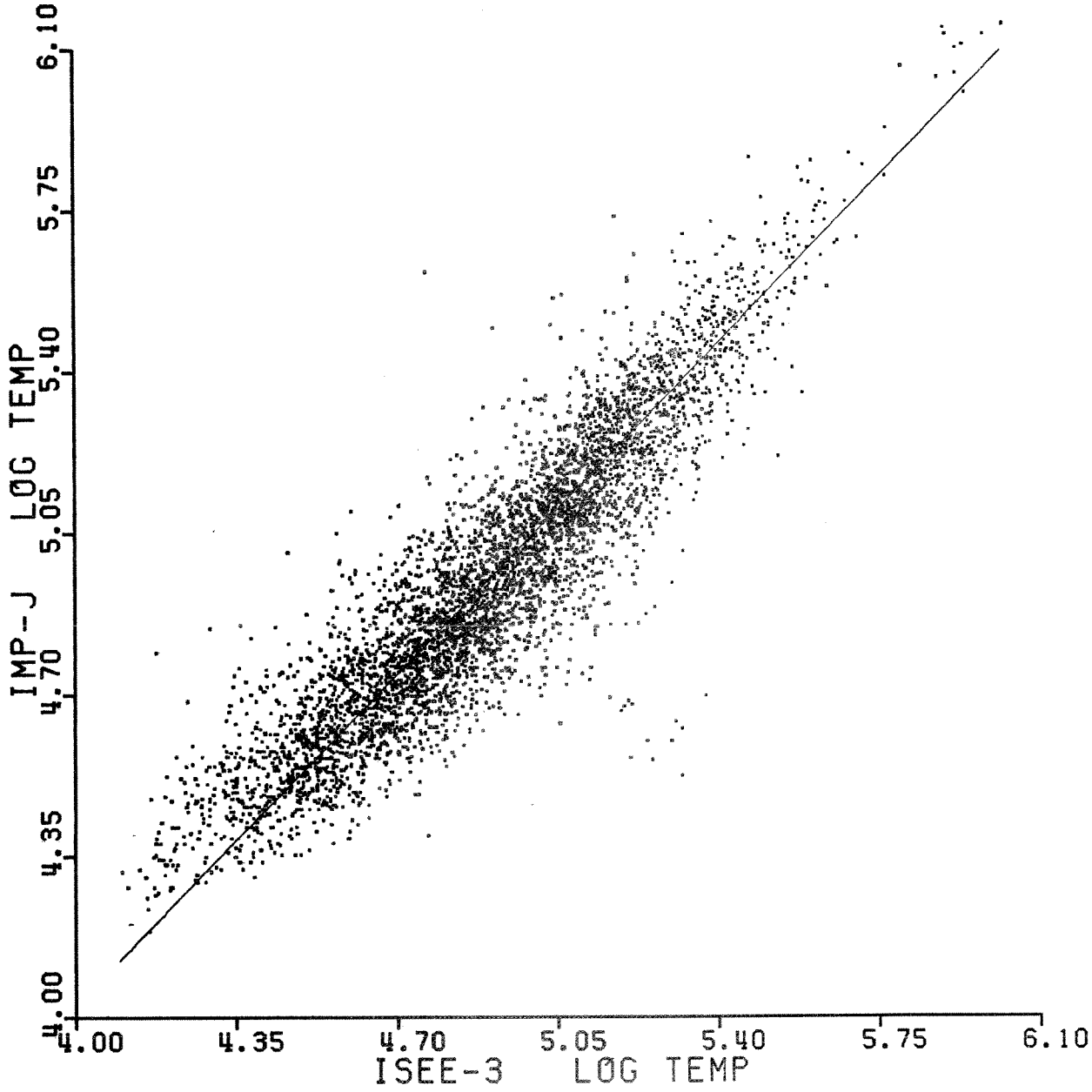

Figure 11. Scatter plot and best fit regression line for IMP 8 and ISEE 3 logarithms of hourly averaged temperature, Aug. 78 - Feb. 80

The scatter function information contained on those figures may be summarized by the first part of Table 2 below and the statement:

If an hourly averaged value of X is obtained for parameter Y from remotely measured but corotation-shifted ISEE 3 fine-scale data, then the near-Earth IMP 8 would measure a value for parameter Y in the range $X \pm Z$ with a 1-sigma (~68%) confidence level, where the Z functions are given below.

TABLE 2. Summary of Hourly Z-Function Information

Y	5-min ion-based speeds used for τ calculation (1978-1980) Z	Hourly electron-based speeds for τ calculation (1979-1983) Z
B_x	1.37 nT	1.63
B_y	1.43	1.80
B_z	1.58	1.88
B_m	0.68	0.75
V	11.9 km/sec	29.3 km/sec
log N	0.10	0.14
log T	0.13	no ion temperatures available

Note that the Z factors differ from the scatter functions by $\sqrt{2}$, as explained previously. We take these values to represent the irreducible random differences arising from the interspersal of ISEE 3 and IMP hour averages. (The right-hand column in Table 2 is discussed below.)

All of the above discussion of time shifting concerned data that were collected prior to day 48, 1980, and used originally in Supplement 2. After this time, the ISEE 3 plasma data available were hourly averaged parameters based on electron observations. The LANL group has carefully normalized their densities and velocities to their ion-based data by comparing parameters when both ion and electron measurements were taken. Nonetheless, we should bear in mind that errors associated with electron-based parameters are somewhat higher than those associated with ion-based parameters.

After day 48, 1980, time shifting of ISEE 3 IMF data was effected using the hourly resolution ISEE 3 speeds. (For late 1982 and 1983 when ISEE 3 IMF data were available but ISEE 3 plasma data were not, hourly resolution IMP 8 speeds were used.) Note that for portions of 1982 and 1983, ISEE 3 was actually tailward of the earth and thus time shift values can be positive or negative. Using the time-shifted ISEE 3 IMF hourly values, regression lines and scatter functions for ISEE 3 vs. IMP 8 were determined for B_x, B_y, B_z and B_m. The scatter functions are summarized in Table 2.

IMF scatter functions calculated when only hourly averaged speeds were available have slightly higher values than those calculated when 5 minute averaged speeds were used for time shifting. This result is not totally unexpected especially when one recalls that the hourly averaged speeds are based on electron measurements. It is also important to point out that the two separate analyses (5-min ion-based speeds and hourly electron-based speeds used for time shifting) were performed on different time intervals. The scatter functions do vary somewhat from year to year and this may account for much of the differences.

In the absence of 5-min resolution plasma data, time shifting of the post day 48, 1980, plasma data involved a much less straightforward procedure than that which was done previously. Each ISEE 3 hourly averaged density and speed was shifted to the Earth using the observed ISEE 3 speed and the corotation delay equation. Typically an ISEE hour (e.g., 0200-0300) shifted to a non-integral Earth hour (e.g., 0245-0345). Earth-time hourly averages (e.g., for 0300-0400) were then built as averages of ISEE values which shifted into the desired Earth hour, weighted by their relative contribution to that hour.

In order to determine the value of the weighted average approach to time shifting, a regression analysis was done between IMP 8 plasma data and ISEE 3 plasma data which were not time shifted. Scatter functions calculated for the "no shift" case were compared with those calculated where weighted averages were used in the time-shifting scheme. Table 3 displays the ratio of these two scatter functions by year for speeds (V) and densities (N). Ratios greater than 1 indicate that the scatter is reduced by time shifting using weighted averages. Also listed in Table 3 are the yearly averages (as measured by ISEE 3) of the solar wind speed and density. We note that the importance of time shifting increases when solar wind speeds are low or when densities are high. Since higher solar wind speeds imply smaller τ's, neglecting τ (by not time shifting) would introduce greater error for low-speed intervals. These results also imply that variability exists in solar wind speeds even when the average speed is low. On the other hand, as evident by the density scatter function ratios, periods of high average density appear to be more variable than low average density intervals.

TABLE 3. Scatter Function Ratios for ISEE 3 vs. IMP 8 Plasma Parameters

Year	# points	$\frac{\sigma_{\text{NO SHIFT}}}{\sigma_{\text{SHIFT (WEIGHTED)}}}$		ISEE 3 Averages	
		V	N	V	N
1979	1148	1.23	1.41	390	6.64
1980	1752	1.34	1.57	378	7.24
1981	1542	1.16	1.10	432	6.01
1982	1112	1.12	2.00	482	8.68

Values of the actual plasma parameter functions are shown in Table 2. Density scatter functions determined using electron-based weighted averages are about 40% higher than those found when 5-min averaged ion-based densities were used. The velocity scatter functions differ by almost a factor of 3. These differences have three possible sources: (1) using electron-based plasma parameters in lieu of ion-based parameters, (2) constructing hourly averages by the method of weighted averages instead of collecting 5-min averages, and (3) the fact that the time periods compared are not the same. Regressing ISEE 3 hourly averaged ion-based densities and velocities to their ISEE 3 electron-based counterparts for 1978 through 1980 results in a Z of .17 for log density and a Z of 33 km/sec for velocity based on 11,770 hours of overlapping data. Hence, we conclude that most of the differences between the density and velocity scatter functions can be attributed to the somewhat larger errors associated with electron-based parameters.

In order to estimate what fraction of the irreducible differences results from the remoteness of ISEE 3, it is of interest to compare the scatter functions from Table 2 with those obtained in cross-normalizing pairs of near-Earth data sets. A special case is the pair of IMP 8 plasma data sets provided by MIT and LANL. Virtually all of these data are from IMP 8 with the exception of some 1977 LANL IMP 7 data. Table 4 summarizes the scatter function data obtained upon cross-normalizing these data sets for 1977 through 1984. A comparison of the Z functions to those of Table 2 suggests that 1/3 to 1/2 of the irreducible differences between ISEE 3 and IMP 8 V and log N values, and a yet smaller fraction for log T, may result from the remoteness of ISEE 3. Note the somewhat greater scatter in the 1980-1982 era.

TABLE 4. MIT vs. LANL Scatter Functions - IMP 8

Year	Number of Hours	Scatter Functions			Z Functions		
		V	log N	log T	V	log N	log T
1977	4465	4.1	.04	.07	5.8	.05	.10
1978	2267	4.9	.04	.10	6.9	.06	.14
1979	2213	4.0	.05	.09	5.7	.06	.13
1980	1938	4.5	.06	.10	6.3	.08	.14
1981	1575	5.5	.07	.12	7.8	.10	.16
1982	1235	6.2	.05	.10	8.7	.08	.14
1983	2400	4.6	.04	.09	6.6	.06	.13
1984	1616	4.9	.03	.08	7.0	.04	.11

In the original *Interplanetary Medium Data Book* of 1977, scatter functions for plasma and field parameters were listed for several pairs of data sets obtained from near-Earth spacecraft between 1963 and 1975. These scatter functions ranged between 7.5 and 17.8 km/s (V), 0.04 to 0.10 (Log-N), and 0.06 to 0.20 (Log-T). There has been a trend towards decreasing random differences between data sets with time, due at least in part to the increasing number of instrument energy channels from whose count rates bulk flow parameters are determined. For magnetic field components, the scatter functions were typically in the 0.7 to 1.1 nT range, while for field magnitudes the scatter functions were either in the 0.3 to 0.6 nT range (8 cases) or 0.9 to 1.1 nT range (4 cases). Unlike the IMP 8 plasma case, there has been no recent case of two magnetometers flown on the same spacecraft. We conclude that the irreducible differences between the IMP 8 and corotationally shifted ISEE 3 hourly averaged IMF data sets are not significantly different statistically from the irreducible differences between non-time-shifted hourly data sets obtained for a pair of near-Earth spacecraft. In this sense, adding corotation-shifted ISEE 3 IMF data to our 1 AU, hourly average data compilation does not significantly diminish the reliability of the compilation.

Cross-Normalization of Data Sets

We consider next the systematic differences between individual data sets. Such differences are in contrast to the previously discussed random differences between data sets, and are reflected in the extent to which "best fit" regression lines deviate from Y=X. Here the concern is to make the data sets contributing to this supplement as mutually consistent as possible, and separately to make these 1977-1985 data as consistent with earlier data as possible. Recall that while all parameters have been cross-compared in the past, only density and temperature have been normalized.

Table 5 summarizes the ISEE 3 versus IMP 8 IMF regression results. In this Table, σ is the scatter function. The "1-σ range" column gives the range of P(ISEE3) over which the regression line lies within one sigma (parallel to ordinate) of Y=X. Typical field components and magnitude values are almost always deep within these ranges. Therefore, concluding that there would be no statistically significant gain in cross-normalizing the field data sets, we have not normalized them.

TABLE 5. IMP 8 vs. ISEE 3 IMF Regression Parameters

$P_{IMP} = a + b\, P_{ISEE\ 3}$

P	a	b	$\sigma_\perp$	1-σ range	
B_x	.04	.98	.97	-66 to 70nT	5-minute ion-based
B_y	.00	.97	1.01	-47 to 47nT	speeds used for τ
B_z	.07	1.03	1.12	-55 to 50nT	calculation
B_m	-.13	1.00	0.48	0 to nT	1978-79
B_x	.01	.98	1.16	-102 to 103nT	hourly electron
B_y	.02	.98	1.27	- 88 to 90nT	based speeds used
B_z	.02	1.00	1.33	-388 to 380nT	τ calculation
B_m	.03	.98	.53	0 to 40nT	1979-83

There are four plasma data sets to be cross-compared. Regression results for flow speeds, densities and temperatures are shown in Tables 6, 7 and 8 respectively. In order to ascertain whether or not the regression parameters are time invariant, each comparison has been presented for each year. Also shown are the ranges of V, N and T over which the regression lines for V, log N and log T lie within one sigma of perfect agreement (Y=X).

Flow speed data generally agree to within a few km/sec. There are some yearly variations, but no trends are apparent. Even though for certain years the 1-σ range for the IMP(LANL) IMP(MIT) velocity regression is not ideal, we have elected not to normalize these data in order to avoid using a time varying normalization. A small but significant number of density and temperature values are measured in the parts of parameter space where the systematic differences are comparable to or greater than random differences. Thus, we shall follow our earlier approach of cross-normalizing the density and temperature data.

ISEE 1 and ISEE 3 plasma data sets were compared to both the LANL and MIT data sets from IMP 8. Chaining of the derived regression equations demonstrates their mutual consistency. For example, the 1977 IMP(LANL) vs. IMP(MIT) and the 1977 IMP(LANL) vs. ISEE 1 relations of Tables 7 and 8 can be combined to yield:

$$\log N_{MIT} = .16 + .84 \log N_{ISEE\ 1}$$
$$\log T_{MIT} = .85 + .83 \log T_{ISEE\ 1}$$

These equations compare favorably to those found from the direct IMP(MIT) vs. ISEE 1 comparison.

It remains to choose what normalization to apply to which data sets. Rather than presume to judge which of the four data sets is more likely to be absolutely correct, we shall normalize all densities and temperatures to IMP(LANL) values for historical consistency. In previous Data Books, the density normalization used for IMP(MIT) data from 1973 to 1978 was:

$$\log N_{LANL} = .12 + .89 \log N_{MIT}$$

This equation is not statistically different from the normalization equation found by cross-comparing data from 1979 to 1984. Hence, we shall normalize the IMP(MIT) density data using the 1973 to 1978 relation.

It is worth noting that although there are yearly variations in the normalization parameters, little is gained by applying a time varying normalization. The σ values are such that the 1-σ range calculated against the proposed normalization for any given year usually encompasses virtually all of the relevant parameter space. For 1980 and 1981 this is not true since the IMP(LANL) IMP(MIT) regression line appears to undergo a "lowering". These "anomalous" years will be addressed subsequently in this section.

The IMP(LANL) vs. IMP(MIT) temperature regression results for 1979 to 1984 shown in Table 8 are essentially identical to the 1973-1978 results of

$$\log T_{LANL} = -.62 + 1.11 \log T_{MIT}$$

Hence for historical consistency the previous normalization will be used. Again, it is worth pointing out the year-to-year variations in the regression parameters.

TABLE 6. Flow Speed Regressions

$V_{LANL} = a + b\, V_{MIT}$ (for IMP 8)

Year	# Points	a	b	$\sigma_\perp$	1 - σ range
1977	4465	-7.0	1.01	4.1	100 to 1000 km/sec
1978	2267	-1.6	1.00	4.9	0 to ∞
1979	2213	-0.6	0.99	4.0	0 to 560
1980	1938	0.2	0.99	4.5	0 to 470
1981	1575	4.3	0.98	5.5	0 to 470
1982	1235	-2.7	0.99	6.2	0 to 1000
1983	2400	1.2	0.99	4.6	0 to 560
1984	1616	1.6	0.99	4.9	0 to 590
1979-1984	10,977	0.3	0.99	4.9	0 to 580

$V_{IMP} = a + b\, V_{ISEE1}$

Year	IMP Instrument	# Points	a	b	$\sigma_\perp$	1 - σ range
1977	LANL	655	3.1	1.01	6.8	0 to 670
1978	LANL	635	-2.0	1.02	11.7	0 to 980
1979	LANL	525	-7.0	1.03	16.9	0 to 1030
1977-1979	LANL	1815	-0.8	1.02	12.1	0 to 1060
1977	MIT	461	12.6	0.99	7.2	220 to 2000
1978	MIT	859	12.8	0.99	9.5	0 to 2300
1979	MIT	921	11.8	1.02	12.3	0 to 330
1977-1979	MIT	2241	17.0	0.99	11.0	120 to 2700

$V_{IMP} = a + b\, V_{ISEE3}$

Year	IMP Instrument	# Points	a	b	$\sigma_\perp$	1 - σ range
1978	LANL	815	8.0	0.99	6.9	0 to 1200
1979	LANL*	1148	-27.2	1.07	15.6	80 to 750
1980	LANL*	1817	21.4	0.96	24.2	0 to 1300
1981	LANL*	1605	-27.3	1.08	21.1	0 to 710
1982	LANL*	1177	-21.8	1.06	17.0	0 to 760
1980-1982	LANL*	4599	- 6.3	1.03	20.8	0 to 1190
1978-1980	MIT	5008	6.0	1.00	8.4	0 to ∞
1979	MIT*	1896	- 4.2	1.03	13.1	0 to 810
1980	MIT*	3097	3.3	1.02	20.9	0 to 1100
1981	MIT*	2794	-19.5	1.07	15.8	0 to 580
1982	MIT*	1930	-17.7	1.07	19.6	0 to 670
1979-1982	MIT*	9717	-10.0	1.05	18.0	0 to 700

*Electron-based ISEE 3 parameters used.

TABLE 7. Density Regressions

$\log N_{LANL} = a + b(\log N_{MIT})$

Year	# Points	a	b	$\sigma_\perp$	1-σ range (N)
1977	4465	.09	.92	.04	2.7 to 41 cm^{-3}
1978	2267	.07	.94	.04	1.3 to 150
1979	2213	.10	.90	.05	2.8 to 57
1980	1938	.05	.85	.06	0.6 to 7.9
1981	1575	.08	.82	.07	0.8 to 9.6
1982	1235	.18	.85	.05	5.1 to 51
1983	2400	.15	.90	.04	10 to 145
1984	1616	.18	.87	.03	12 to 55
1979-198	10,977	.09	.91	.07	0.9 to 110

$\log N_{IMP} = a + b(\log N_{ISEE1})$

Year	IMP Instrument	# Points	a	b	$\sigma_\perp$	1-σ range (N)
1977	LANL	655	.24	.77	.08	3.6 to 30
1978	LANL	635	.14	.92	.09	1.7 to 1200
1979	LANL	525	.16	.88	.10	1.5 to 320
1977-1979	LANL	1815	.18	.85	.09	2.3 to 110
1977	MIT	461	.19	.84	.06	4.6 to 54_{14}
1978	MIT	859	.06	.99	.07	10^4 to 10^{14}
1979	MIT	921	.04	.98	.07	10^{-4} to 10^8
1977-1979	MIT	2241	.07	.96	.07	.2 to 10^4

$\log N_{IMP} = a + b(\log N_{ISEE3})$

Year	IMP Instrument	# Points	a	b	$\sigma_\perp$	1-σ range (N)
1978	LANL	815	.19	0.85	.09	3.6 to 136
1979	LANL*	1148	.16	0.88	.07	2.8 to 164
1980	LANL*	1817	.07	0.83	.10	0.4 to 16
1981	LANL*	1605	.05	0.85	.09	0.3 to 15
1982	LANL*	1177	.14	0.82	.07	1.8 to 18
1980-1982	LANL*	4599	.06	0.85	.09	0.4 to 20
1978-1980	MIT	5008	.09	0.93	.07	0.9 to 740
1979	MIT*	1896	.05	0.99	.06	10^{-4} to 10^{11}
1980	MIT*	3097	.00	0.99	.09	10^{-20} to 10^{20}
1981	MIT*	2794	.01	0.96	.07	.01 to 660
1982	MIT*	1930	-.09	1.02	.09	.07 to 10^7
1979-1982	MIT*	9717	.00	0.98	.08	10^{-5} to 10^5

*Electron-based ISEE 3 parameters used.

TABLE 8. Temperature Regressions

$\log T_{LANL} = a + b(\log T_{MIT})$

Year	# Points	a	b	$\sigma_\perp$	1-σ range (T)	
1977	4465	-.77	1.15	.07	2.0×10^4 to 4.6×10^5	°K
1978	2267	-.75	1.16	.10	8.3×10^3 to 6.6×10^5	
1979	2213	-.87	1.18	.09	1.5×10^4 to 3.9×10^5	
1980	1938	-1.14	1.24	.10	1.3×10^4 to 1.9×10^5	
1981	1575	- .43	1.11	.11	3.5×10^2 to 3.7×10^5	
1982	1235	.25	0.96	.10	7.1×10^2 to 4.5×10^9	
1983	2400	- .72	1.15	.09	1.0×10^4 to 5.3×10^5	
1984	1616	- .04	1.02	.08	5.0×10^{-5} to 1.3×10^9	
1979-1984	10,977	- .62	1.13	.10	4.4×10^3 to 5.2×10^5	

$\log T_{IMP} = a + b(\log T_{ISEE1})$

Year	IMP Instrument	# Points	a	b	$\sigma_\perp$	1-σ range (T)
1977	LANL	655	.21	0.95	.06	1.7×10^2 to 2.1×10^5
1978	LANL	635	.30	0.93	.09	2.0×10^2 to 8.7×10^5
1979	LANL	525	-.97	1.17	.14	3.6×10^4 to 1.2×10^7
1977-1979	LANL	1815	.14	0.96	.11	0.4 to 3.4×10^6
1977	MIT	461	.81	.84	.08	1.8×10^4 to 4.9×10^5
1978	MIT	859	.80	.83	.11	6.3×10^3 to 3.7×10^5
1979	MIT	921	.46	.86	.14	10^2 to 4.6×10^4
1977-1979	MIT	2241	.85	.80	.14	2.5×10^3 to 2.2×10^5

$\log T_{IMP} = a + b(\log T_{ISEE3})$

Year	# Points	a	b	$\sigma_\perp$	1-σ range (T)
1978-1980	5008 (MIT)	-.06	1.04	.08	.02 to 1.6×10^5
1978	815 (LANL)	.34	0.94	.06	3.3×10^4 to 2.2×10^7

Cross-comparisons of ISEE 1 with either IMP instrument were performed on a fairly small number of points. Thus the significance of the year-to-year variations is not easily determined. Chaining the IMP(LANL)-IMP(MIT) with the IMP(MIT)-ISEE 1 equations yields results consistent with the direct IMP(LANL) ISEE 1 equations for both densities and temperatures. Temperatures will not be normalized since the 1977-1979 regression parameters do not differ significantly from Y=X. We do normalize ISEE 1 density as indicated in Table 9.

A cross-comparison of ion-based ISEE 3 densities with IMP(MIT) densities was done for 1978 through day 48, 1980 (Table 7). Similar regression parameters are obtained when ISEE 3 electron-based densities are used for 1979.

The IMP(LANL) ISEE 3 density regression parameters for 1979 and 1982 lie within a 1-σ range of the normalization used in Supplement 2 (log N_{LANL} = .20 + .83 log $N_{ISEE\ 3}$). However, 1980 and 1981 IMP(LANL) ISEE 3 regression parameters have a different character. The regression line appears to be lowered in a similar manner to that found from the IMP(LANL)-IMP(MIT) cross-comparison. Since IMP(MIT) ISEE 3 regression parameters do not exhibit any anomalies for 1980 and 1981, we assume that any instrumental time variability is in the IMP(LANL) instrument. Thus we normalize all IMP(MIT) and ISEE 3 densities using the same relation that was used in Supplement 2. As explained earlier, IMP(MIT) parameter values are selected preferentially over IMP(LANL) values when both are available for any given hour. Because of this, there is only a small number (~300) of 1980-1981 hours having IMP(LANL) data.

To further support the ignoring of time variations in the normalizations, we depict in Figure 12 the yearly averages of the densities, velocities, and temperatures for the two IMP plasma instruments. These averages are based on the overlapping hours listed in the first part of Tables 6, 7 and 8. Velocities agree quite closely. Average temperatures are not as close, but LANL temperatures are consistently higher than MIT temperatures. The average LANL densities are lower than MIT densities for 1980 and 1981 yet higher for all other years.

Table 9 summarizes the normalizations used in this book.

TABLE 9. Normalization Parameters for N and T

$P_{NORM} = a + b\ P_{DS}$

	P = log N		P = log T	
DS	a	b	a	b
IMP-LANL	0	1.00	0	1.00
IMP-MIT	.12	0.89	-.62	1.11
ISEE 3	.20	0.83	-.55	1.07
ISEE 1	.18	0.85	0	1.00

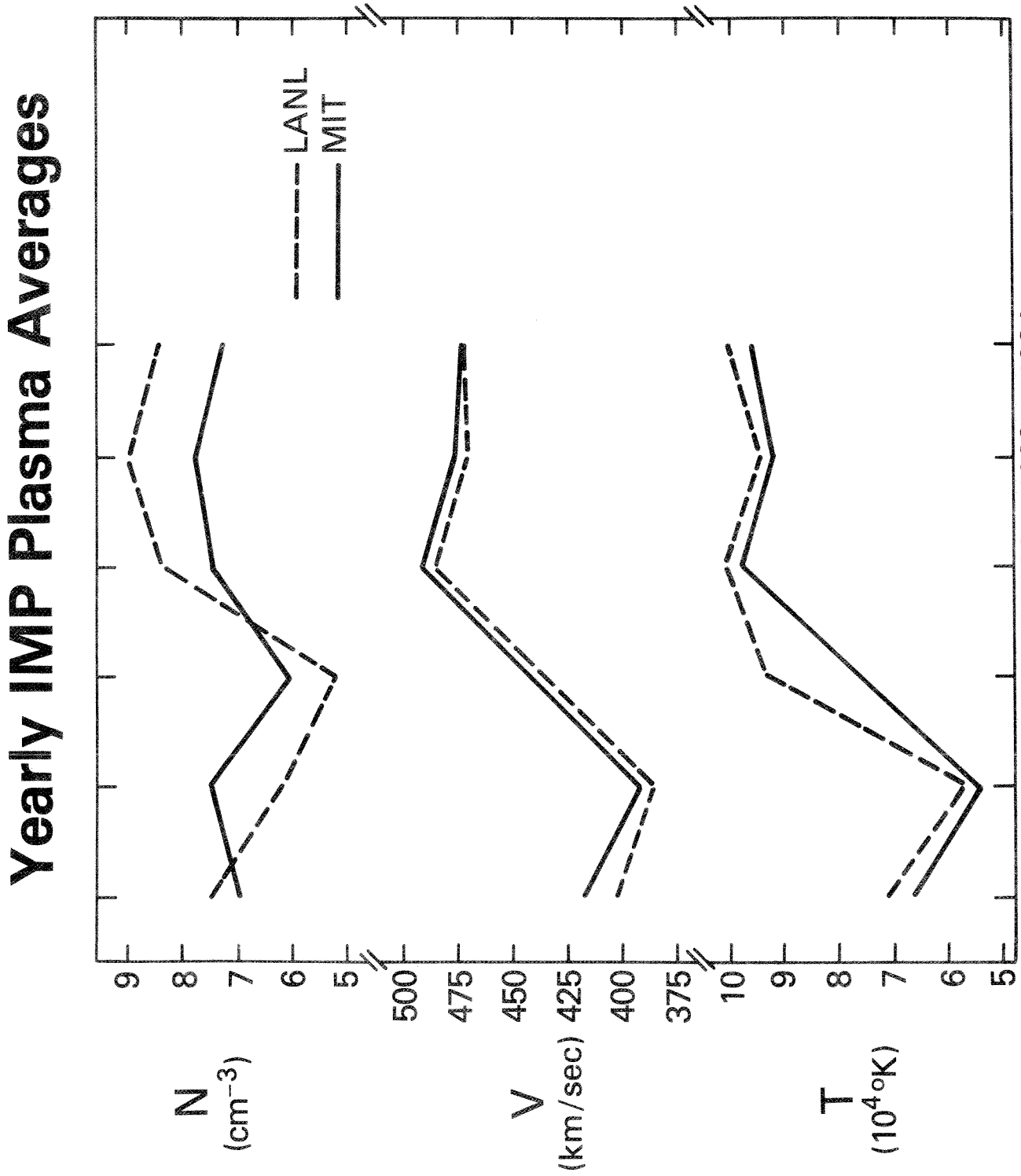
Yearly IMP Plasma Averages
LANL
MIT
N
(cm^{-3})
V
(km/sec)
T
(10^4°K)
1979
1980
1981
1982
1983
1984

Figure 12

Data Coverage

The percent of coverage of the composite data set over the 1963 to 1985 time period is shown in Figure 13. Of the 188,568 hours included in Bartels' solar rotations 1783 to 2073, there are 98,771 hours with field and plasma data of which 72,548 hours have field and plasma data from a common spacecraft, 22,031 hours with field data only, 24,960 hours with plasma data only, and 42,806 hours with no interplanetary plasma or field data.

Data Presentation

This third Data Book Supplement consists of graphical (Volume 3) and tabular (Volume 3A) presentations of some of the parameters of the composite data set. In Volume 3, there are two plots for each solar rotation in which any plasma or field data were obtained. On facing pages, for convenience in lining up features in the data, are found a plot of plasma data (bulk speed, density, and proton temperature) and a plot of field data (average magnitude, geocentric solar magnetospheric (GSM) B_Z component, and geocentric solar ecliptic (GSE) latitude and longitude angles of the average field vector). Note that on those rare occasions when the parameter values exceed the allowed range, a heavy mark is placed near the edge of the plot. For such cases the reader is advised to consult the data listings (Volume 3A) for appropriate numerical values.

Additional Data Availability

In addition to the parameters listed and plotted herein, the data set from which this Data Book Supplement was generated also contains additional IMF parameters (e.g., By, Bz in GSE coordinates), additional plasma parameters (flow direction), standard deviations in IMF and plasma parameters, and geophysical and solar activity indices (Kp, C9, Dst, R).

This data set is available both online, on the NSSDC VAX, and on magnetic tape. The data set is updated as NSSDC receives additional relevant data, at a typical frequency of every several months. New hardcopy Supplements are issued only every few years.

A word on day-numbering conventions is appropriate. When the first OMNItape was created, most input data used the convention that January 1 is Day 0. This convention was employed for the OMNItape, and has been continued for all subsequent tape versions. However, it is recognized that this is a minority convention. Accordingly, the Data Books and the recently created online "OMNIfile" both use the convention that January 1 is Day 1.

In all versions of this data set, missing parameter values are filled with zeros.

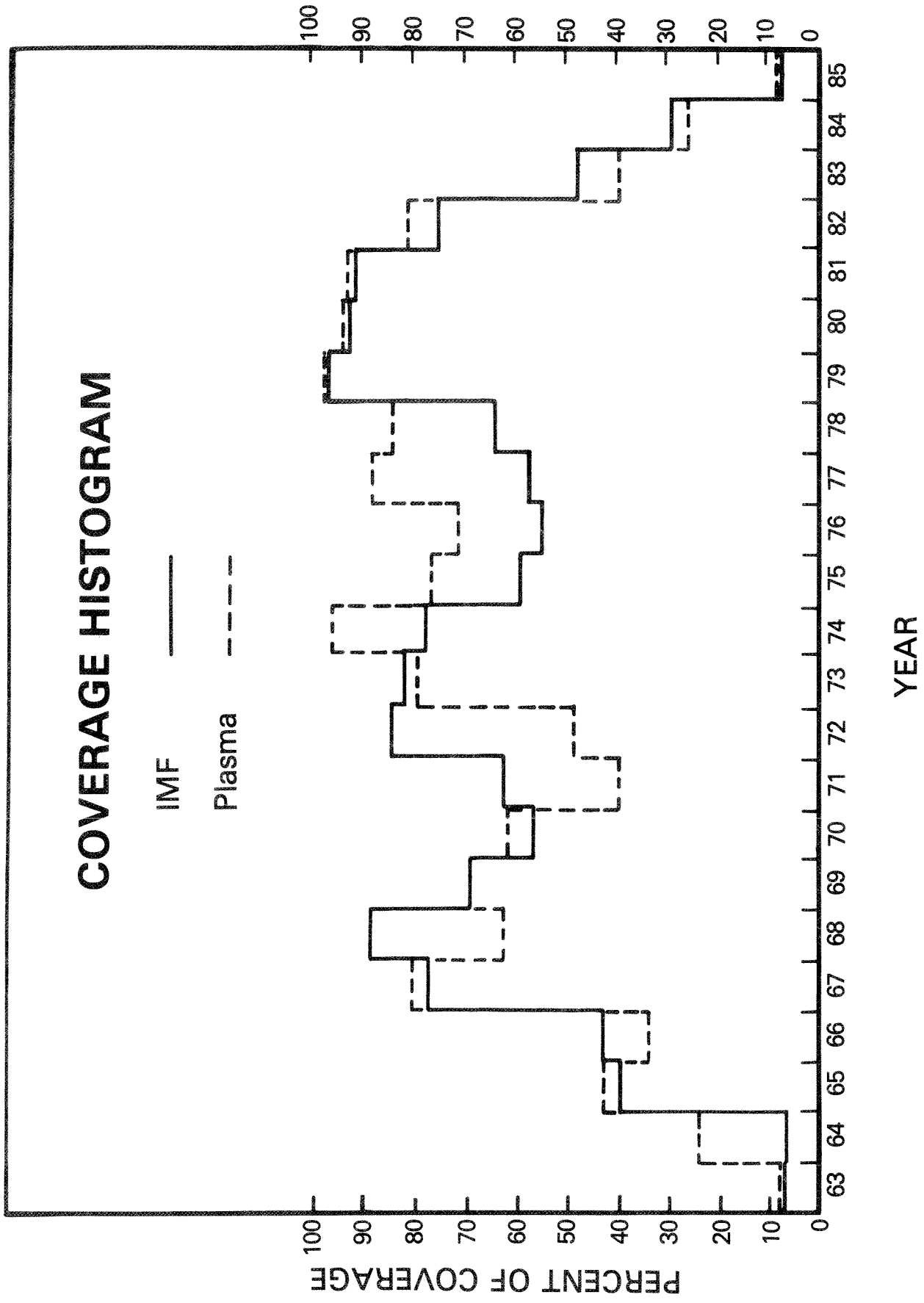
COVERAGE HISTOGRAM
IMF
Plasma
PERCENT OF COVERAGE
YEAR
0
10
20
30
40
50
60
70
80
90
100
63
64
65
66
67
68
69
70
71
72
73
74
75
76
77
78
79
80
81
82
83
84
85

Figure 13

The Online File

The data set is online from 1976 onward. Earlier portions can be brought online in response to demand. The data set may be accessed over SPAN by $SET HOST NSSDC, USERNAME=NSSDC. This interface gives a menu of NSSDC online services, one of which is access to the "OMNIfile." Currently, the user may view the file format and may select and list at his terminal any subset of parameters for any days of interest. Additional capabilities, such as linking to an NSSDC-supplied READ subroutine to read OMNIfile records, and creating a subfile for downloading to the user's VAX, are currently being developed.

The Magnetic Tape

ASCII or IBM/binary magnetic tape versions of the data set from 1963 onward are also available. Copies of either of these tapes (or a reformatted version), with documentation, may be ordered electronically from another menu option of the USERNAME=NSSDC account discussed in the previous paragraph, or by request to:

National Space Science Data Center
Code 633.4
NASA/Goddard Space Flight Center
Greenbelt, MD 20771
Telephone: (301) 344-6695
Telex No.: 89675 NASCOM GBLT
TWX No.: 7108289716

Researchers who reside outside the United States would contact:

World Data Center A for Rockets and Satellites
Code 630.2
NASA/Goddard Space Flight Center
Greenbelt, MD 20771 U.S.A.
Telephone: (301) 344-6695
Telex No.: 89675 NASCOM GBLT
TWX No.: 7108289716

NSSDC NATIONAL SPACE SCIENCE DATA CENTER

WORLD DATA CENTER A for ROCKETS AND SATELLITES 89-17

Interplanetary Medium Data Book—Supplement 4, 1985–1988

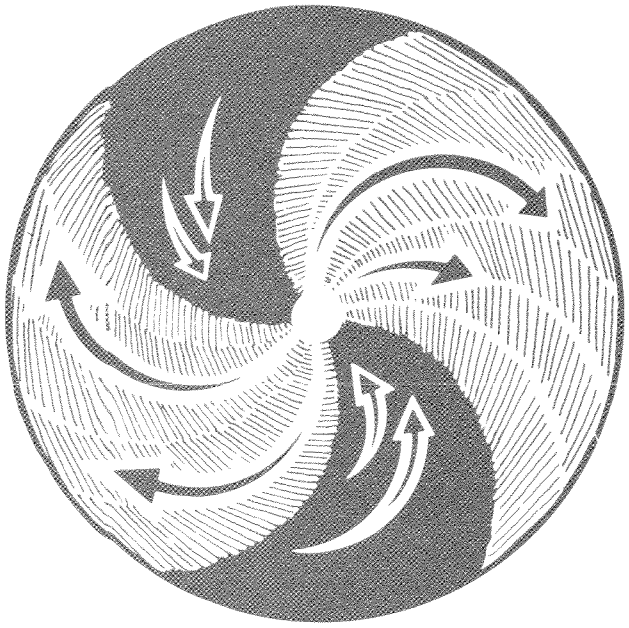

September 1989

NASA
National Aeronautics and Space Administration

Goddard Space Flight Center

NSSDC/WDC-A-R&S 89-17

Interplanetary Medium Data Book—Supplement 4, 1985-1988

By

Joseph H. King

September 1989

National Space Science Data Center (NSSDC)/
World Data Center A for Rockets and Satellites (WDC-A-R&S)
National Aeronautics and Space Administration
Goddard Space Flight Center
Greenbelt, Maryland 20771

Introduction

This publication represents an extension of the series of *Interplanetary Medium Data Books* and supplements that have been issued by the National Space Science Data Center since 1977. This volume contains solar wind magnetic field (IMF) and plasma data from the IMP 8 spacecraft for 1985 through 1988, and 1985 IMF data from the Czechoslovakian/Soviet Prognoz 10 spacecraft (also called Intershock). The normalization of the MIT plasma density and temperature, which has been discussed at length in previous volumes, is implemented as before, using the same normalization constants for 1985-88 data as for the earlier data.

The data books and supplements, all available from NSSDC, are produced from the NSSDC-maintained OMNItape, which now spans 1963-88. The 1973-88 portion of the OMNItape's contents is available on line for electronic browse and access, with time and parameter subsetting capability. (From a SPAN node, SET HOST NSSDCA, then USERNAME=NSSDC, then follow the prompts and menus.)

The plots and listings of this supplement are of the same format as in previous supplements. Days for which neither IMF nor plasma data were available for any hours are omitted from the listings. Note that data source identifiers J and P are used for IMP 8 and for Prognoz 10, respectively.

The figure that follows shows the fractional IMF and plasma data coverage for each year since 1973, the IMP 8 launch year.

Prognoz 10 IMF Data

Prognoz 10 was launched April 26, 1985, into a highly eccentric orbit of apogee 31 Earth radii and orbital period 4.0 days. Its spin axis was maintained within 10 deg of the solar direction, and its spin rate was in the range 1.5 to 2.4 rpm. It was instrumented to measure in situ magnetic fields, waves, plasmas, and energetic particles; its primary scientific objective was the study of interplanetary shocks.

Prognoz 10 provided useful data from launch through November 11, 1985. Overall management of the Prognoz 10 mission was shared between the Astronomical Institute of the Czechoslovak Academy of Sciences and the Space Research Institute of the Soviet Academy of Sciences.

The spacecraft carried a boom-mounted triaxial magnetometer provided by the Principal Investigator, Dr. E. Yeroshenko of IZMIRAN/USSR. In its nonshock mode, the instrument made one measurement of the ambient magnetic field every 10.24 sec; the resolution in each sensor measurement was 0.5 nT. Data processing was carried out by the principal investigator and colleagues, who then provided 10-min averaged magnetic field vectors, for times when Prognoz was in the solar wind, to World Data Center-B2 for

Solar Terrestrial Physics (A. Feldstein, Moscow). These data were sent to NSSDC for dissemination to the U.S. space physics community.

Dr. David Sibeck of the Johns Hopkins University's Applied Physics Laboratory took the 10-min data from NSSDC, determined that a 1.0 nT offset had to be applied to the Bx(GSE) component to obtain consistency with simultaneously measured IMP 8 values of Bx(GSE), applied the offset, computed hourly averages, and provided these data back to NSSDC for inclusion in the OMNItape. Note that the X(GSE) component, being approximately along the Prognoz spin vector, is the least well-determined component, whereas the IMP 8 Bx(GSE) is highly reliable owing to its being normal to the IMP spin vector.

Acknowledgments

The IMP 8 IMF and plasma data were provided by Dr. Ronald Lepping of Goddard Space Flight Center and Dr. Alan Lazarus of the Massachusetts Institute of Technology. The Prognoz 10 data were provided by Dr. E. Yeroshenko of IZMIRAN, through Dr. A. Feldstein of WDC-B2 (Moscow). Dr. David Sibeck of the Applied Physics Laboratory analyzed the consistency of the Prognoz 10 and IMP 8 IMF data, and normalized the former. Howard Leckner of NSSDC has been instrumental in keeping the OMNItape, and its online version, current, and in generating the plots and listings of this supplement. Robert Tice of the NSSDC photo lab and Ronald Blitstein of the NSSDC operations group contributed significantly to the final preparation of this document. Dr. Susan Kayser of NSSDC has also contributed to the OMNItape maintenance since the last supplement was issued in 1986. I thank all these persons for their contributions.

NSSDC
WDC-A-R&S

77-04

National Space Science Data Center/
World Data Center A For Rockets and Satellites

Interplanetary Medium Data Book

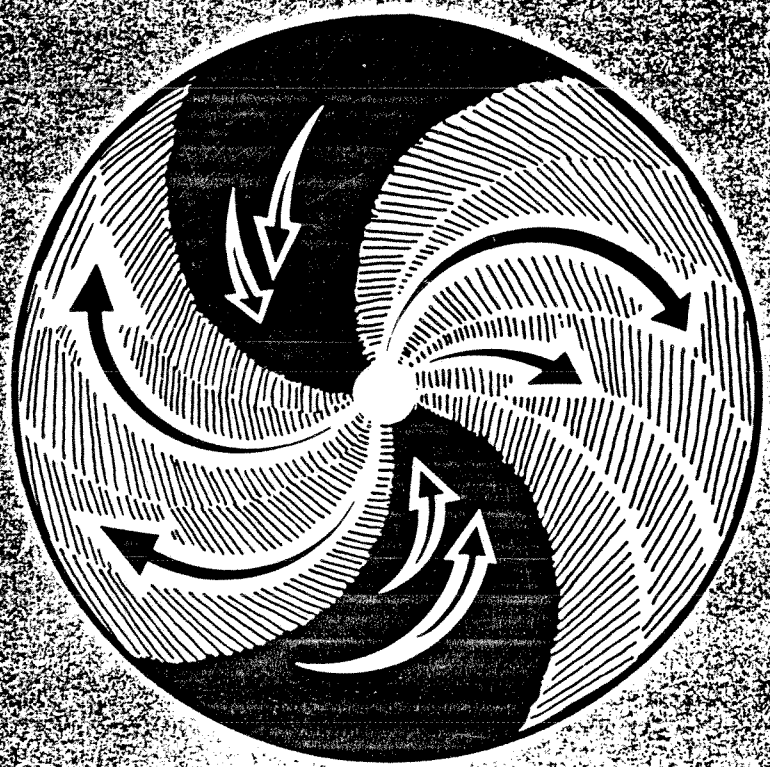

September 1977

NSSDC/WDC-A-R&S 77-04

Interplanetary Medium Data Book

by

Joseph H. King

September 1977

National Space Science Data Center
National Aeronautics and Space Administration
Goddard Space Flight Center
Greenbelt, Maryland 20771

ACKNOWLEDGMENTS

The skilled efforts of a great many individuals were required to make this Data Book a reality. These individuals include those involved in the conception, design, and construction of the spacecraft and of the plasma and magnetic field detectors with which the data were obtained; those involved in the data acquisition, reduction, and analysis phases during which sensor outputs were transformed into reliable, physically meaningful information; and those involved in the actual generation of this Data Book.

Those people particularly helpful in supplying data and suggestions include: S. J. Bame, W. C. Feldman, J. T. Gosling, and J. R. Asbridge of the Los Alamos Scientific Laboratory (LASL); H. S. Bridge, A. J. Lazarus, and J. D. Sullivan of the Massachusetts Institute of Technology (MIT); M. Neugebauer of the Jet Propulsion Laboratory (JPL); N. F. Ness, K. W. Ogilvie, D. H. Fairfield, K. W. Behannon, R. P. Lepping, and L. F. Burlaga of the Goddard Space Flight Center (GSFC); and P. C. Hedgecock of the Imperial College, London.

Acknowledgements are also due to L. Svalgaard of Stanford University for his contribution to the section, "IMF Vector Standard Deviation," and to C. T. Russell of the University of California at Los Angeles (UCLA) who transformed the interplanetary magnetic field (IMF) data of the earlier composite data set from geocentric solar ecliptic (GSE) to geocentric solar magnetospheric (GSM) coordinates and who provided to the National Space Science Data Center (NSSDC) camera-ready plots and listings of these GSM data at a time when a GSM IMF Data Book was under serious consideration. (Since this *Interplanetary Medium Data Book* contains GSM IMF data, the need for a separate GSM IMF Data Book is eliminated.)

Many of my colleagues at NSSDC have provided valuable assistance, suggestions, and encouragement. These include S. G. Morris and E. A. Scarzafava who performed a number of the required data mergings and who generated the listings and 27-day plots, D. V. Reames who set up the GSE/GSM transformations, and J. Kubica and M. J. Teague who generated the scatter plots.

INTRODUCTION

Many unresolved questions on the physics of the solar wind and its effects on magnetospheric processes and cosmic ray propagation can be addressed with hourly averaged interplanetary plasma and magnetic field data. A wealth of such data has been accumulated for almost two decades. Recently, much of these data have been assembled onto a single magnetic tape available from NSSDC.

The purposes of this report are: (1) to describe this composite data set - its content and extent, its sources, its limits of validity, and the mutual consistency studies and normalizations to which the input data were subjected, and (2) to present in the form of digital listings and 27-day plots hourly (or 3-hourly) averaged parameters. The listings are contained in the separately bound Appendix to this Data Book.

DATA CONTENTS AND COVERAGE

The composite data set contains: (1) interplanetary magnetic field (IMF) vector data in geocentric solar ecliptic (GSE) and geocentric solar magnetospheric (GSM) coordinate systems, (2) interplanetary plasma parameters, and (3) geomagnetic (K_p and C_9) and solar (sunspot number R) activity indexes. The interplanetary field and plasma data were all obtained by spacecraft in geocentric or selenocentric orbit when those spacecraft were outside the Earth's bow shock. The identifications of interplanetary periods for these spacecraft were made by the experimenters who supplied the data to NSSDC; these identifications are occasionally difficult to make. The geomagnetic and solar activity indexes were taken from a compilation prepared and periodically updated by the European Space Agency's European Space Operations Center and are described in *Lenhart* (1968).

The field parameters consist of field magnitudes, cartesian components, direction angles, and certain standard deviations. The plasma parameters consist of bulk flow speed (V), proton density (N), proton temperature (T), flow direction longitude (ϕ_V) and latitude (θ_V), and certain standard deviations (σ). As is detailed below, not all the plasma parameters were contained in each source data set. Thus, for some hours of the composite data set, only a subset of the identified plasma parameters are given.

The basic unit of time for the composite data set is 1 hour. All field data and much plasma data were available in the form of hourly averages. For those source plasma data sets, identified below, in which only 3-hour values are available, the 3-hour values were assigned to each of the 3 hours of the averaging interval. The 3-hour K_p index and the daily C_9 and R indexes were treated similarly. For example, a given value of C_9 is repeated in 24 successive hourly records on the composite magnetic tape.

Although the details of data merging are given later, it is useful to note here the general outline of the procedure followed. All the source plasma data sets were combined onto a single, time-ordered magnetic tape. For any hour, there were data given separately from up to five sources. A similar composite IMF tape was also generated, with separate data from up to three spacecraft for each hour. A normalized composite plasma tape was generated from a slightly edited version of the tape with the unnormalized experimenter-supplied data. The composite IMF tape, the normalized composite plasma tape, and the tape containing the solar and geomagnetic activity indexes were merged to yield the final composite tape. The plasma parameters contained on the final tape for a given hour were selected from one of the possibly several sources available for that hour. Field parameters were selected in a similar manner. Each of the tapes involved in the preparation of the final composite tape is available from NSSDC.

The percent of coverage of the composite data set over the 1963 to 1975 time period is shown in Figure 1 for each Bartels' solar rotation number. Of the 106,920 hours included in Bartels' solar rotation 1783 to 1947, there are 45,399 hours with field and plasma data of which 23,613 hours have field and plasma data from a common spacecraft, 19,755 hours with field data only, 15,779 hours with plasma data only, and 25,987 hours with no interplanetary plasma or field data. The time intervals of field and plasma data are Nov. 27, 1963, to Oct. 28, 1975, and Nov. 27, 1963, to Dec. 30, 1975, respectively. Of the 61,178 hourly records with plasma data, 29,160 records actually contain 3-hour averages. It is contemplated that this composite data set will be updated as additional data become available.

DATA SOURCES

General

All the source spacecraft used in compiling this composite data set are identified in Table 1 in chronological sequence. Each spacecraft is assigned a numeric and an alphabetic identifier. The numeric identifier represents how a given spacecraft is specified on the magnetic tape and in tables and figures in this document. The alphabetic identifiers are used in the listing found in The Data Book Appendix. In Table 1, it is indicated whether plasma and/or field data from a given spacecraft are used in this compilation.

Plasma Data

The 11 source data sets from which the plasma data of the new composite data set were obtained are listed in Table 2. For each source data set, the spacecraft, the principal investigator and his institution, the averaging interval, the time span, the number of hours on the final

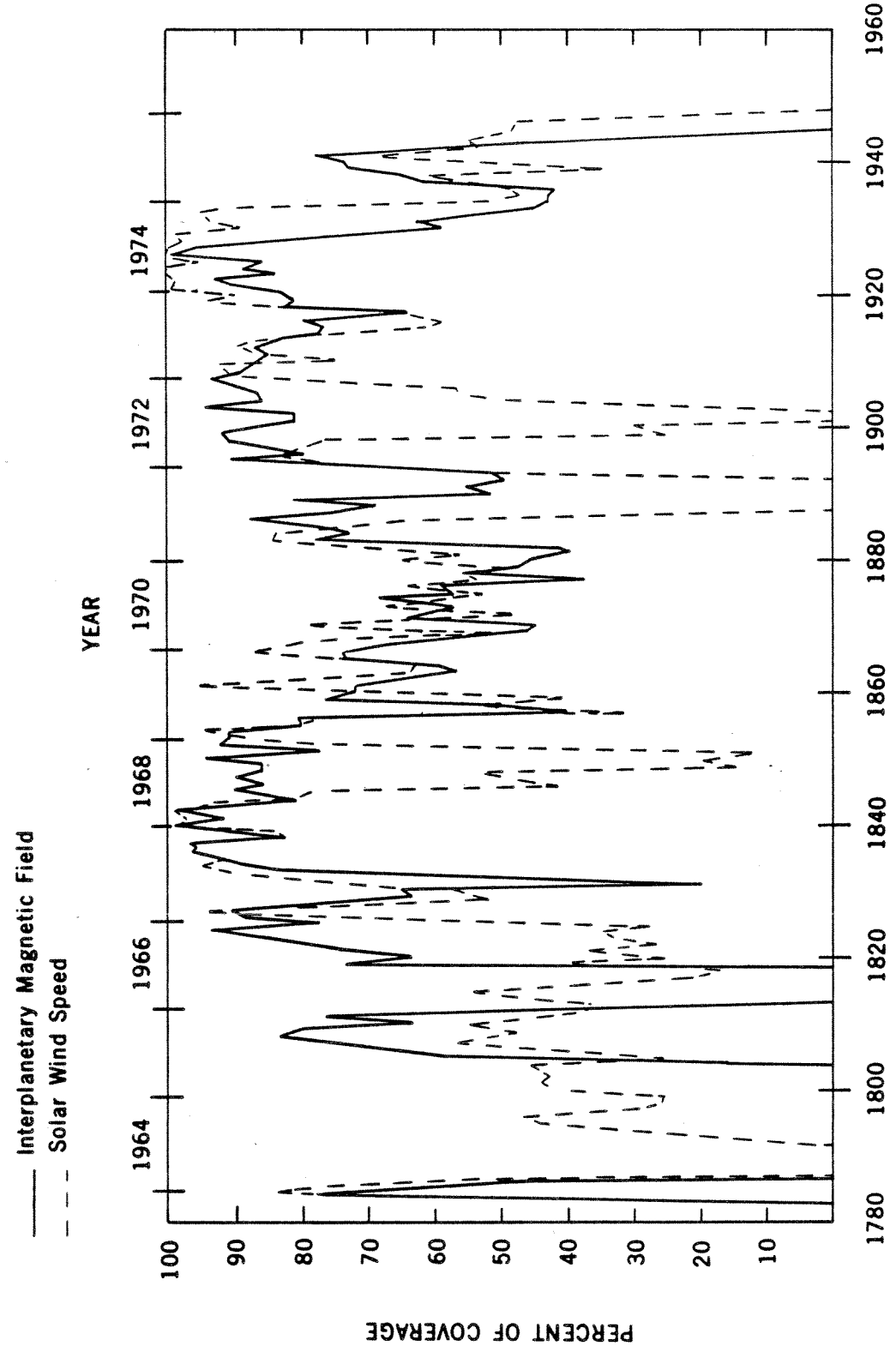

Figure 1. Composite Data Set Temporal Coverage

Table 1. Spacecraft Providing Interplanetary Medium Data

Spacecraft	Numeric Identifier	Alphabetic Identifier	Plasma Data	Field Data
Explorer 18 (IMP 1, IMP A)	18	A	X	X
Merged Vela (Vela 2-6)	99	V	X	
Vela 3	3	V	X	
Explorer 28 (IMP 3, IMP C)	28	C		X
Explorer 33 (AIMP 1, IMP D)	33	D	X	X
Explorer 34 (IMP 4, IMP F)	34	F	X	X
Explorer 35 (AIMP 2, IMP E)	35	E	X	X
OGO 5	5	O	X	
HEOS	1	X	X	X
Explorer 41 (IMP 5, IMP G)	41	G		X
Explorer 43 (IMP 6, IMP I)	43	I	X	X
Merged IMP (IMP 6-8)	98	L	X	
Explorer 47 (IMP 7, IMP H)	47	H		X
Explorer 50 (IMP 8, IMP J)	50	J	X	X

Table 2. Source Plasma Data Set Characteristics

Spacecraft	P.I. (Institution)	Averaging Time (Hours)	Time Period	Number of Hours	T	N	V	ϕ_V	θ_V	σ_T	σ_N	σ_V	σ_ϕ	σ_θ
Explorer 18	Bridge (MIT)	3	11/27/63 - 2/22/64	1,485		20%	10%							
Merged Vela	Bame (LASL)	3	7/21/64 - 3/18/71	10,273			X							
Vela 3	Bame (LASL)	3	7/26/65 - 11/13/67	5,721	10%	25%	5%	1.6°		X	X	X	X	
Explorer 33	Bridge (MIT)	1	7/6/66 - 9/23/69	5,637	X	X	X	X	X	X	X	X	X	X
Explorer 34	Ogilvie (GSFC)	1	6/3/67 - 12/16/67	2,282	X	10%	3%			X	X	X		
Explorer 35	Bridge (MIT)	1	7/28/67 - 7/3/68	3,642	X	X	X	1.5°	.75°	X	X	X	X	X
OGO 5	Neugebauer (JPL)	1	3/5/68 - 4/29/71	2,564	15%	8%	1%	X	X					
HEOS 1	Bonetti (CNR, Italy)	3	12/11/68 - 4/15/70	3,142		X	X							
Explorer 43	Bame (LASL)	1	3/18/71 - 3/27/73	7,998	X	X	X							
Merged IMP	Bame (LASL)	3	3/18/71 - 12/31/74	8,539	15%	30%	2%							
Explorer 50	Bridge (MIT)	1	12/1/73 - 12/30/75	9,895	X	X	X	X	X	X	X	X	X	X

composite tape, and an identification of which plasma parameters were available are shown. The Vela 3 data set is a composite of data from the Vela 3A and Vela 3B satellites. The sources listed as Merged Vela and Merged IMP refer to data sets, generated by the LASL plasma physics team, that contain data from Velas 2, 3, 4, 5, and 6, and Explorers 43, 47, and 50 (IMPs 6, 7, and 8), respectively. Because the LASL Explorer 43 data set has a time resolution of 1 hour, it has been used (after normalizing densities and deleting some suspicious hours) rather than the 3-hour resolution Merged IMP data set, when possible. However, LASL personnel have normalized and edited their Explorer 43 data and have folded them into the Merged IMP data set.

Note that an "X" is used in Table 2 to indicate the availability of some parameters, while, for others, estimates of uncertainties found in the literature are given. During a discussion of the mutual consistency studies carried out in assembling this composite data set, questions of the levels of reliability of various parameters will be further discussed.

The number of hours, listed in Table 2, that each source data set contributes to the final composite data set is only a fraction of the available hours for that source data set. The fraction depends on the data selection priority scheme (discussed later) and the availability of simultaneous data. The fraction ranges from 40 percent for the Merged IMP set to 100 percent for the Explorer 18 and 50 sets.

The bulk plasma parameters of each source data set were determined by each experimenter group by averaging over fine-time scale values of these bulk parameters. (The number of such values contributing to each hourly or 3-hourly average is given on the final composite tape for all source data sets except those from Explorers 18 and Merged IMP.) Fine-time scale bulk parameters were derived from the spectral and directional distributions of sensor outputs along with sensor calibration information. An assumption of the nature of the governing particle distribution function (e.g., convected isotropic Maxwellian distribution) was also made. Generally speaking, fine-time scale plasma parameter derivation has improved with time as spacecraft telemetry rates have increased, thereby permitting improved temporal, spectral, and directional resolution of sensor outputs.

Because each experimental group providing data has generally used the same instrumentation repeatedly and the same parameter derivation technique, the following discussion is of the data sources grouped by institution.

All the Massachusetts Institute of Technology (MIT) data have been obtained with modulated grid split-collector Faraday cups. The basic theory of these instruments is discussed in *Bridge et al.* (1960). In the derivation of the parameters, it was assumed that the governing distribution was a convected isotropic Maxwellian or a convected isotropic Kappa

distribution. The latter distribution is a variation of the former with a high energy tail. The Explorer 18 measurement sequence and some key results are discussed in *Bridge et al.* (1965), *Olbert* (1968), and *Egidi et al.* (1969). Explorer 33 details are given in *Lyon et al.* (1968), while Explorer 35 details are given in *Lyon et al.* (1967). For a discussion of the flow direction angle determination from Explorers 33 and 35, see *Egidi et al.* (1977).

All the Los Alamos Scientific Laboratory (LASL) data have been obtained using hemispherical electrostatic analyzers for energy-per-charge selection and an electron multiplier for particle counting. Typically, a convected bi-Maxwellian distribution has been assumed in the bulk parameter derivation. The single temperature contained in the LASL-supplied data sets is related to the perpendicular and parallel temperatures according to $T = 1/3(T_{\|} + 2\ T_{\perp})$. Further details on the LASL instruments and data are given in *Hundhausen et al.* (1967), *Gosling et al.* (1967), *Bame et al.* (1967) and *Hundhausen et al.* (1970) for Velas 2 and 3; *Montgomery et al.* (1970) and *Hones et al.* (1972) for Vela 4; *Bame et al.* (1971) for Velas 5 and 6; *Feldman et al.* (1973) for Explorer 43; and *Asbridge et al.* (1976) for Explorers 47 and 50. Discussions of the Merged Vela and IMP data sets are found in *Gosling et al.* (1976) and *Feldman et al.* (1976).

The Goddard Space Flight Center (GSFC) Explorer 34 plasma instrumentation consisted of a curved plate electrostatic analyzer for energy-per-charge selection, followed by a crossed electric field/magnetic field device (Wein filter) for velocity selection, followed by a particle counter. Plasma parameters were derived by taking moments of the observed distribution function. Further details on the instrumentation and data analysis are found in *Ogilvie et al.* (1968a), *Oglivie et al.* (1968b), and *Burlaga and Oglivie* (1968).

The Jet Propulsion Laboratory (JPL) OGO 5 plasma instrumentation consisted of a modulated grid Faraday cup and a curved plate electrostatic analyzer. Plasma parameters were determined iteratively by appropriately combining the outputs of the two sunward-looking sensor systems. Details are provided in *Neugebauer* (1970). Because of its greater reliability, the total charge density obtained from the Faraday cup flux, rather than the ion flux inferred from the electrostatic analyzer, is given in the new composite data set. It is of interest to note that, except for the attitude-stabilized OGO 5, all the spacecraft providing plasma data for the new composite data set were spin stabilized.

The Consiglio Nazionale delle Richerche (CNR, Italy) HEOS 1 plasma instrumentation consisted of a hemispherical electrostatic analyzer followed by a Faraday cup. A convected isotropic Maxwellian distribution function was assumed in the plasma parameter derivation. Details are provided in *Bonetti et al.* (1969). *Diodato et al.* (1975) have presented listings of 3-hour averaged bulk speeds and densities from Vela 3, Explorers 33, 34, and 35, and HEOS 1. The listed averages consist of com-

bined data from as many spacecraft as were available for each 3-hour averaging period. Before averaging, the data for each data set were normalized to Vela 3 values, using the results of the *Moreno and Signorini* (19 regression analysis. As input to our composite data set, only those Diodato-listed, 3-hour averages resulting from HEOS 1 only were taken, and they have been denormalized. That is, the inverse of the previously used normalization equations were applied.

Magnetic Field Data

The 10 IMF source data sets are listed in Table 3. All were provided by N. F. Ness and colleagues at GSFC, except the HEOS data set, which is a merged HEOS 1/HEOS 2 data set provided by P. C. Hedgecock of Imperial College, London. All the source data sets consisted of 1-hour averages obtained from fluxgate magnetometer data. All the magnetometers were triaxial except those on Explorers 18 and 28, which were biaxial. All but the Explorers 18 and 28 and HEOS magnetometers were flippable to assist in sensor zero-level determinations. See *Hedgecock* (1975a) for a discussion of zero-level determination in the absence of sensor flip capability. Sensor signal digitization resolution was typically between 0.1 and 0.2 gamma. Estimated upper limits of spacecraft magnetic fields at magnetometer locations (ends of booms) ranged from .5 gamma for early spacecraft to .1 gamma or less for recent spacecraft.

The parameters available in the source data sets consist of hourly averaged field cartesian components in solar ecliptic coordinates, the magnitude and direction angles of the field vector made up by these three average cartesian components, and the averaged field magnitude. For the HEOS data set, hourly averaged direction angles and the standard deviations in the averaged magnitude and direction angles were also given. For the Explorer data sets, standard deviations in the cartesian component averages and, for all but Explorers 33, 34, and 35, in the field magnitude average were also given. Field components in GSM coordinates were computed at NSSDC from GSE components, as will be discussed.

Hourly averaged values were constructed from fine-time scale field values (obtained either by measurement or by averaging yet finer scale data). The fine-time scale was 327 s for Explorers 18 and 28, 48 and 32 s for HEOS 1 and 2, and between 1 and 5 s for the remaining Explorers. The 327-s resolution field magnitudes are the magnitudes of field vectors made up of 327-s averaged cartesian components. Thus, field directional fluctuations with frequencies between 5 s and 327 s will cause Explorer 18 and 28 hourly averaged magnitudes to be somewhat smaller than corresponding averaged magnitudes based on 1- to 5-s resolution magnitudes.

Much of the IMF data of the new composite data set was already presented, in GSE components only, in *King* (1975). The present compilation supersedes that earlier document.

Table 3. Source Magnetic Field Data Set Characteristics

Spacecraft	Time Period	Number of Hours	Reference
Explorer 18	11/27/63 - 2/15/64	1,215	*Ness et al.*, 1964
Explorer 28	5/30/65 - 1/29/67	6,233	*Ness et al.*, 1964
Explorer 33	7/4/66 - 7/13/68	8,032	*Behannon*, 1968
Explorer 34	5/26/67 - 12/27/68	5,888	*Fairfield*, 1969
Explorer 35	7/26/67 - 11/10/69	2,825	*Ness et al.*, 1967
HEOS	12/11/68 - 10/28/75	15,139	*Hedgecock*, 1975b
Explorer 41	6/21/69 - 10/26/72	7,373	*Fairfield and Ness*, 1972
Explorer 43	3/13/71 - 7/21/74	8,690	*Fairfield*, 1974
Explorer 47	9/26/72 - 4/3/73	1,645	*Mish and Lepping*, 1976
Explorer 50	10/29/73 - 8/26/75	8,114	*Mish and Lepping*, 1976

MUTUAL CONSISTENCY

General

In the creation of the composite interplanetary medium data set, we have examined the mutual consistency of the source data sets. For the plasma data, consideration of regression analysis results and visual inspection of corresponding scatter plots yielded normalization equations that were applied to some of the experimenter-supplied parameter values. In this section, the regression analysis used is described and the results are discussed for plasma data and for field data. A series of sample scatter plots, found in the back sections of this document, are discussed, and the plasma parameter normalizations utilized are listed. The limits of accuracy of the various parameters in this composite data set are also discussed.

A linear regression analysis, in which equal random error is assumed in both variables, was applied to the simultaneously determined data of several pairs of spacecraft. See, for example, *Madansky* (1959) for details. This approach was chosen because both data sets do have random error in fact and because the unavoidable chaining of regression equations for spacecraft A/B and B/C to obtain A/C relations is more legitimate with this approach.

This approach is in contrast to the more often used approach that assumes no error in the "independent variable." See, for example, *Neugebauer* (1976) and *Moreno and Signorini* (1973). (The present data have been run through a no-error-in-the-independent-variable regression analysis, and regression parameter values were found that are more nearly similar to those of Neugebauer and of Moreno and Signorini than are the following parameter values.)

In the present analysis, the regression parameters a and b in the equation

$$P_{s1} = a\, P_{s2} + b$$

(where s_1 and s_2 denote the two source data sets, and P identifies the physical parameter) are determined in a way geometrically equivalent to minimizing the sum of squares of perpendicular distances between data points and regression line.

Before proceeding, it should be noted that, although differences between data sets are emphasized in the following discussion, the level of agreement is really very high considering that the data were obtained and processed at different times using differing instrumentation flown on various spacecraft by various principal investigators and their colleagues. The high levels of agreement attest to the skill and care with which the data were acquired and processed.

Plasma Data

The results of the regression runs for the logarithms of temperature and density and for the bulk speed are presented in Figures 2, 3, and 4. Logarithms were chosen for temperature and density because their distributions were more Gaussian than were the linear values of temperature and density. Each figure shows several regression lines and their equations. Also shown for each line is a slope range that would correspond to 95 percent confidence limits in the absence of autocorrelations in the time series being regressed (and to somewhat lower confidence limits in the presence of such autocorrelations). In addition, the root-mean-square perpendicular distance ($\sigma_\perp$) between data points and regression line is listed and is plotted with the center at the position of the average value on the regression line. The number of hours folded into each regression run and the distribution of values found in the composite data set after normalization are also given in these figures.

The slope ranges of these figures make it clear that there is a statistically significant difference from unity in the slope values for many pairs of spacecraft. Further, a regression equation whose slope is consistent with unity, but whose intercept is comparable to or larger than the listed root-mean-square perpendicular distance, is also statistically inconsistent with $y = x$.

The distributions of values in the final composite data set, indicated in Figures 2, 3, and 4, are not identical to the distributions in the determination of any one of the regression lines, but they can be used as measures of the region of parameter space from which the data points were taken and outside of which the regression lines are meaningless. The percentages of hours with temperatures, densities, and bulk speeds lying outside the ranges in Figures 2, 3, and 4 are 0.4, 0.8, and 2.9, respectively.

The hours included in the determination of the regression equations in Figures 2, 3, and 4 were all hours of simultaneous data, regardless of the number of fine-time scale points per hour and regardless of whether a given hourly value was, in fact, a 3-hour average. The difference in regression parameters obtained was examined with the restriction that each hourly average be comprised of at least three fine-time scale values a restriction used by some earlier workers. For most spacecraft pairs there were only negligible changes in the regression parameters; typically 1 to 2 percent in slope and 1 to 10 percent in intercept and in root-mean-square perpendicular distance. However, for regressions of OGO 5 data with Explorers 33 and 35 data, some significant changes resulted. With the three fine-time-scale-points-per-hour restriction, the following equations were obtained

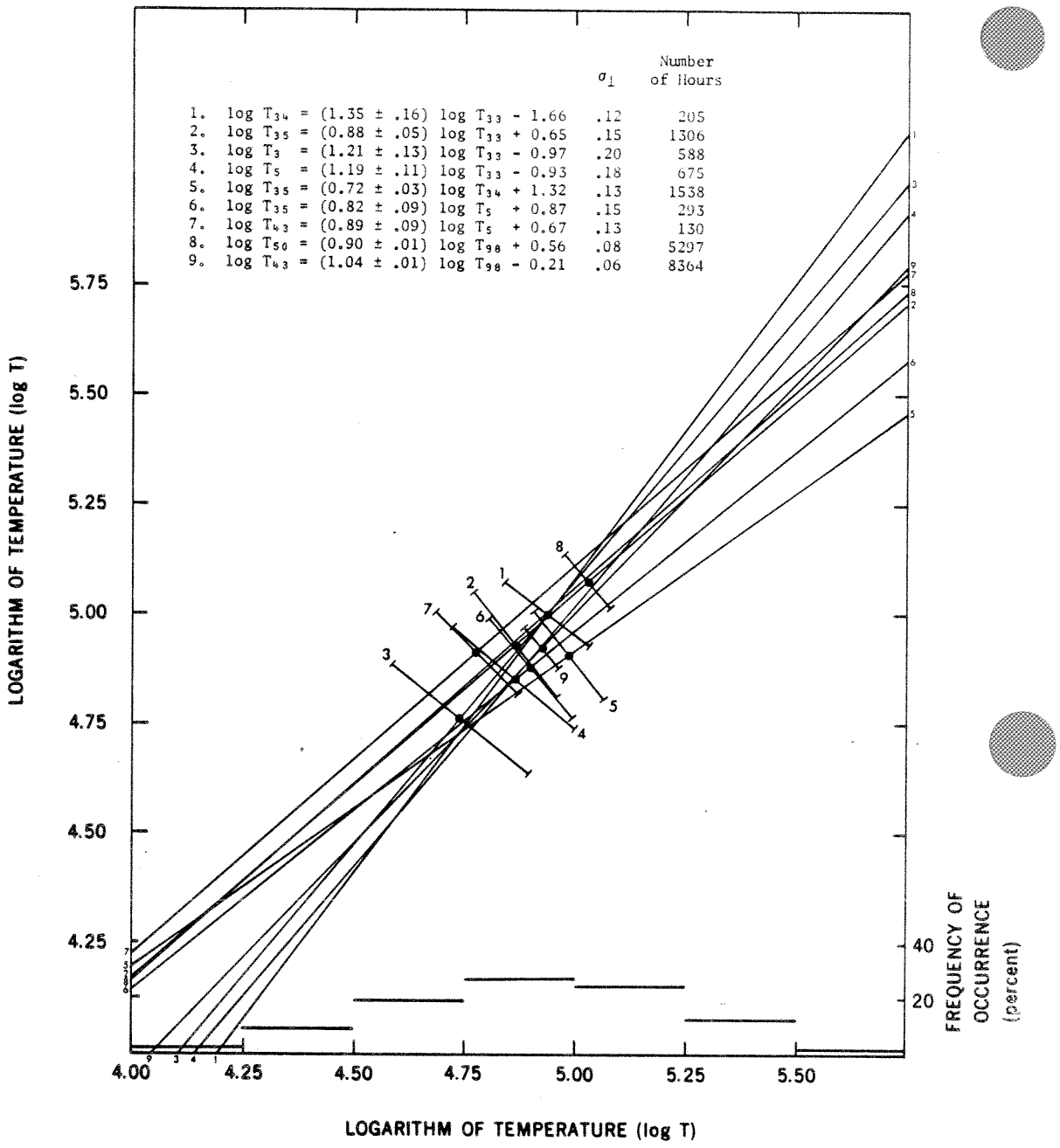

Figure 2. Plasma Temperature Regression Results

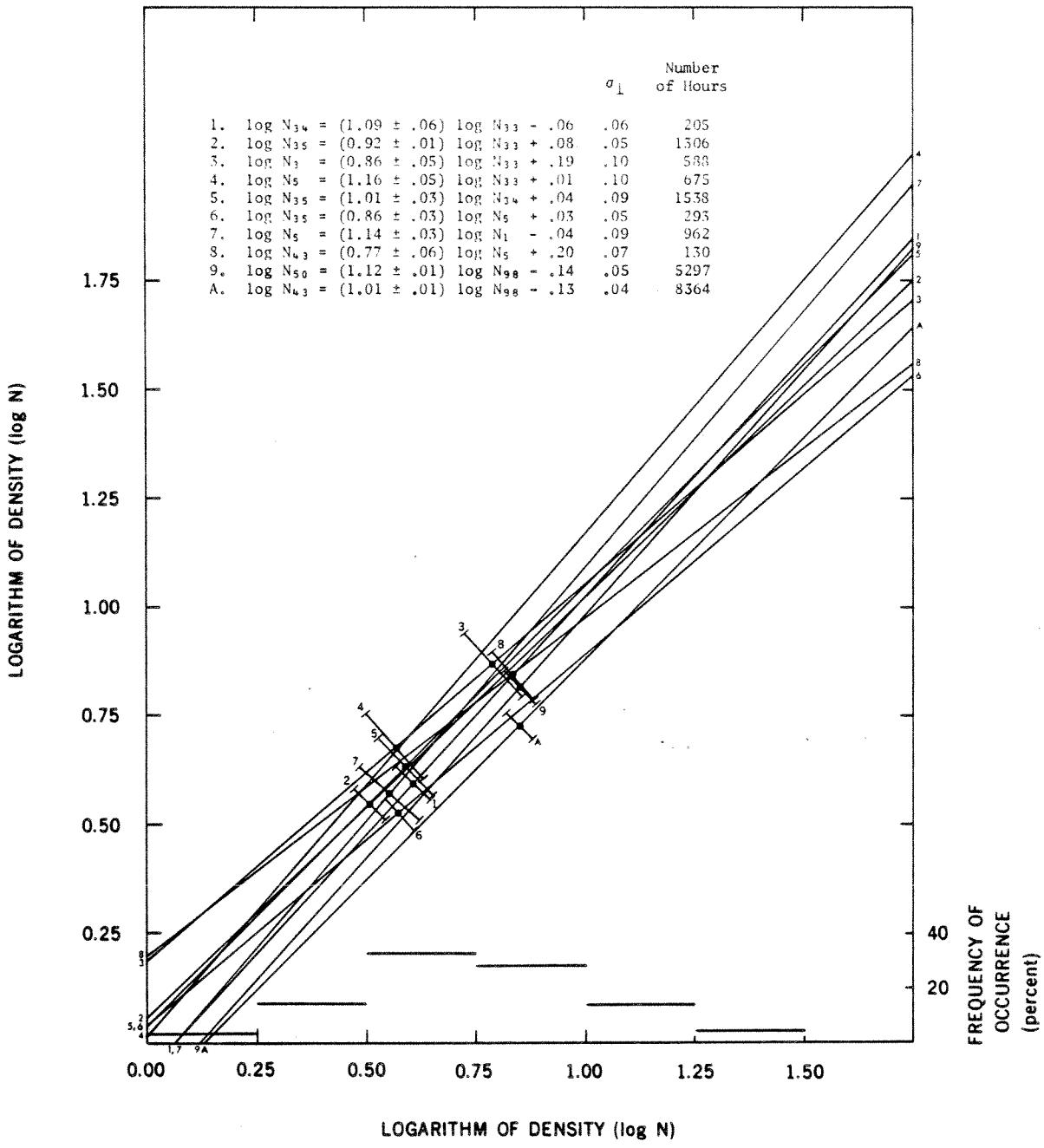

Figure 3. Plasma Density Regression Results

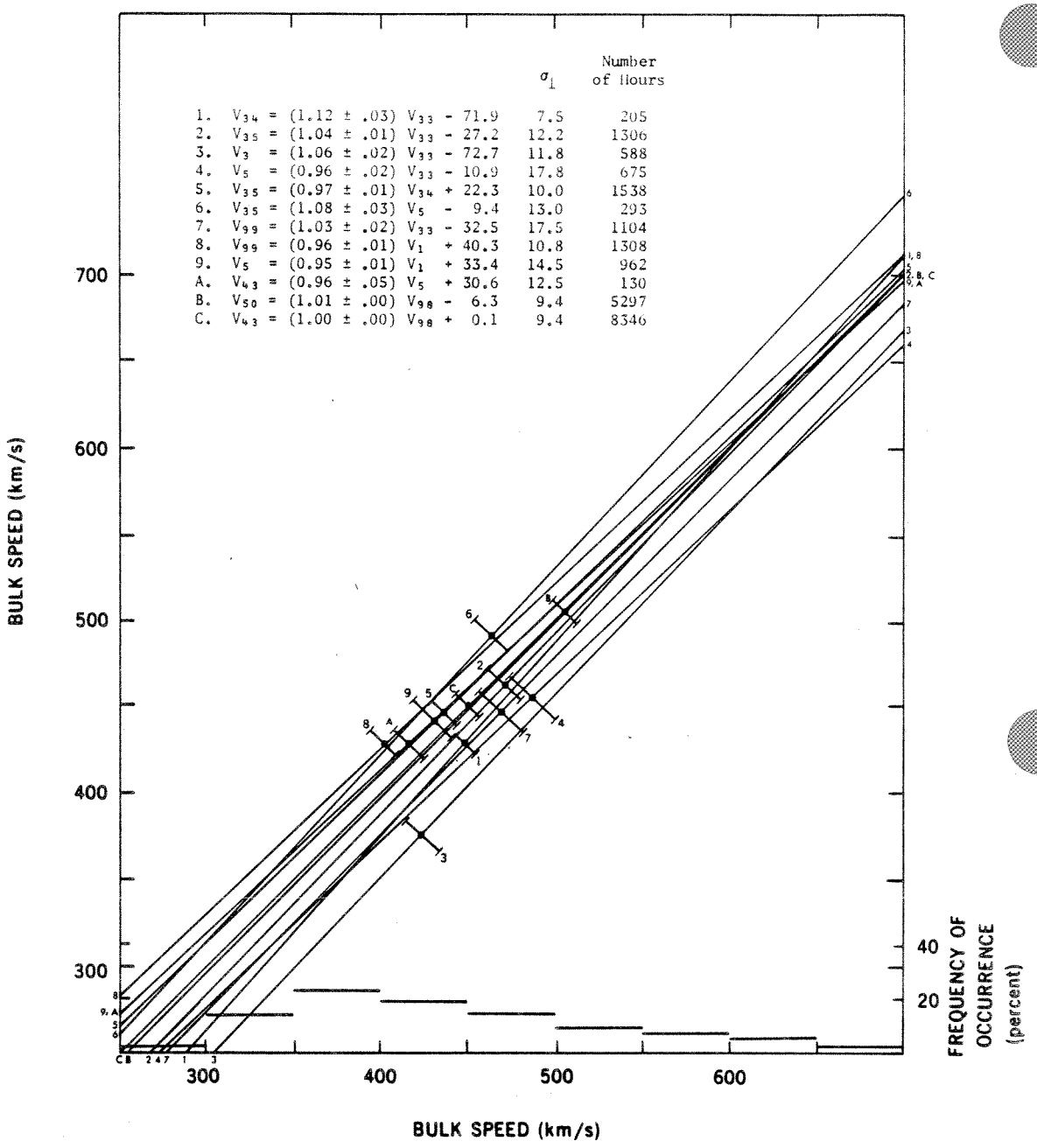

Figure 4. Plasma Bulk Speed Regression Results

		$\sigma_\perp$	Number of Hours
$\log T_5$	$= (1.08 \pm .09) \log T_{33} - 0.37$	0.17	547
$\log T_{35}$	$= (0.91 \pm .10) \log T_5 + 0.45$	0.11	269
$\log N_5$	$= (1.12 \pm .04) \log N_{33} + 0.01$	0.08	547
$\log N_{35}$	$= (0.86 \pm .03) \log N_5 + 0.03$	0.05	269
V_5	$= (1.00 \pm .02) V_{33} - 31.8$	12.7	547
V_{35}	$= (1.08 \pm .03) V_5 - 11.2$	11.4	269

These are to be compared to the appropriate equations in Figures 2, 3, and 4. No significant change in the OGO 5/HEOS regression parameters was found.

Note that no regressions involving flow directions are presented, nor are flow direction angles listed or plotted in this Data Book. This is because such direction angles are given only in a small number of the source data sets (cf. Table 2), and because the potential error of measurement relative to the expected range of flow angles is significantly larger than the relative error in other plasma parameters. Flow direction angles, as received from the experimenters, are found on the magnetic tape from which this Data Book was created.

Scatter plots 1-4, 5-8, and 9-12 are plots for the logarithm of temperature, logarithm of density, and bulk speed, respectively. These correspond to a representative portion of the regression analysis results summarized in Figures 2, 3, and 4. Based on some preliminary scatter plots and other considerations, a modest number (less than 1 percent) of questionable experimenter-supplied data hours from Explorer 34, 35, 43, and 50 were eliminated from the composite data set before the reported regression runs were made.

Note the anomalously low slope in the V_{35} versus V_{34} bulk speed data between about 330 and 380 km/s. This anomaly also occurs in V_{35} versus V_{33} and V_{35} versus V_5 scatter plots (not shown), but in no other scatter plots. The conclusion is that the anomaly is in the Explorer 35 data. No special allowance was made for this apparent Explorer 35 anomaly in creating the composite data set.

Consider the spread of data points about the regression line. This variance may arise from a number of sources related to the instruments, the plasma parameter derivation from sensor outputs, the inadvertent inclusion of averages affected by terrestial or lunar effects, and the solar wind variability itself. This latter effect may be significant insofar as two spacecraft may be measuring at least partly different plasma regimes during a given hour (or 3-hour interval) because of their differing spatial locations and/or their sampling at differing portions of an averaging interval. Recall that two source spacecraft contributing to this composite data set may be separated by a few tens of Earth radii (R_E) in

a solar wind flowing at 200 - 300 R_E/h. This spacecraft separation effect was not accounted for in building the composite data set, a fact that yields a slight "fuzziness" in the very concept of the hourly averaged value of an interplanetary parameter for the Earth. That this effect of solar wind variability is not the dominant cause of data point scatter is suggested by the fact that the point spread for the 50/98 (Explorer 50/Merged IMP) regression lines for all 3 plasma parameters is small relative to the spread for other spacecraft pairs, even though the 50/98 regression involves 1-hour (50) and 3-hour (98) averages.

However, whatever the source of the spread of data points, this spread, rather than quoted errors in individually determined plasma parameters, determines the limits of validity of the composite data set created by interspersing normalized hourly (or 3-hourly) averages from many spacecraft. Based on root-mean-square perpendicular distances between data points and regression lines, as listed in Figures 2, 3, and 4, irreducible uncertainties in temperatures are estimated as $\approx$ 40 percent early ($\lesssim$ 1971) and $\approx$ 20 percent late ($\approx$ 1971), in densities as $\approx$ 20 percent early and $\approx$ 10 percent late, and in speeds as 15 km/s early and 10 km/s late.

Thus, for example, it is estimated that the probability that any given (normalized) early-period temperature value is in error by more than 40 percent is $\approx$ 0.32, which is the probability that a sample point taken from a Gaussian distribution lies more than one σ away from the population mean value.

Having examined the irreducible variance in the composite data set, it is desirable to normalize the source data sets to the extent that a significant improvement in mutual consistency may be achieved. A complicating factor in the attempt to find appropriate normalizations is that there are many pairs of overlapping spacecraft. Each of several of these pairs is not independent of combinations of other pairs. For example, regression analyses have been run for Explorers 33/34, 33/35, and 34/35. These runs involved 205 common 33/34 hours between days 236 - 257 of 1967, 1306 common 33/35 hours between day 236 of 1967 and day 98 of 1968, and 1538 common 34/35 hours between days 205 - 344 of 1967. Combining the 33/34 and 33/35 results (cf. Figures 2, 3, and 4) to infer 34/35 relations and comparing these to the directly obtained 34/35 relations yields reasonable consistency in temperature and bulk speed, but a poor measure of consistency in density.

Inferred	Observed
$\log T_{35} = .65 \log T_{34} + 1.73$	$\log T_{35} = .72 \log T_{34} + 1.32$
$\log N_{35} = .84 \log N_{34} + 0.13$	$\log N_{35} = 1.01 \log N_{34} + 0.04$
$V_{35} = .93 \quad V_{34} + 40.0$	$V_{35} = 0.97 \quad V_{34} + 22.3$

To some extent, this apparent discrepancy may arise from the different time periods over which these data were taken, combined with some un-

detected or inadequately treated temporal dependence in sensor characteristics. Although this possibility is examined in more detail in connection with magnetic fields, temporal variation in sensor characteristics has generally been neglected in this data compilation, with some minor exceptions to be noted later. It is of interest that upon comparing inferred and observed 34/35 relations based on only 166 hours of simultaneously available 33, 34, and 35 data, a high level of consistency was found.

The possibility of seasonal variation in the Explorer 33/35 regressions, which might arise from the fact that the Explorer 33 spin vector lay in the ecliptic plane, was examined. (All subsequently launched Explorer spacecraft used in this compilation had spin vectors normal to the ecliptic plane.) For days 236 - 255 of 1967, and then days 18 - 98 of 1968, it was found that

		$\sigma_\perp$	Number of Hours
1967	$\log T_{35} = (0.89 \pm .06) \log T_{33} + 0.59$	0.15	1061
	$\log N_{35} = (0.91 \pm .02) \log N_{33} - 0.08$	0.05	
	$V_{35} = (1.04 \pm .01) V_{33} - 29.3$	12.8	
1968	$\log T_{35} = (0.67 \pm .10) \log T_{33} + 1.62$	0.11	245
	$\log N_{35} = (1.04 \pm .03) \log N_{33} - 0.02$	0.03	
	$V_{35} = (1.08 \pm .04) V_{33} - 42.1$	8.6	

There are apparently significant changes in these two subsets of the Explorer 33/35 data. Nevertheless, because inspection of the appropriate scatter plots revealed that the 245 data points for 1968 populate a region of parameter space (for each of the three parameters) entirely populated by some of the 1061 points for 1967, the choice was made to neglect seasonal variations in performing plasma parameter normalizations. Further, since the 33/35 regression parameters for all 1306 points of 1967 to 1968 are close in value to the corresponding 33/35 parameters for the 1061 points of 1967 only, it appears that seasonal variation is not responsible for the previously discussed discrepancy in observed and inferred 35/34 regression parameters.

Because of many uncertainties in the analysis (dependence of regression results on data subset used, occurrence of spurious points despite attempts to eliminate such points, possible time dependence in spacecraft and/or sensor characteristics, autocorrelations in time series being regressed, etc.), and because of the need to perform normalizations simultaneously and consistently for many overlapping data sets, it was decided to normalize temperatures and densities only when visually better fits to $y = x$ in scatter plots could be achieved. Bulk speed data have been normalized on the basis of the regression equations in Figure 4, as discussed further below.

The normalized parameter values T_n, N_n, and V_n found in the final composite data set are related to the experimenter-supplied values thr the normalization equations listed in Table 4. Many points deserve no

1. The Explorer 18 densities and speeds overlapped with no other available data and could not be normalized. Their limits of validity, relative to the rest of the data set, is uncertain.

2. The "Merged Vela" speeds were separately considered for periods before and after Jan. 1, 1968, and different normalization equations were chosen.

3. The early data (sources 1, 3, 5, 33, 34, 35, and 99) were normalized independently of the later data (sources 43, 50, and 98). In the later period, the 43 and 50 data were normalized to the 98 data. This separation into early and late data follows from the fact that the only overlap between an early period source and a late period source is the set of 130 OGO 5/Explorer 43 common hours obtained in March and April of 1971. (cf. scatter plots 3, 7, and 11.) Given the smallness of this number of hours, and given the fact that the OGO 5 instrumentation was 3 years postlaunch during these hours, it did not seem justifiable to use the OGO 5/Explorer 43 regression to normalize the early and/or late period data to a common standard. This inability to make a dependable early/late normalization will probably not introduce any gross errors into the study of solar cycle variations with this data set; nevertheless, this point should be kept in mind in such studies.

4. Many speeds have been normalized by relatively small amounts, because reliability in absolute speed values is important for studies attempting to link features at 1 AU with solar features. (Note that a 10 to 15 km/s uncertainty in speed for an ≈400 km/s solar wind yields a solar source longitude uncertainty of 1.4° to 2.1° with the frequently used constant radial velocity approximation.) In the early data ($\lesssim$ 1971), speed normalizations were chosen using the numerous regressions between Explorer 33 and other spacecraft. It was assumed that a weighted average of these equations would yield a relationship between Explorer 33 speeds and "true" speeds and that this relationship could then be used with the Explorer 33/Spacecraft X regression result to yield a relationship between Spacecraft X speeds and "true" speeds.

Table 4. Normalization Equations Used

Spacecraft Identifier	$\log T_n$ =	$\log N_n$ =	V_n =
18	-	$\log N_{18}$	V_{18}
3	$.8 + .83 \log T_3$	$-.222 + 1.16 \log N_3$	$26 + .99 V_3$
99 ($\leq$ '67)	-	-	$26 + .99 V_{99}$
99 ($\geq$ '68)	-	-	V_{99}
33	$\log T_{33}$	$\log N_{33}$	$-44 + 1.05 V_{33}$
34	$1.2 + .75 \log T_{34}$	$\log N_{34}$	$9 + .98 V_{34}$
35	$\log T_{35}$	$\log N_{35}$	$-8 + V_{35}$
5	$\log T_5$	$.9 \log N_5$	$-10 + 1.05 V_5$
1	-	$\log N_1$	$32 + .98 V_1$
98	$\log T_{98}$	$\log N_{98}$	V_{98}
43	$\log T_{43}$	$.097 + \log N_{43}$	V_{43}
50	$-.62 + 1.1 \log T_{50}$	$.121 + .89 \log N_{50}$	V_{50}

5. There was a certain amount of arbitrariness in arriving at the normalization equations given in Table 4. However, for the most part, other reasonable choices of normalization parameters would lead to normalized parameter values different from the values obtained by amounts less than the previously discussed intrinsic uncertainties in the composite data set. Nevertheless, the composite unnormalized solar wind tape is available from NSSDC if the reader wishes to make a different normalization.

Magnetic Field Data

The regression analysis results for the interplanetary magnetic field data are given in Tables 5 and 6. The notation follows from an equation of the form

$$P_{s1} = a\, P_{s2} + b,$$

where P denotes the parameter, s_1 and s_2 identify the two spacecraft, and a is the slope and b is the intercept. Note that slope values are given with limits that would correspond to 95 percent confidence limits in the absence of autocorrelations and which, given the presence of some autocorrelations, in fact correspond to somewhat lower confidence limits. The column labeled $\sigma_\perp$ gives the root-mean-square perpendicular distance between data points and the "best fit" regression line. Table 5 relates to field cartesian components (solar ecliptic coordinates), and Table 6 relates to the average field magnitudes and to direction angles derived from averaged cartesian components.

The units of the b and $\sigma_\perp$ columns are gammas and degrees, as appropriate. In selecting hourly averages for analysis, no restriction on the minimum number of fine-time scale points per hour was imposed. That there are fewer hours in the field longitude regression equation determination than for other parameters results from the exclusion of hours when $|\phi_{s1} - \phi_{s2}| > 180°$. (Such hours of, for example, $\phi_{s1} \approx 10°$ and $\phi_{s2} \approx 350°$ are appropriate for inclusion in regression analysis for other parameters; that such hours were not included in the ϕ regression, with ϕ_{s1} set equal to 370° in the example given, is expected to introduce no bias in the ϕ regression results.)

Scatter plots 13-27 correspond to selected regression runs in Table 5. From inspection of this table and those figures, several points may be made:

1. The slopes are different from unity by several percent in many cases. This implies errors of several percent in effective sensitivity factors in one or both spacecraft involved (*King and Ness*, 1977). There is no unique and con-

Table 5. Regression Results for Field Cartesian Components

$$P_{S1} = a\, P_{S2} + b$$

S1	S2	Number of Points	P	a	b	$\sigma_\perp$
28	33	1183	B_x	1.00 ± .02	0.16	0.99
			B_y	0.93 ± .02	-0.02	1.05
			B_z	1.04 ± .06	-0.05	1.55
34	33	1497	B_x	0.94 ± .02	0.03	0.83
			B_y	0.96 ± .01	-0.03	0.77
			B_z	0.97 ± .03	0.10	0.97
33	35	3040	B_x	1.09 ± .01	0.01	0.75
			B_y	1.09 ± .01	0.03	0.74
			B_z	1.07 ± .02	0.80	0.96
34	35	3145	B_x	0.91 ± .03	-0.17	1.79
			B_y	1.09 ± .01	0.09	0.83
			B_z	0.91 ± .02	0.61	1.14
1	35	1156	B_x	1.08 ± .02	0.17	1.01
			B_y	1.09 ± .02	-0.01	1.07
			B_z	1.01 ± .02	0.72	1.05
41	1	2021	B_x	1.00 ± .01	-0.09	0.72
			B_y	0.99 ± .01	0.00	0.70
			B_z	0.99 ± .02	-0.10	0.66
41	43	1424	B_x	1.03 ± .01	-0.07	0.50
			B_y	1.01 ± .01	0.05	0.52
			B_z	0.98 ± .02	0.05	0.56
47	43	755	B_x	1.05 ± .03	0.00	0.98
			B_y	1.01 ± .03	0.13	0.99
			B_z	1.02 ± .04	0.19	1.40
50	43	1657	B_x	0.89 ± .02	0.15	1.35
			B_y	1.01 ± .02	-0.06	0.82
			B_z	0.94 ± .02	0.08	0.85
1	43	4898	B_x	0.98 ± .01	-0.03	1.17
			B_y	1.00 ± .01	0.03	0.94
			B_z	0.98 ± .01	0.09	0.90
1	47	1675	B_x	0.98 ± .02	0.03	1.00
			B_y	1.01 ± .02	0.03	1.09
			B_z	0.99 ± .03	-0.11	0.91
1	50	3130	B_x	1.04 ± .01	0.00	0.94
			B_y	0.97 ± .02	0.10	1.07
			B_z	1.00 ± .02	0.08	0.88

Table 6. Regression Results for Field Magnitude and Angles

$$P_{S1} = a\, P_{S2} + b$$

S1	S2	Number of Points	P	a	b	$\sigma_\perp$
28	33	1183	B	0.96 ± .02	-0.07	0.61
		1183	θ	1.13 ± .08	1.28	15.18
		1130	φ	1.01 ± .02	1.52	17.20
34	33	1497	B	0.97 ± .01	-0.01	0.34
		1497	θ	1.01 ± .04	1.18	12.14
		1418	φ	1.00 ± .01	0.19	15.24
33	35	3040	B	1.06 ± .01	0.02	0.40
		3040	θ	1.01 ± .01	8.73	11.92
		2930	φ	1.00 ± .01	-0.19	15.26
34	35	3145	B	0.84 ± .02	0.99	0.94
		3145	θ	0.99 ± .03	7.91	12.87
		2969	φ	0.98 ± .01	5.96	20.09
1	35	1156	B	1.06 ± .03	-0.07	0.97
		1156	θ	0.95 ± .04	7.74	13.06
		1098	φ	1.01 ± .02	-1.13	17.10
41	1	2021	B	1.00 ± .01	0.06	0.35
		2021	θ	1.00 ± .02	-1.10	9.02
		1959	φ	0.99 ± .01	4.88	15.19
41	43	1424	B	1.01 ± .01	-0.03	0.31
		1424	θ	0.98 ± .02	1.05	8.32
		1381	φ	0.99 ± .01	3.47	11.44
47	43	755	B	1.02 ± .01	0.05	0.30
		755	θ	1.01 ± .06	2.70	13.05
		729	φ	1.01 ± .02	-0.76	16.85
50	43	1657	B	0.80 ± .02	1.21	1.17
		1657	θ	1.02 ± .03	1.31	9.11
		1583	φ	1.00 ± .01	-4.05	12.85
1	43	4898	B	0.93 ± .01	0.38	0.96
		4898	θ	1.00 ± .02	1.24	9.47
		4649	φ	0.99 ± .01	1.90	15.02
1	47	1675	B	0.98 ± .01	-0.04	0.41
		1675	θ	0.97 ± .03	-1.93	12.02
		1584	φ	1.01 ± .01	-6.19	18.53
1	50	3130	B	1.01 ± .01	-0.07	0.35
		3130	θ	1.01 ± .02	1.07	11.11
		2927	φ	1.00 ± .01	3.59	19.04

sistent way to determine in which source data sets these apparent errors occur, despite the availability of several different spacecraft pairs.

2. The root-mean-square perpendicular distance between data points and regression line is typically of the order of 0.5 - 1.0 gamma. Variability between spacecraft pairs results from both differing widths of the main clusters of points as well as different numbers of far-outlying points. The factors yielding non-zero root-mean-square perpendicular distances are addressed in the preceding discussion of plasma data. The significance of these point spreads is that they yield the limits of validity of the corresponding parameter. Thus, a listed value of B_x represents the "true" hourly averaged IMF B_x component for Earth to within 0.5 to 1.0 gamma.

3. The regression line intercepts are always less than 0.2 gamma (and often less than 0.1 gamma) except for those involving B_z as measured by Explorer 35. It appears that the Explorer 35 B_z values are too small (too negative) by about 0.7 gamma, and that sensor zero levels for the other spacecraft involved in the regressions have been well determined. It is appropriate to note that in *King* (1975) it was found that, when B_z was averaged over all available hours separately for each source data set, all such averages were within 0.2 γ of zero, except for Explorer 18 (B_z = -1.0 γ based on 1215 hours) and Explorer 35 (B_z = -0.7 γ).

Inspection of Table 6 reveals that typical uncertainties in the "true" hourly averaged IMF magnitude, latitude, and longitude angles for Earth are $\approx$0.3 to 1.0 γ, $\approx$10° to 15°, and $\approx$15° to 20°, respectively. The previously noted ~0.7 γ offset in Explorer 35 B_z is reflected in the $\approx$8° offset in the θ regression runs involving Explorer 35. Otherwise, intercepts for the θ regressions are all reasonably close to zero. The intercepts for the ϕ regressions exhibit a surprisingly large range of up to $\approx$6°, although there is no unique and consistent way to assign angle offsets to specific source data sets.

It is apparent from Table 6 that the field magnitude regression slope has an unusually low value (0.80) for Explorer 50/Explorer 43. This is in contrast to the fact that Explorer 50/HEOS and Explorer 43/HEOS field magnitude regression slopes are both much closer to unity (1.01 and 0.93). A similar inconsistency is visible in the 34/33, 35/33, and 34/35 regression runs.

Given the availability of more than 3 years of overlapping HEOS/Explorer 43 data, the possibility of time dependencies in regression param-

eters that might be at least partially responsible for such inconsistencies has been examined. The results are summarized in Table 7. Note that there is a slight trend for the field component regression line slopes to decrease with time, with a statistically significant decrease of about 10 percent in 1974 relative to 1973. Note the more dramatic variation in the field magnitude regression line slopes. This difference in the character of the temporal changes between field magnitude and field component regression parameters is, at least in part, due to the application of the same regression analysis to dissimilar distributions of field component values (quasi-normal) and field magnitude values (non-normal).

It appears that time variations in sensor characteristics may yield some inconsistencies in comparing results from apparently redundant triads of spacecraft pairs. Nevertheless, it is difficult to uniquely assign time variations to specific source data sets.

Despite the present findings of regression line slopes different from unity, and some intercepts different from zero, no IMF data normalizations have been performed because the line $y = x$ passes through the main cluster of IMF data points on the scatter plots shown (and on those not shown). Equivalently, the changes in parameters brought about by appropriate normalization would be less than the previously discussed uncertainties in these parameters.

These mutual consistency results have been included to give the potential data user both quantitative and qualitative insight into the limits of validity of the composite data set. If the reader believes a specific study would profit from data normalizations, it is advised that normalization be done. The magnetic tape containing up to three sets of IMF data from different spacecraft per hour is available from NSSDC if the reader wishes to test data mutual consistency in some manner other than that employed herein.

DATA SELECTION

The final composite data set was assembled from the composite IMF tape, the normalized composite plasma tape, and a tape with geomagnetic and solar activity indexes. For a given hour, the plasma and field data were each taken from one of possibly several available source data sets according to the following priority scheme.

Plasma data were considered first. If the plasma spacecraft used for the preceding hour was available, and it had a 1-hour resolution, it was chosen. If the plasma spacecraft used for the preceding hour was not available, or if it had a 3-hour resolution, that source having at least three fine-time scale points per hour and having the highest priority was chosen. The priority ordering was (high to low) 33, 35, 34, 3, 50, 43, 5, 1, 99, and 98, determined somewhat arbitrarily on the basis of available

Table 7. Regression Results for HEOS/Explorer 43 Field Data

$$P_1 = a\, P_{43} + b$$

Year	Number of Points	P	a	b	σ_1
1971	102	B_X	1.03 ± .06	0.28	0.64
		B_y	1.06 ± .10	0.03	1.07
		B_z	1.06 ± .13	0.01	0.75
		B	0.95 ± .04	0.47	0.26
1972	1425	B_X	1.04 ± .02	-0.08	0.79
		B_y	1.02 ± .01	0.06	0.78
		B_z	1.02 ± .02	0.02	0.83
		B	1.08 ± .02	0.43	0.75
1973	1592	B_X	1.01 ± .02	-0.08	0.90
		B_y	1.02 ± .02	-0.02	0.98
		B_z	1.02 ± .03	0.02	0.89
		B	1.01 ± .01	-0.08	0.33
1974	1779	B_X	0.90 ± .03	0.14	1.57
		B_y	0.96 ± .02	0.03	1.01
		B_z	0.90 ± .03	0.06	0.96
		B	0.71 ± .05	1.67	1.27

parameters and temporal resolution. If no source was chosen using the just mentioned criteria, the fine-time-scale-points-per-hour criterion dropped, and the same priority criterion was reapplied.

Then IMF data were taken from the same spacecraft, if available, from which the plasma data were just chosen. However, if this spacecraft was not available, if it was Explorer 35, or if there were no plasma data for the current hour, IMF data were taken from the spacecraft providing IMF data for the previous hour. Again, if this spacecraft was not available or was Explorer 35, IMF data were taken from the highest priority spacecraft available, according to the priority ordering (high to low) 50, 47, 43, 1, 41, 34, 33, 28, and 35. Note that Explorer 35 IMF data appear in the final composite data set only for those 2825 hours when IMF data were available from no other source.

FIELD COMPONENT TRANSFORMATIONS

There are several orthogonal, right-handed coordinate systems in which interplanetary vector quantities are usefully expressed. In geocentric solar ecliptic (GSE) coordinates, the X-axis points from the Earth to the Sun and the Z-axis is normal to the ecliptic plane, positive northward. Geocentric solar equatorial coordinates also have an X-axis pointing from the Earth to the Sun, but have a Y-axis lying in a plane parallel to the solar equatorial plane, positive in a direction roughly opposite that of planetary motion. In this system, which differs from the GSE system by 7.25° at most, the ideal spiral magnetic field (*Parker*, 1958) has no Z component. In geocentric solar magnetospheric (GSM) coordinates, the X-axis again points from the Earth to the Sun, while the Z-axis lies in a plane containing the X-axis and the Earth's magnetic dipole axis and is positive northward. The GSM system is appropriate for studies of magnetospheric effects of IMF variations. See *Russell* (1971) for a more detailed discussion of these and other coordinate systems and the transformations among them.

The solar wind flow direction angles were provided in GSE coordinates and are contained on the composite tape in these coordinates only. The IMF data, given only in GSE coordinates in the source data sets and in the predecessor to this Data Book (*King*, 1975), are given in the present composite data set in both GSE and GSM coordinate systems. The required transformations were performed at NSSDC.

IMF VECTOR STANDARD DEVIATION

As indicated previously, standard deviations for hourly averages of various IMF parameters were made available in various source data sets. However, there was no parameter for which a standard deviation was given in all source data sets.

In order to have a consistent measure of field fluctuations for the composite data in the predecessor to this Data Book, a "vector standard deviation" was computed as $(\sigma_{B_X}{}^2 + \sigma_{B_Y}{}^2 + \sigma_{B_Z}{}^2)^{1/2}$ for Explorer data sets and as $(\sigma_B{}^2 + B^2\,\sigma_\theta{}^2 + B^2\cos^2\theta\,\sigma_\phi{}^2)^{1/2}$ for HEOS records. In so far as these expressions represented the lengths of the diagonals of "uncertainty elements" at the tips of the hourly averaged field vectors, they were taken to yield a quasi-homogeneous set of data when interspersed.

However, it has subsequently been pointed out (*Svalgaard*, 1976) that the expression $\sigma_{B_X}{}^2 + \sigma_{B_Y}{}^2 + \sigma_{B_Z}{}^2$ is analytically equivalent to the expression $\sigma_B{}^2 + B^2 - F^2$, where B is the average field magnitude, σ_B its standard deviation, and F the length of the vector constituted by the averaged cartesian components. Accordingly, the vector standard deviation contained in the new composite data set (tape and listings of this Data Book) is $(\sigma_{B_X}{}^2 + \sigma_{B_Y}{}^2 + \sigma_{B_Z}{}^2)^{1/2}$ for Explorer records and $(\sigma_B{}^2 + B^2 - F^2)^{1/2}$ for HEOS records.

DATA PRESENTATION

The composite interplanetary plasma/magnetic field data set has been assembled onto a single magnetic tape with one record for each hour of Bartels' solar rotations 1783 through 1947 (Nov. 2, 1963 to Jan. 12, 1976). The data found in a given record consist of a flag to indicate whether there are plasma and/or field data (or neither) for that hour, time information and Bartels' rotation number, identifiers for the plasma and field source spacecraft, numbers of fine-time scale points in the plasma and field averages, average field magnitude and GSE and GSM cartesian components, magnitude and latitude and longitude angles of the vector comprised by the GSE cartesian components, standard deviations in the average magnitude and in cartesian component averages (Explorer IMF data) or in field angle averages (HEOS IMF data), field vector standard deviation (see previous section for discussion of this parameter), proton temperature, proton density, bulk flow speed and direction angles, standard deviations in the plasma parameters, geomagnetic activity indexes K_P and C_9, and the sunspot number R. The initial flag, the time and solar rotation words, and the geomagnetic activity indexes and sunspot number words have meaningful values for all hours. Plasma (field) words are filled with zeros for hours when no plasma (field) data were available. In addition, individual words corresponding to parameters not provided in the source data set are also filled with zeros. This tape (which may be updated as warranted) is available from NSSDC with a detailed format statement.

The Data Book consists of graphical and tabular presentations of some of the parameters of the composite data set. There are two plots for each solar rotation in which any plasma or field data were obtained. On facing pages, for a convenience in lining up features in the data, are found a plot of plasma data (temperature, density, and bulk speed) and a plot of field data (average magnitude, GSM B_Z component, and GSE latitude and longi-

tude angles of the average field vector). Note the 450° range in the cyclic field longitude angle, employed to decrease the number of times the trace crosses the plot in response to small excursions in the field direction. Note that on those rare occasions when the parameter values exceed the allowed range, a heavy mark is placed near the edge of the plot. For such cases, the reader is advised to consult the data listings in the Appendix for appropriate numerical values.

In a separately bound Appendix to this *Interplanetary Medium Data Book* are found listings of selected hourly parameters, which include plasma temperature (in units of 1000°K), proton density (cm^{-3}), bulk speed (km/s), and an identifier of the spacecraft from which the plasma data were taken. Also found with the plasma data are the field parameters: average magnitude, GSM cartesian components, latitude and longitude angles of the vector made up of the average GSE field components, the previously discussed vector standard deviation, and an identifier of the IMF spacecraft. Note that to economize space, one-character alphabetic spacecraft identifiers have been used (as in this document's predecessor, *Interplanetary Magnetic Field Data Book*) although numeric identifiers are used on the magnetic tape for convenience. (See Table 1 for definitions of the identifiers.) Also note that the data are listed in 1-day blocks and that days with no field or plasma data are omitted from the listings.

REFERENCES

Asbridge, J.R., S.J. Bame, W.C. Feldman, and M.D. Montgomery, "Helium and Hydrogen Velocity Differences in the Solar Wind," *J. Geophys. Res.*, *81*, 2719, 1976.

Bame, S.J., J.R. Asbridge, H.E. Felthauser, E.W. Hones, and I.B. Strong, "Characteristics of the Plasma Sheet in the Earth's Magnetotail," *J. Geophys. Res.*, *72*, 113, 1967.

Bame, S.J., E.W. Hones, Jr., S.I. Akasofu, M.D. Montgomery, and J.R. Asbridge, "Geomagnetic Storm Particles in the High Latitude Magnetotail," *J. Geophys. Res.*, *76*, 7566, 1971.

Behannon, K.W., "Mapping of the Earth's Bow Shock and Magnetic Tail by Explorer 33," *J. Geophys. Res.*, *73*, 907, 1968.

Bonetti, A., G. Moreno, S. Cantarano, A. Egidi, R. Marconero, F. Palutan, and G. Pizzella, "Solar Wind Observations with Satellite ESRO HEOS-1 in December 1969," *Nuovo Cimento*, *46B*, 307, 1969.

Bridge, H.S., C. Dilworth, B. Rossi, F. Scherb, and E.F. Lyon, "An Instrument for the Investigation of Interplanetary Plasma," *J. Geophys. Res.*, *65*, 3053, 1960.

Bridge, H.S., A. Egidi, A. Lazarus, and E. Lyon, "Preliminary Results of Plasma Measurements on IMP-A," *Space Research V*, 969, North Holland Pub. Co., Amsterdam, 1965.

Burlaga, L.F., and K.W. Ogilvie, "Observations of the Magnetosheath-Solar Wind Boundary," *J. Geophys. Res.*, *73*, 6167, 1968.

Diodato, L., G. Moreno, and C. Signorini, "Compilation of Normalized Solar Wind Densities and Velocities (1965/1971)," *Astron. Astrophys. Suppl.*, *20*, 313, 1975.

Egidi, A., G. Moreno, and J. Sullivan, "North-South Motions in the Solar Wind," *J. Geophys. Res.*, *82*, 2187, 1977.

Egidi, A., G. Pizzella, and C. Signorini, "Measurement of the Solar Wind Direction with The IMP 1 Satellite," *J. Geophys. Res.*, *74*, 2807, 1969.

Fairfield, D.H., "Bow Shock Associated Waves Observed in the Far Upstream Interplanetary Medium," *J. Geophys. Res.*, *74*, 3541, 1969.

Fairfield, D.H., "Whistler Waves Observed Upstream from Collisionless Shocks," *J. Geophys. Res.*, *79*, 1368, 1974.

Fairfield, D.H., and N.F. Ness, "IMP 5 Magnetic Field Measurements in the High Latitude Outer Magnetosphere near the Noon Meridian," *J. Geophys. Res.*, *77*, 611, 1972.

Feldman, W.C., J.R. Asbridge, S.J. Bame, and J.T. Gosling, "High-Speed Solar Wind Flow Parameters at 1 AU," *J. Geophys. Res.*, *81*, 5054, 1976.

Feldman, W.C., J.R. Asbridge, S.J. Bame, and M.D. Montgomery, "Double Ion Streams in the Solar Wind," *J. Geophys. Res.*, *78*, 2017, 1973.

Gosling, J.T., J.R. Asbridge, S.J. Bame, and W.C. Feldman, "Solar Wind Speed Variations: 1962-1974," *J. Geophys. Res.*, *81*, 5061, 1976.

Gosling, J.T., J.R. Asbridge, S.J. Bame, and I.B. Strong, "Vela 2 Measurements of the Magnetopause and Bow Shock Positions," *J. Geophys. Res.*, *72*, 101, 1967.

Hedgecock, P.C., "A Correlation Technique for Determining Magnetometer Zero Levels," *Space Science Instrumentation*, *1*, 74, 1975a.

Hedgecock, P.C., "Magnetometer Experiments in the ESRO-HEOS Satellites," *Space Science Instrumentation*, *1*, 53, 1975b.

Hones, E.W., J.R. Asbridge, S.J. Bame, M.D. Montgomery, S. Singer, and S.I. Akasofu, "Measurements of Magnetotail Plasma Flow Made with Vela 4B," *J. Geophys. Res.*, *77*, 5503, 1972.

Hundhausen, A.J., J.R. Asbridge, S.J. Bame, H.E. Gilbert, and I.B. Strong, "Vela 3 Satellite Observations of Solar Wind Ions: A Preliminary Report," *J. Geophys. Res.*, *72*, 87, 1967.

Hundhausen, A.J., S.J. Bame, J.R. Asbridge, and S.J. Sydoriak, "Solar Wind Proton Properties: Vela 3 Observations from July 1965 to June 1967," *J. Geophys. Res.*, *75*, 4643, 1970.

King, J.H., *Interplanetary Magnetic Field Data Book*, NASA/NSSDC 75-04, Greenbelt, Maryland, 1975.

King, J.H., and N.F. Ness, "Lunar Magnetic Permeability Studies and Magnetometer Sensitivity," *Geophys. Res. Lett.*, *4*, 129, 1977.

Lenhart, K.G., "Geomagnetic and Solar Data for Use with Digital Computers," *Trans. A.G.U.*, *49*, 463, 1968.

Lyon, E., A. Egidi, G. Pizzella, H. Bridge, J. Binsack, R. Baker, and R. Butler, "Plasma Measurements on Explorer 33 (I) Interplanetary Region," *Space Research VIII*, 99, North Holland Pub. Co., Amsterdam, 1968

Lyon, E.F., H.S. Bridge, and J.H. Binsack, "Explorer 35 Plasma Measurements in the Vicinity of the Moon," *J. Geophys. Res.*, *72*, 6113, 1967.

Mish, W.H., and R.P. Lepping, *Magnetic Field Experiment Data Processing Systems: Explorers 47 and 50*, NASA/GSFC X-694-76-158, Greenbelt, Maryland, 1976.

Madansky, A., "The Fitting of Straight Lines When Both Variables are Subject to Error," *J. Am. Statistical Assn.*, *54*, 173, 1959.

Montgomery, M.D., J.R. Asbridge, and S.J. Bame, "Vela 4 Plasma Observations near the Earth's Bow Shock," *J. Geophys. Res.*, *75*, 1217, 1970.

Moreno, G., and C. Signorini, "Comparison of Interplanetary Plasma Experiments," ELDO/ESRO *Sci. Tech. Rev.*, *5*, 401, 1973.

Ness, N.F., K.W. Behannon, C.S. Scearce, and S.C. Cantarano, "Early Results from the Magnetic Field Experiment on Lunar Explorer 35," *J. Geophys. Res.*, *72*, 5769, 1967.

Ness, N.F., C.S. Scearce, and J.B. Seek, "Initial Results of the IMP 1 Magnetic Field Experiment," *J. Geophys. Res.*, *69*, 3531, 1964.

Neugebauer, M., "Initial Deceleration of Solar Wind Positive Ions in the Earth's Bow Shock," *J. Geophys. Res.*, *75*, 717, 1970.

Neugebauer, M., "The Quiet Solar Wind," *J. Geophys. Res.*, *81*, 4664, 1976.

Ogilvie, K.W., L.F. Burlaga, and T.D. Wilkerson, "Plasma Observations on Explorer 34," *J. Geophys. Res.*, *73*, 6809, 1968a.

Ogilvie, K.W., N. McIlwraith, and T.D. Wilkerson, "A Mass-Energy Spectrometer for Space Plasmas," *Rev. Sci. Inst.*, *39*, 441, 1968b.

Olbert, S., "Summary of Experimental Results from M.I.T. Detector on IMP-1," *Physics of the Magnetosphere*, 641, D. Reidel Pub. Co., Dordrecht, The Netherlands, 1968.

Parker, E.N., "Dynamics of the Interplanetary Gas and Magnetic Fields," *Astrophys. J.*, *128*, 664, 1958.

Russell, C.T., "Geophysical Coordinate Transformations," *Cosmic Electrodynamics*, *2*, 184, 1971.

Svalgaard, L., Private Communication, 1976.

SCATTER PLOTS

The following pages contain plasma and magnetic field scatter plots for selected pairs of spacecraft.

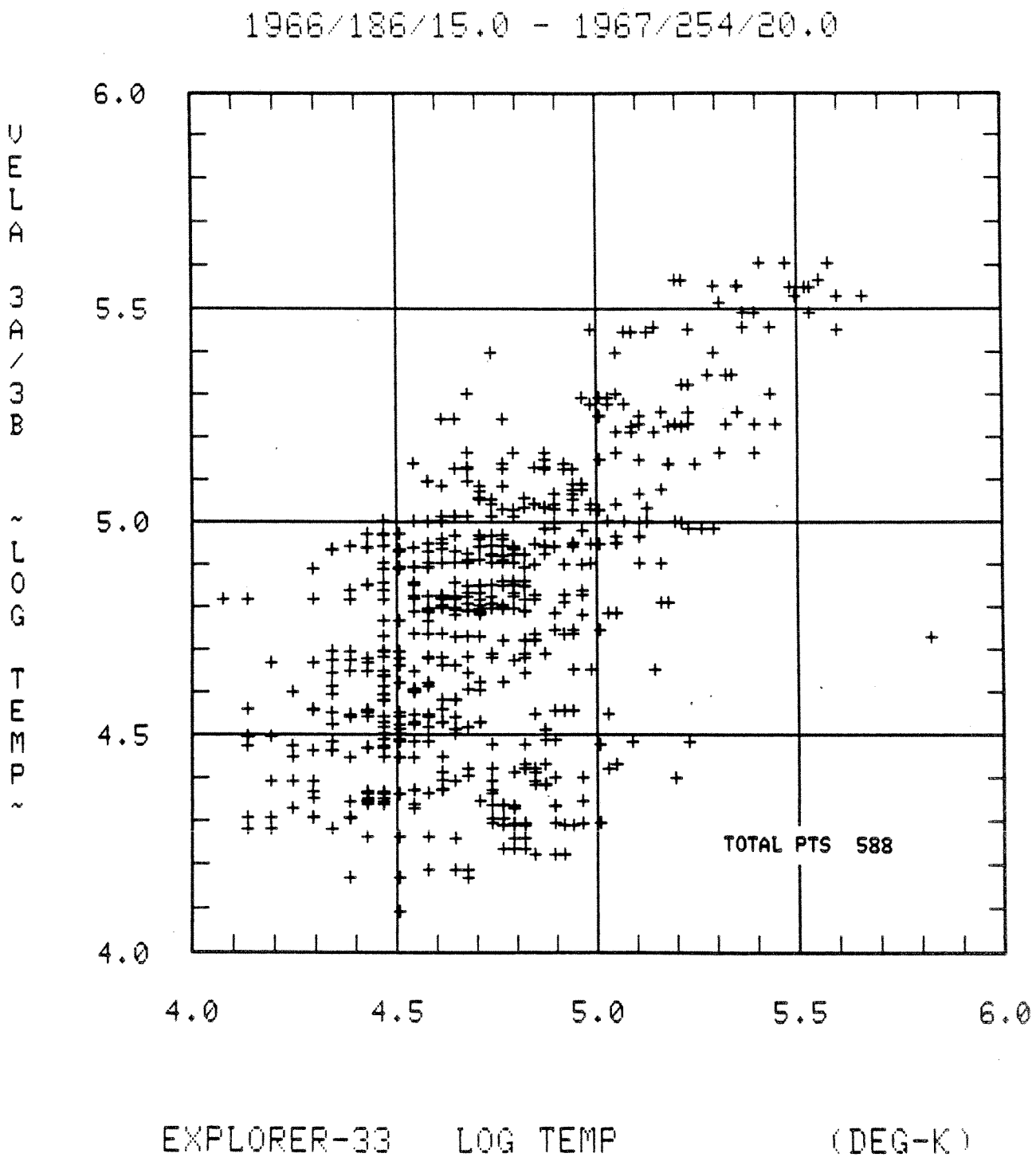

Scatter Plot 1

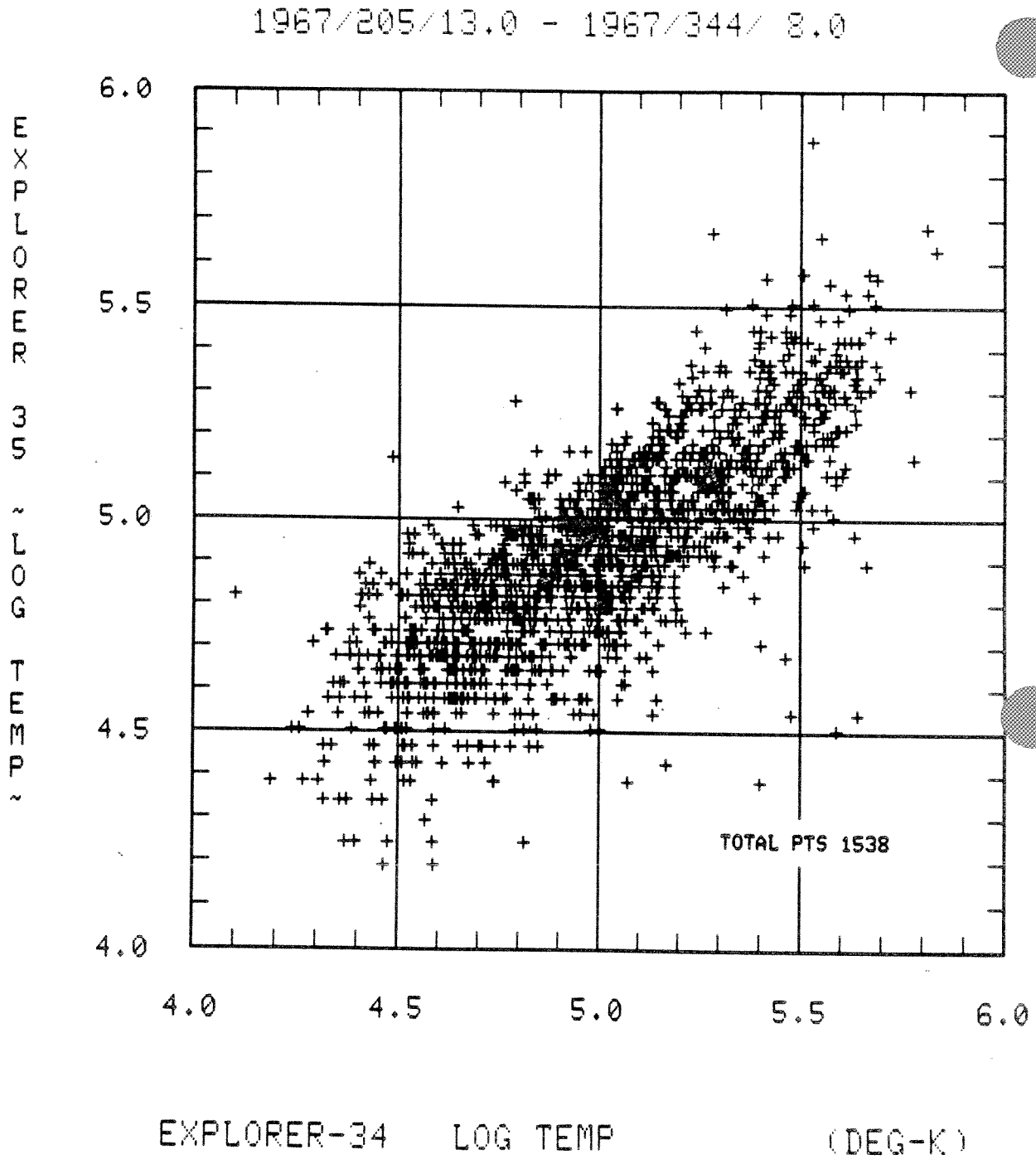

Scatter Plot 2

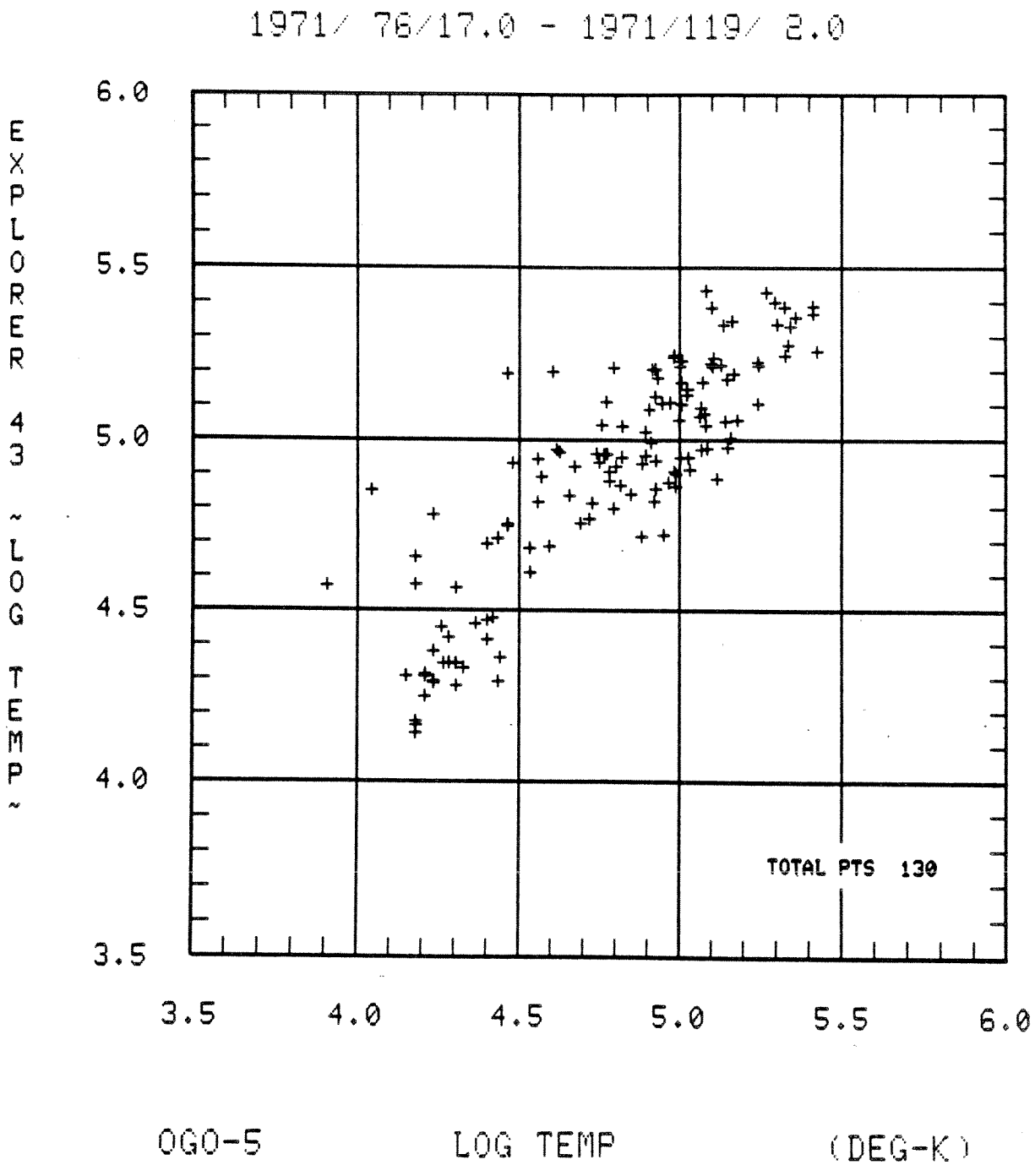

Scatter Plot 3

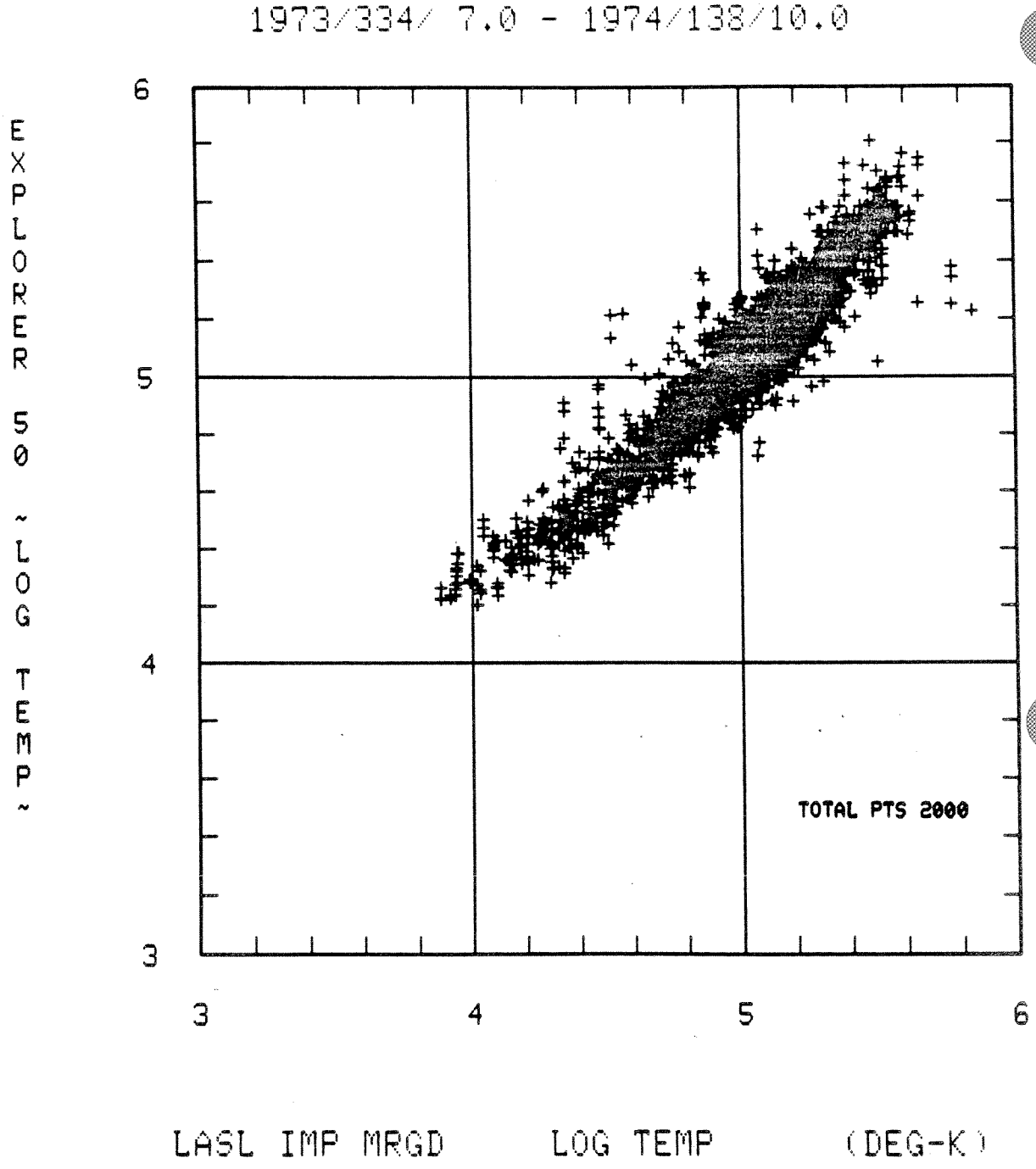

Scatter Plot 4

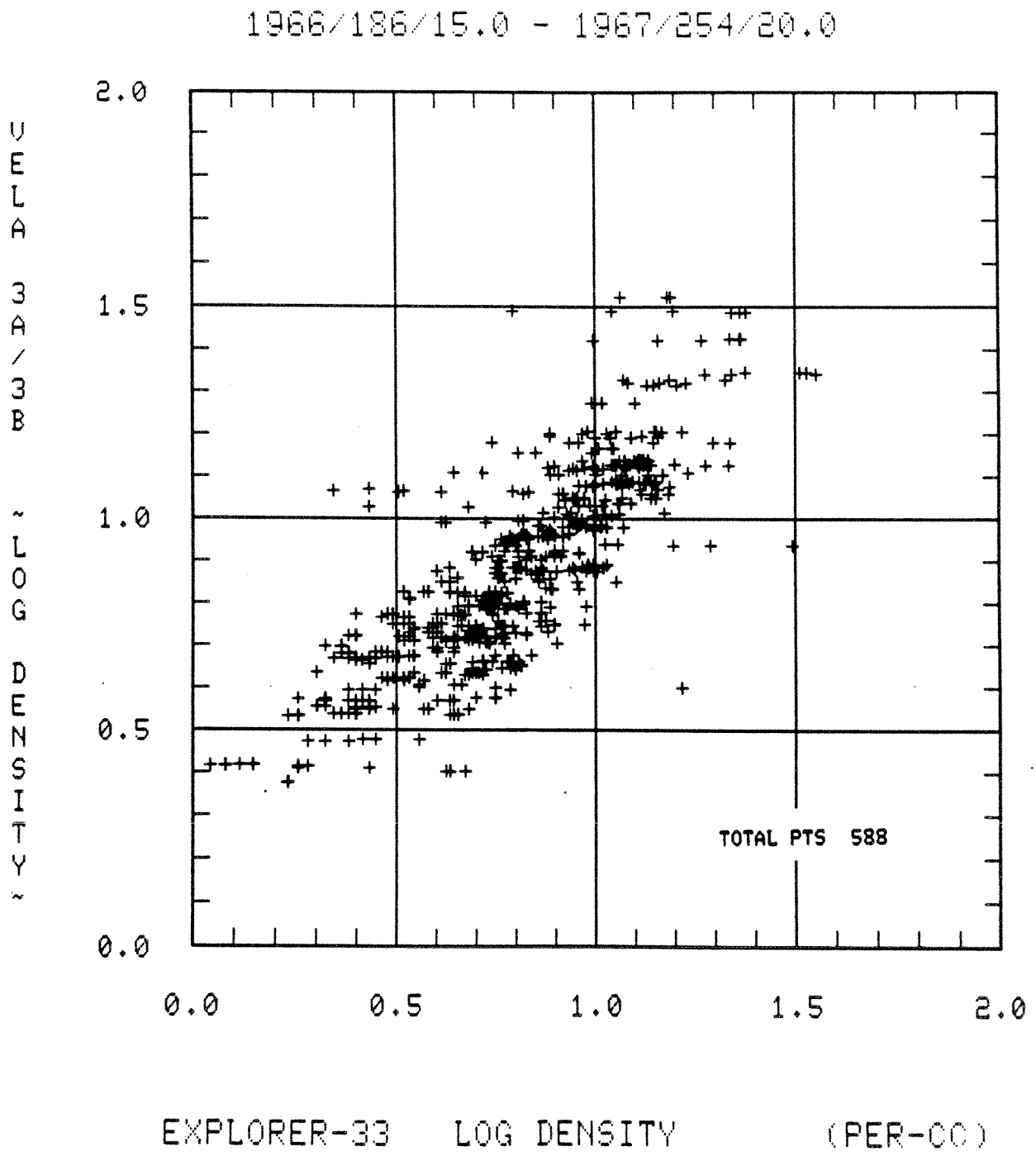

Scatter Plot 5

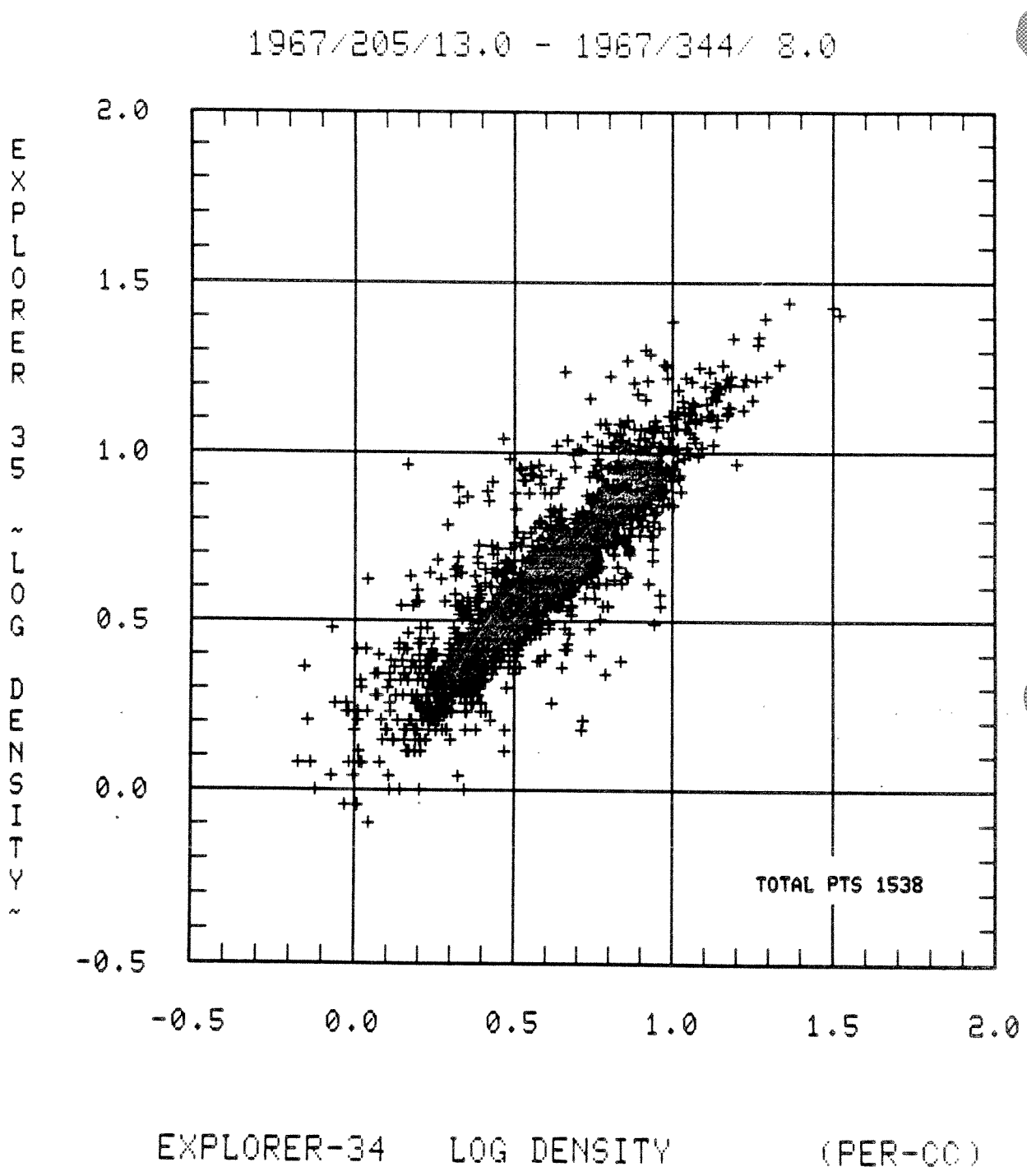

Scatter Plot 6

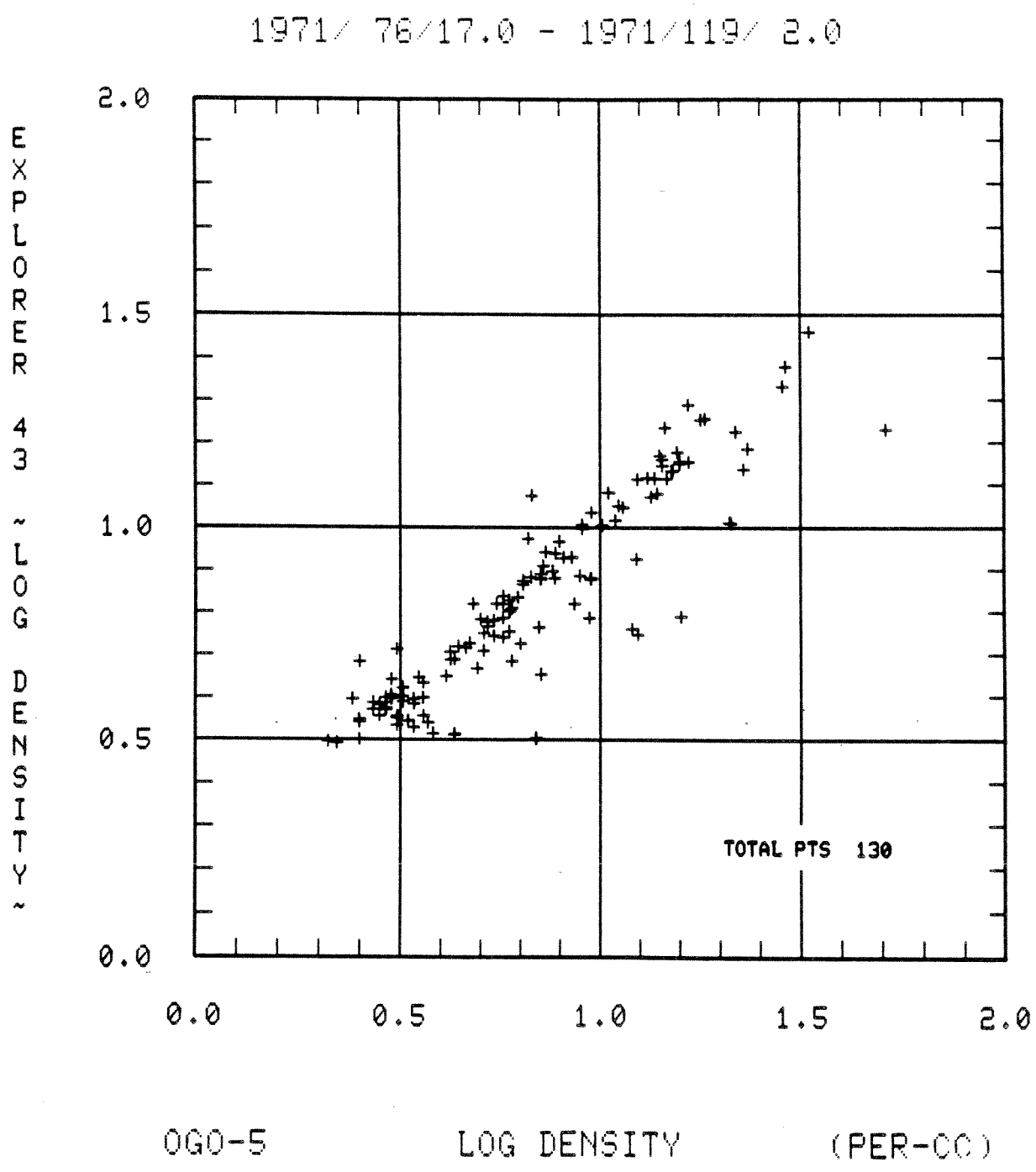

Scatter Plot 7

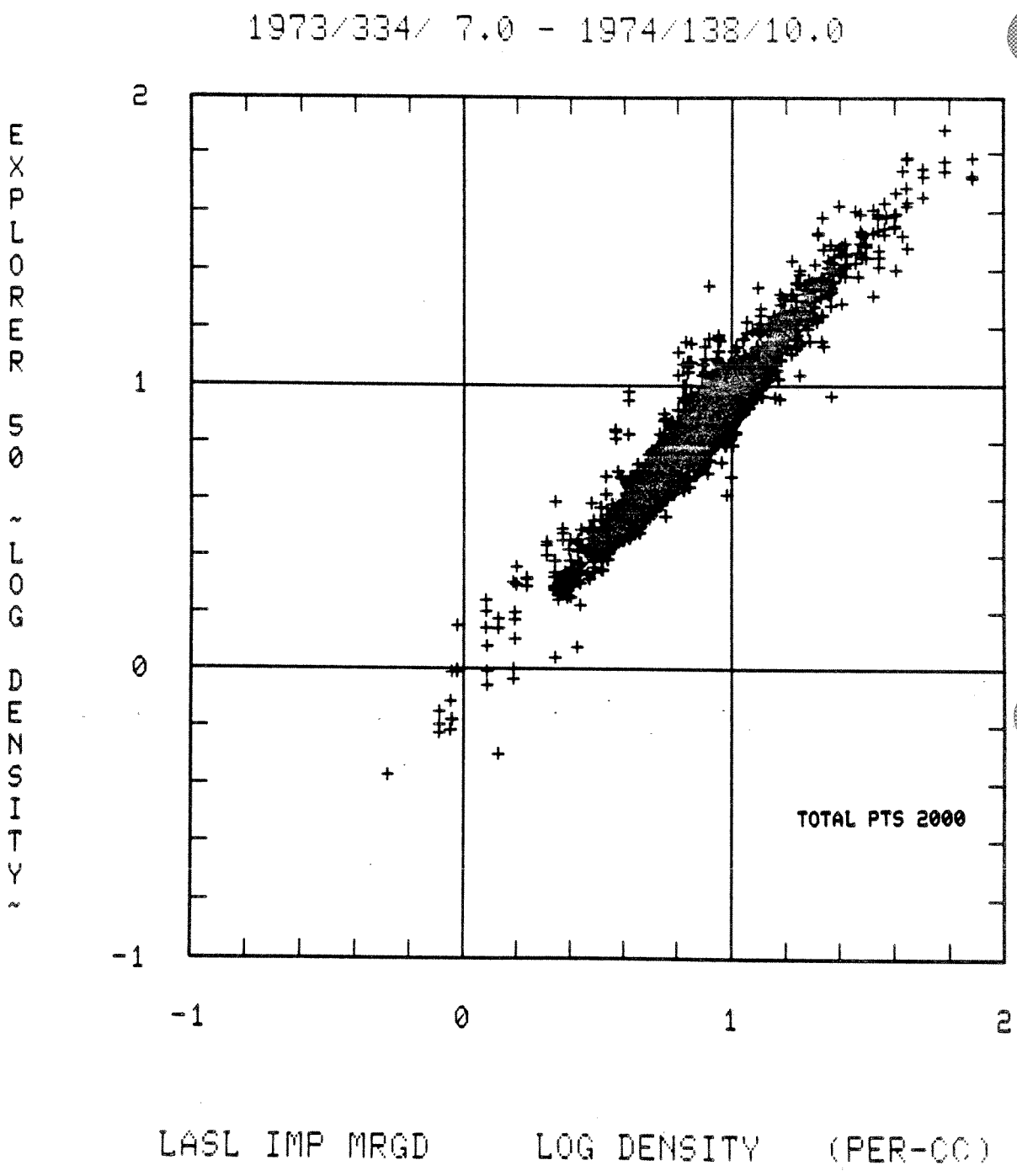

Scatter Plot 8

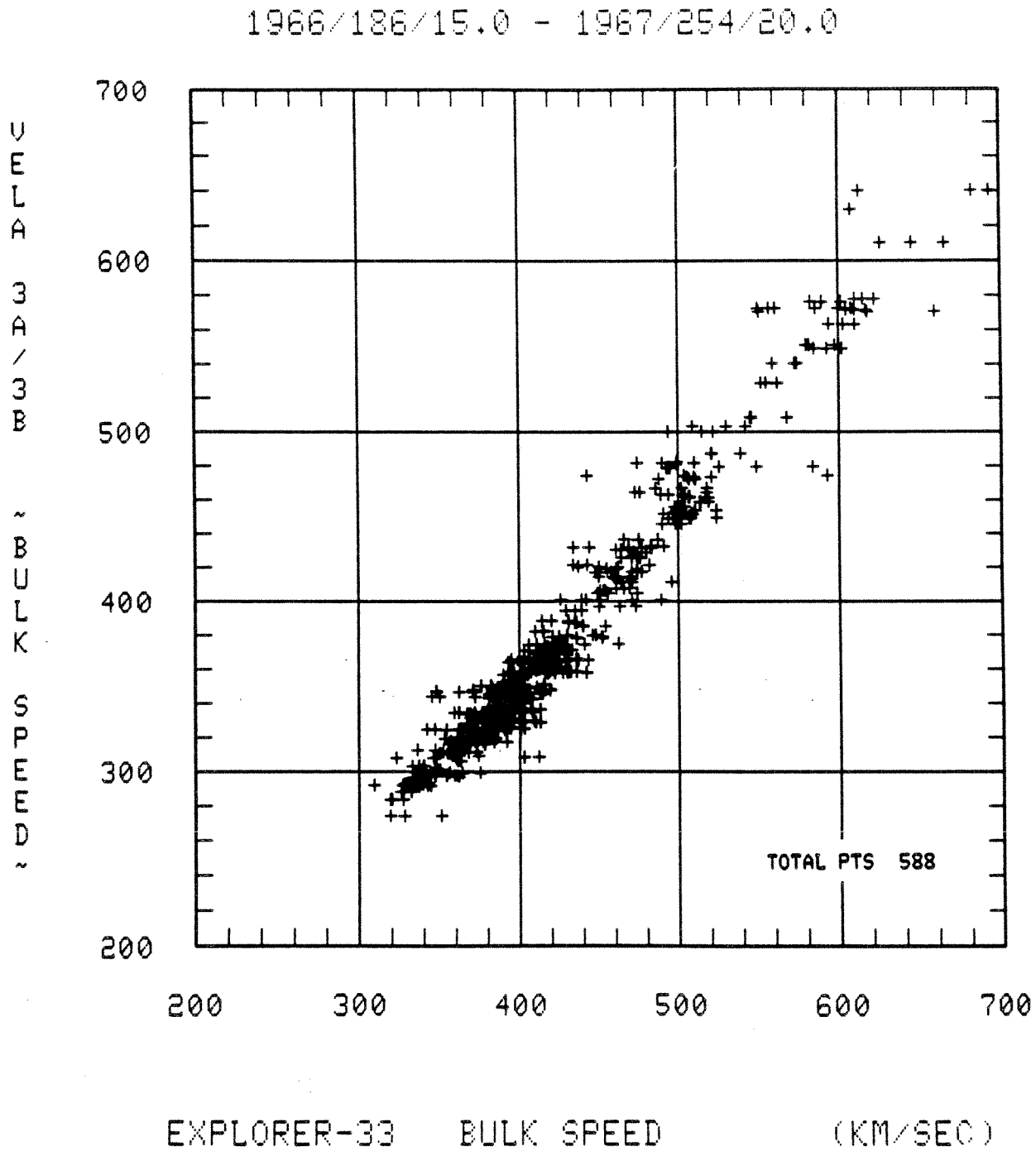

Scatter Plot 9

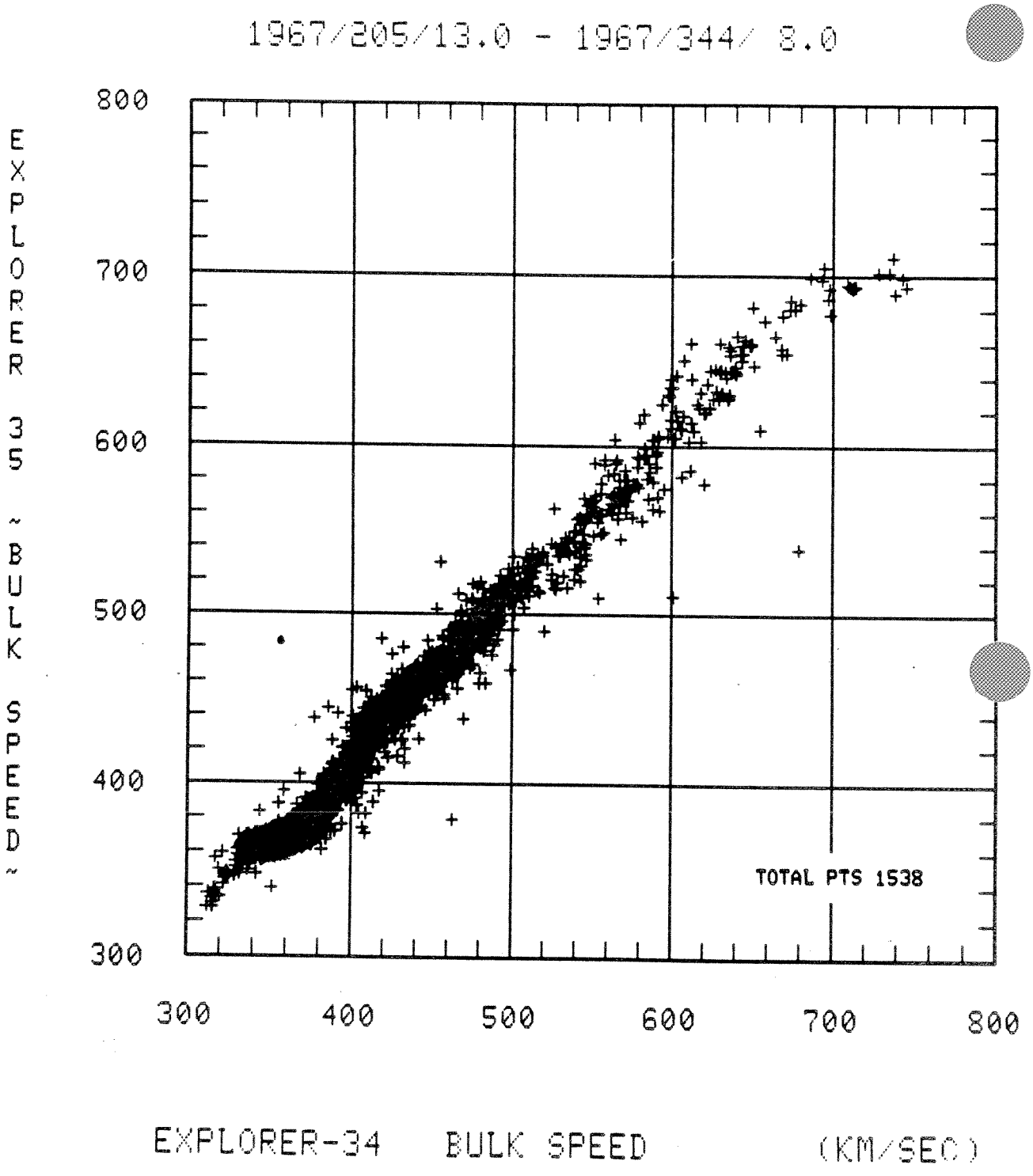

Scatter Plot 10

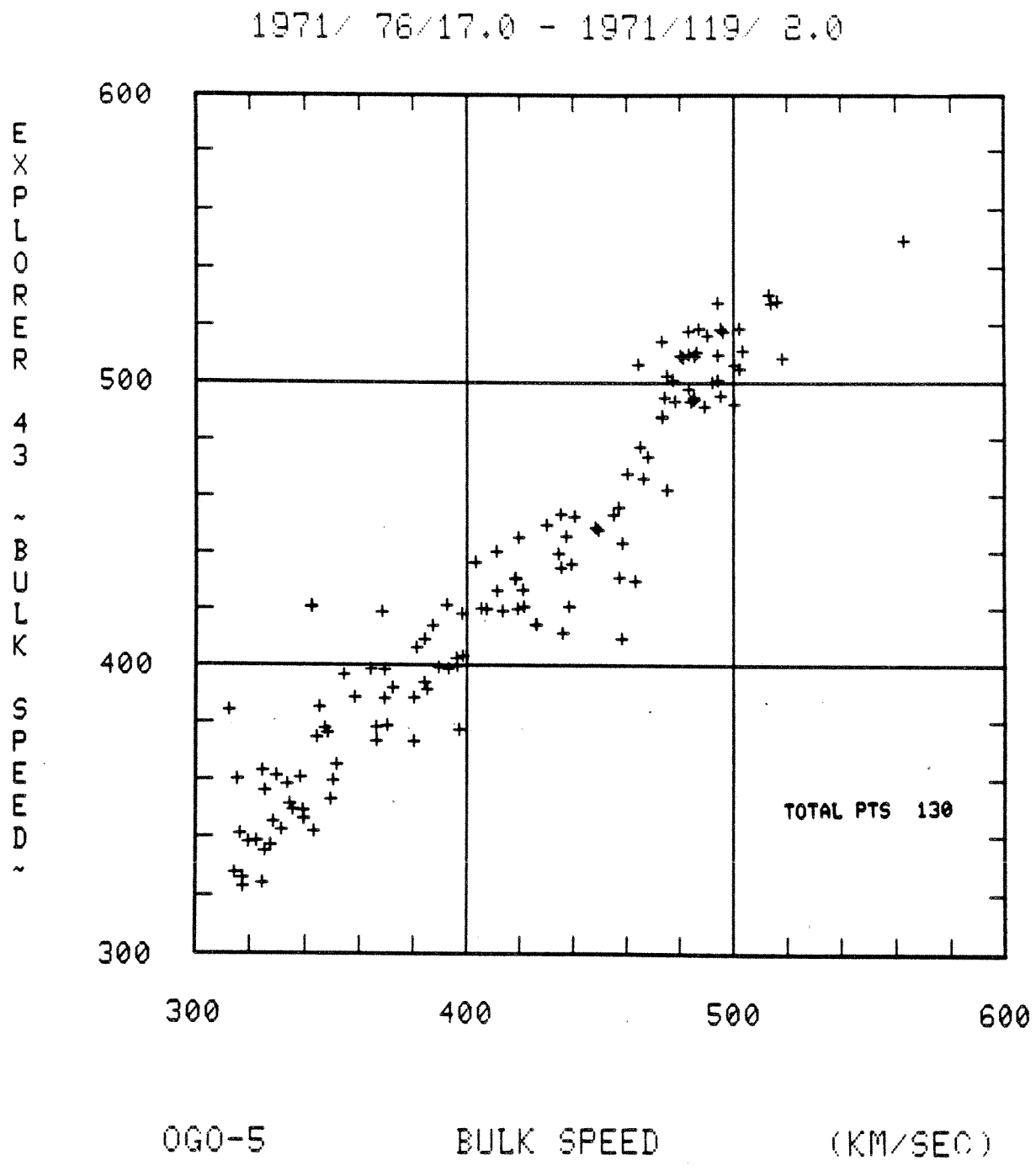

Scatter Plot 11

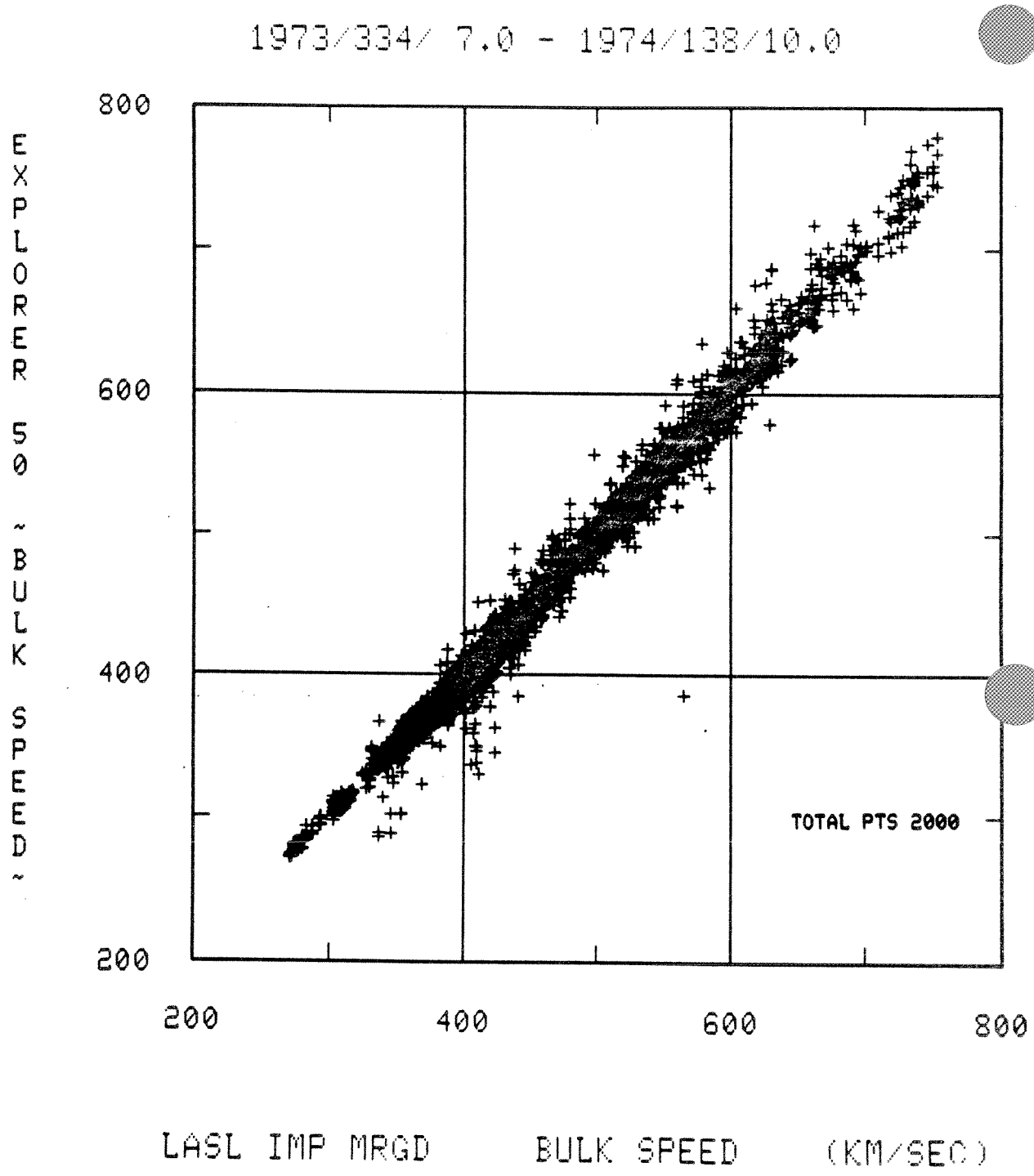

Scatter Plot 12

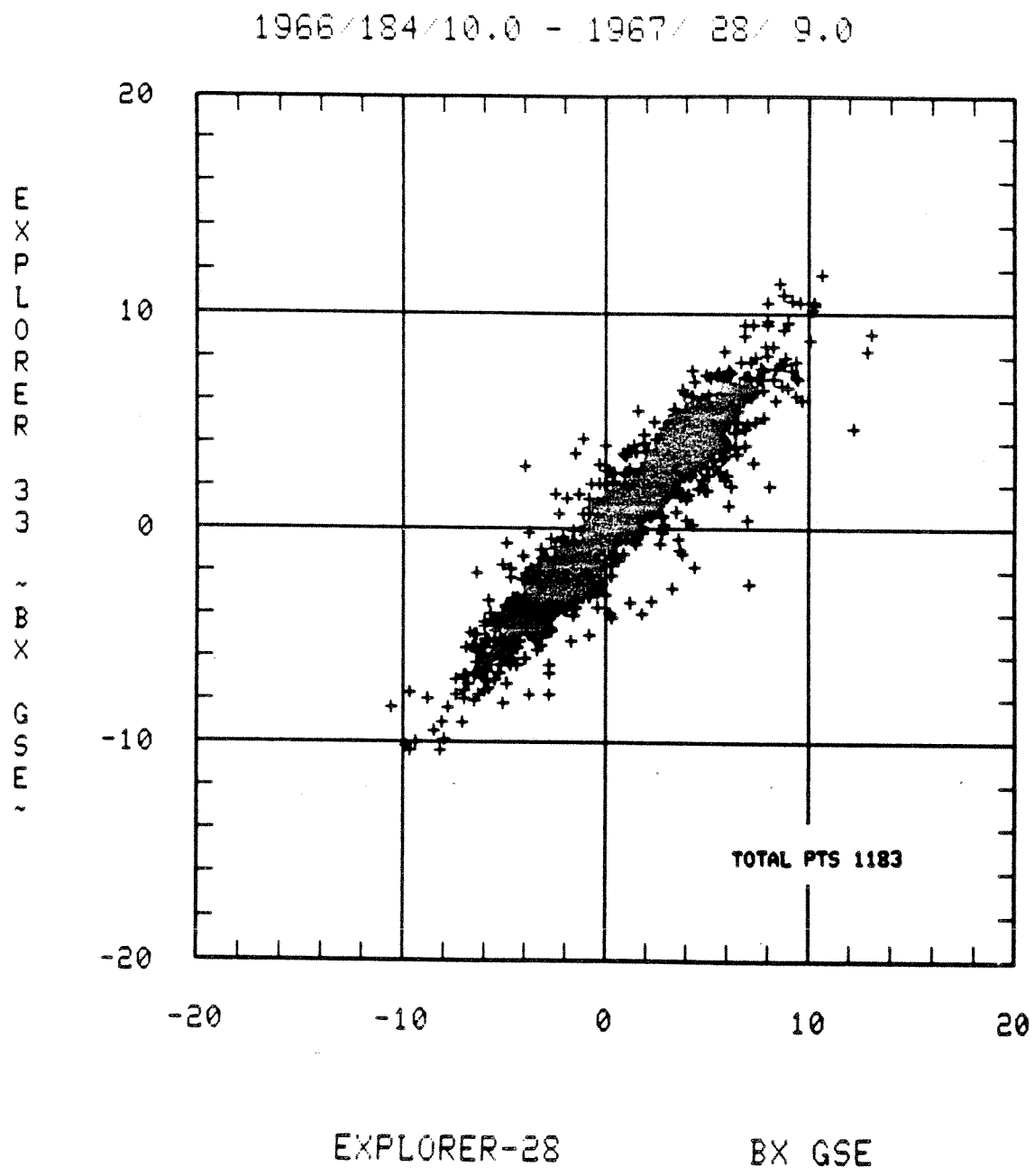

Scatter Plot 13

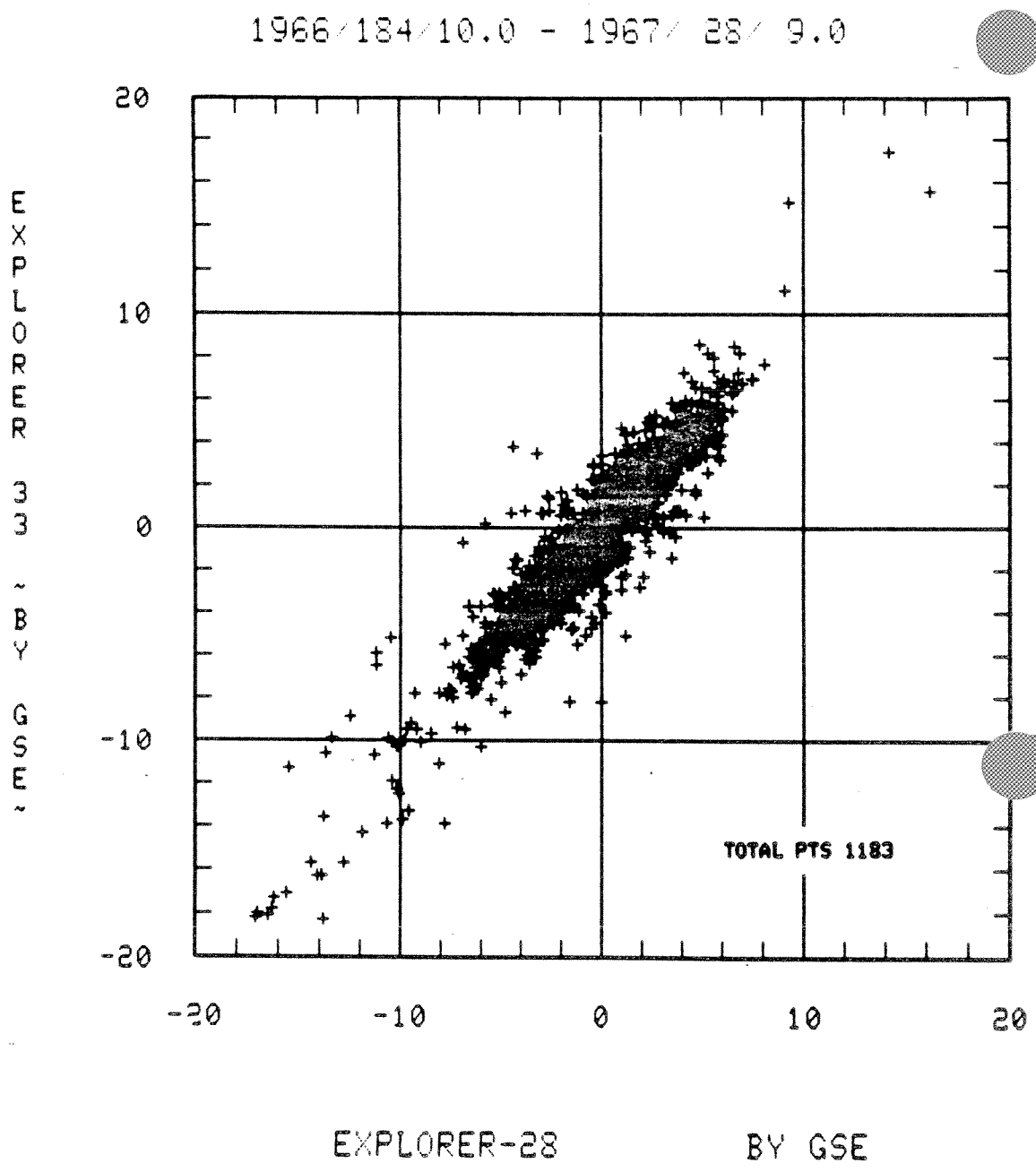

Scatter Plot 14

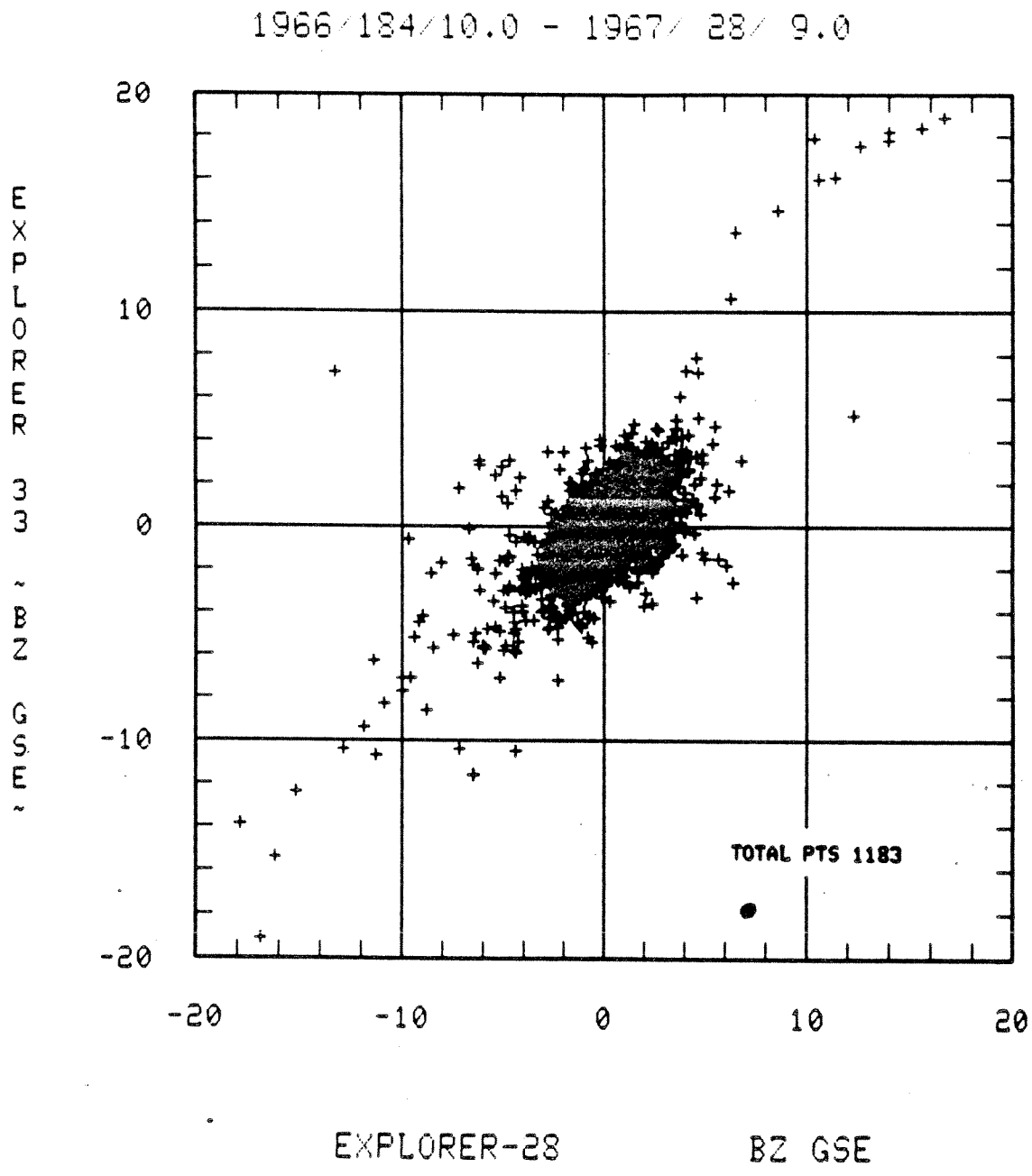

Scatter Plot 15

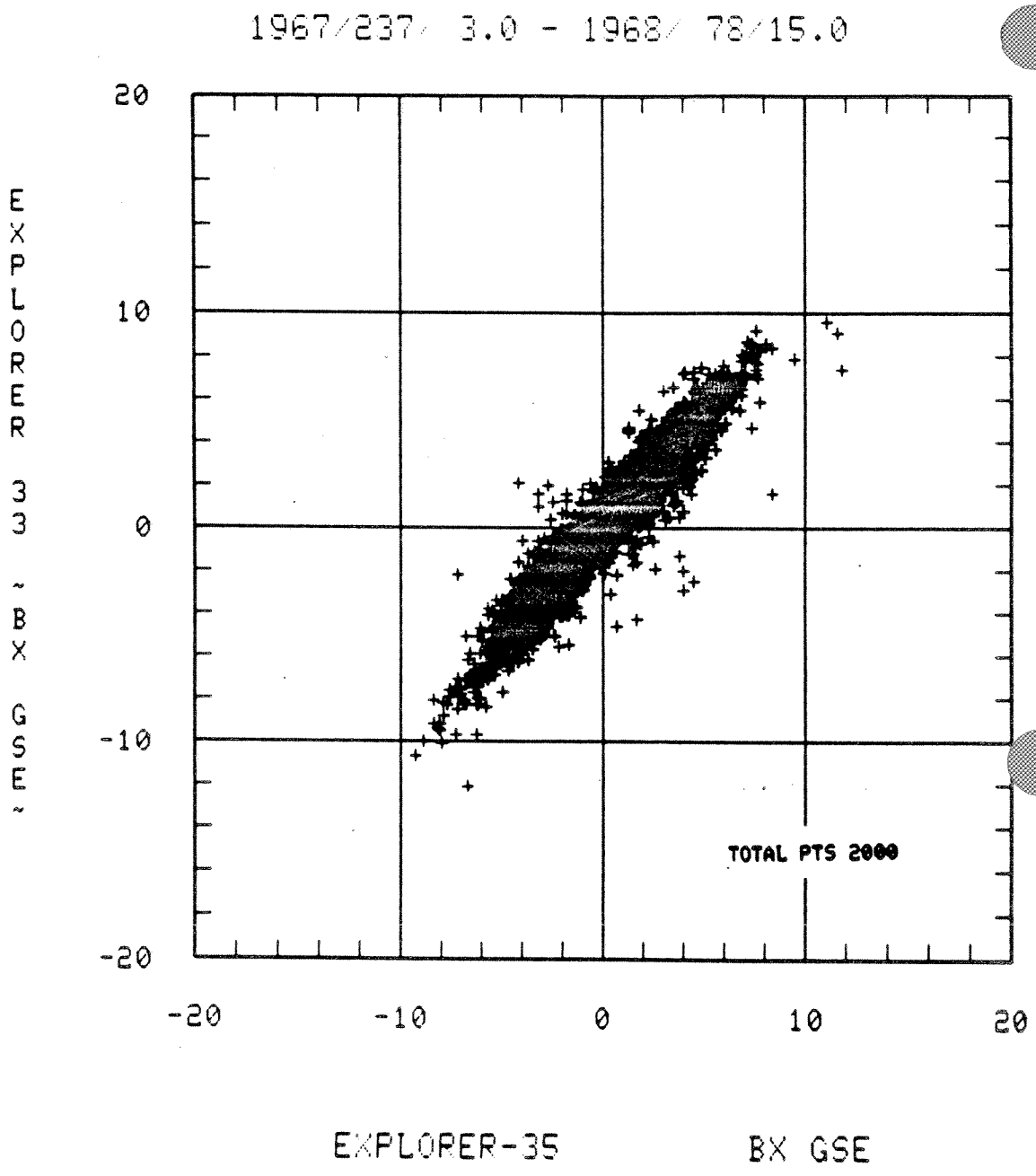

Scatter Plot 16

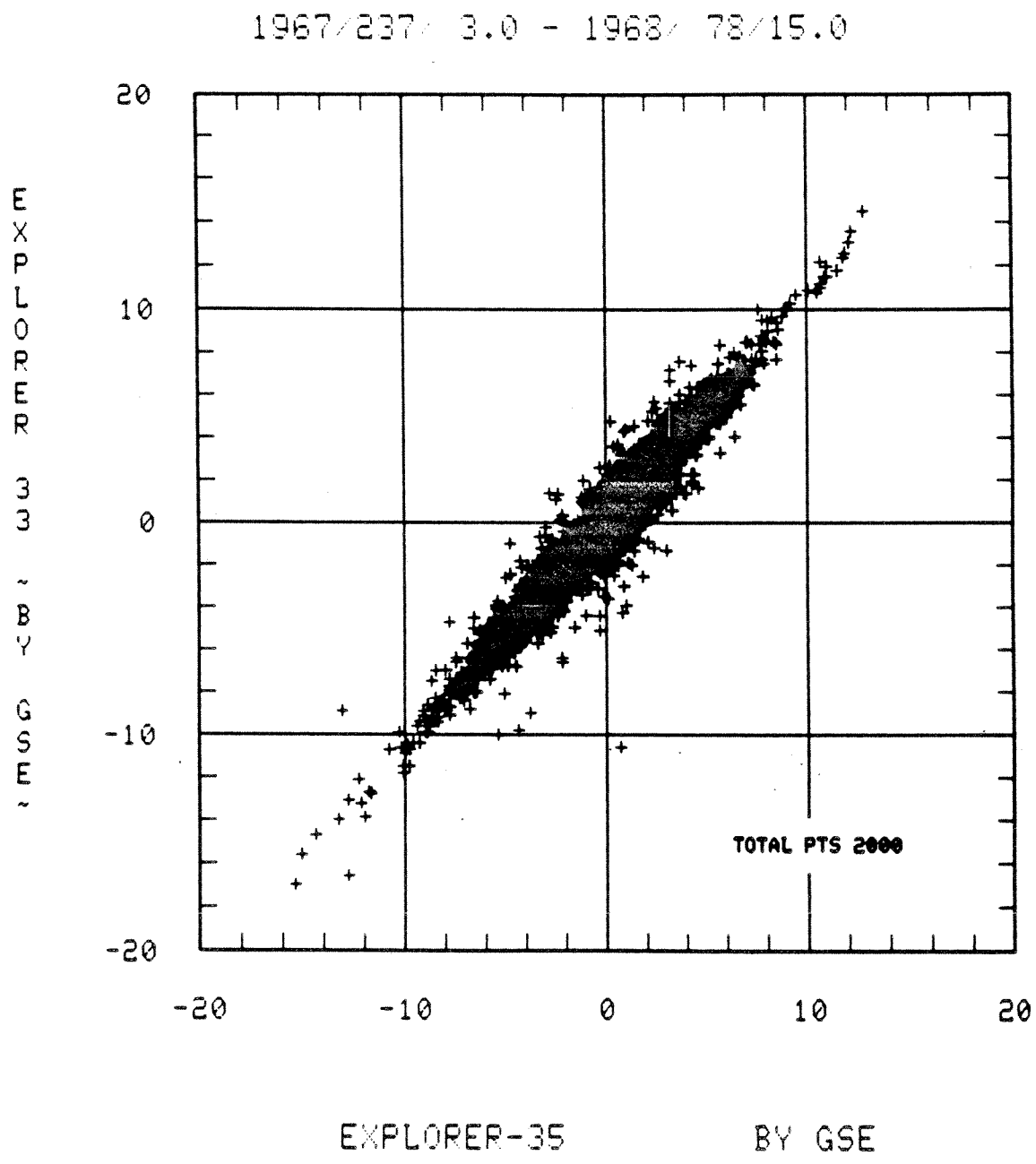

Scatter Plot 17

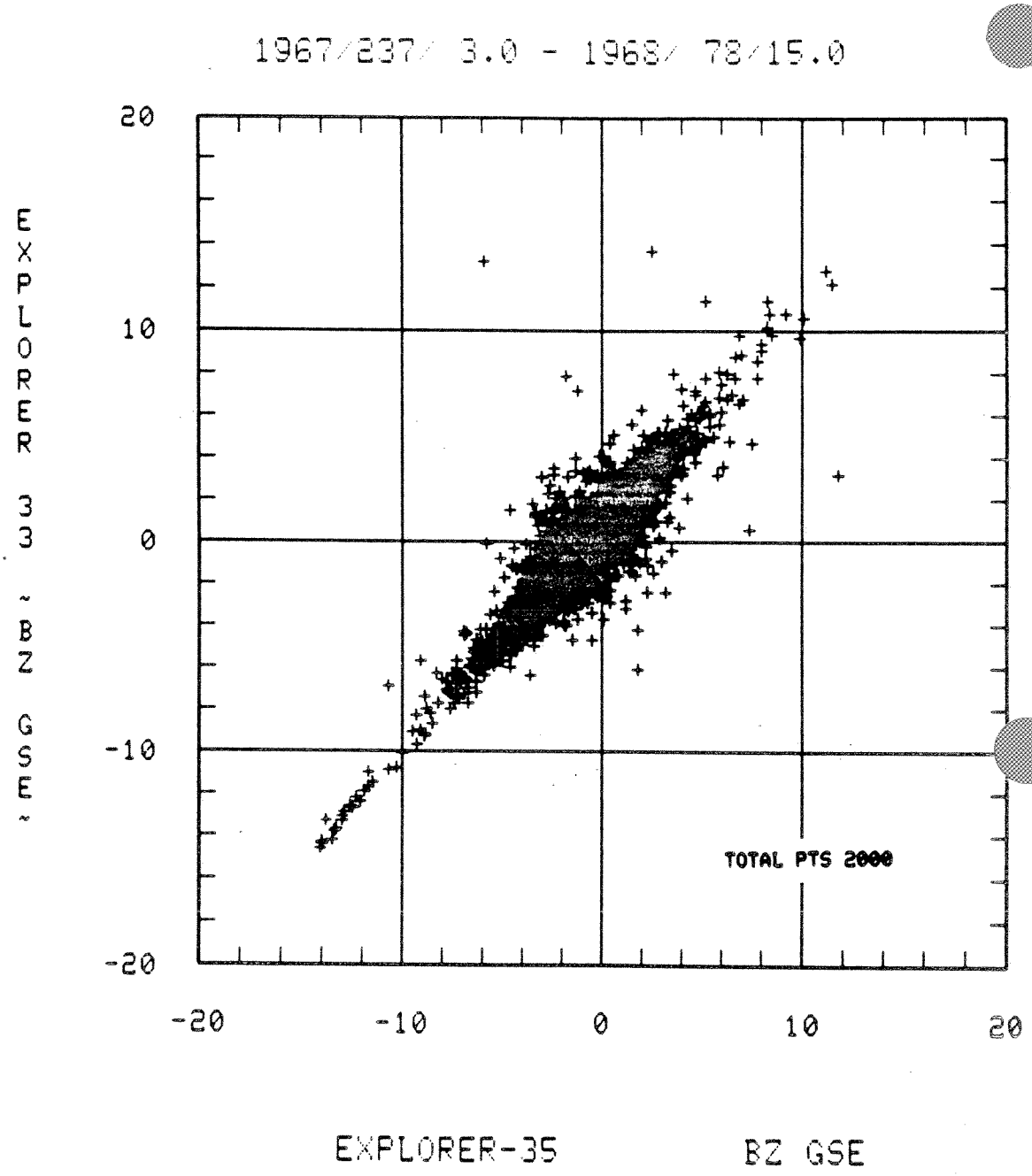

Scatter Plot 18

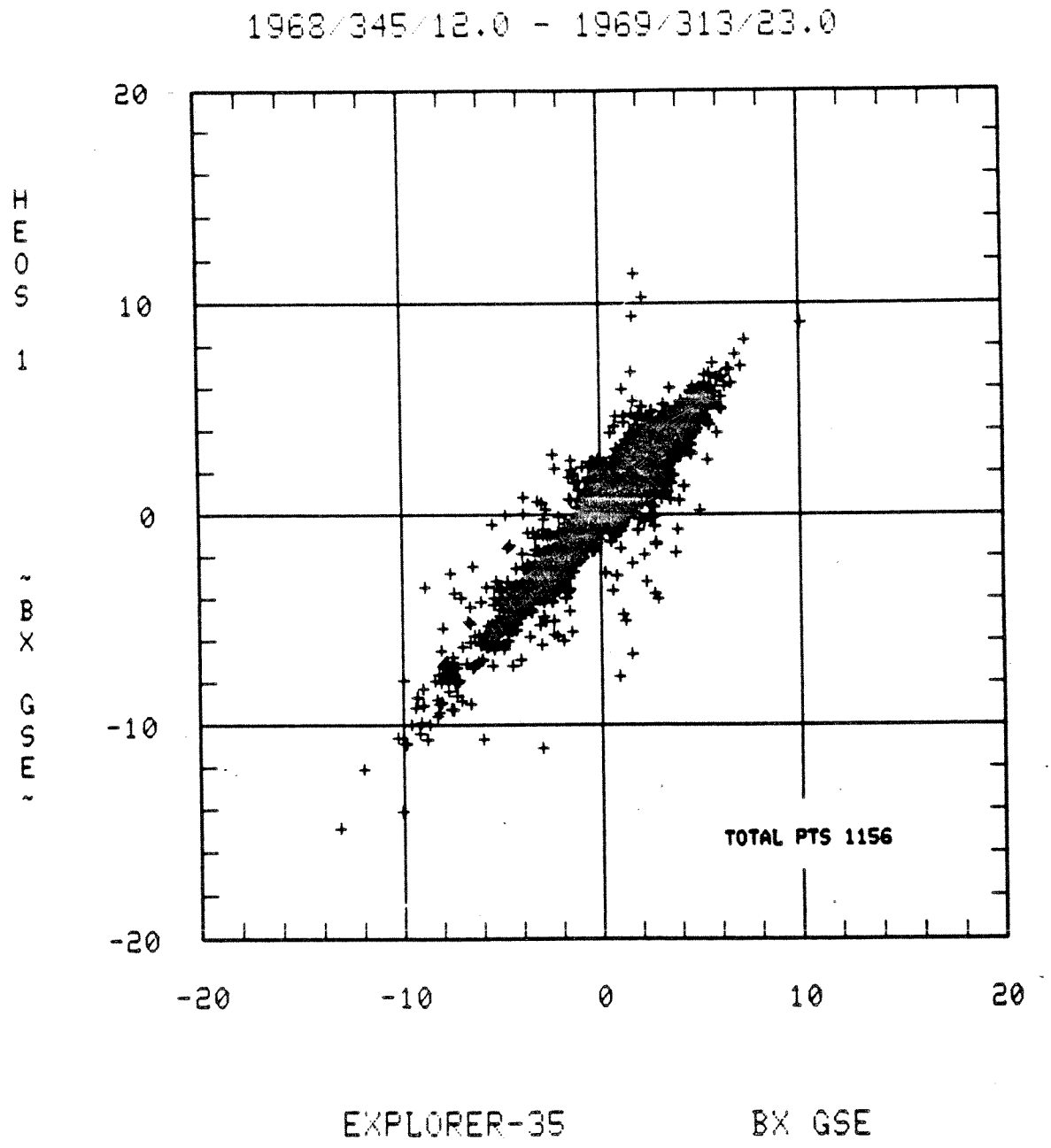

Scatter Plot 19

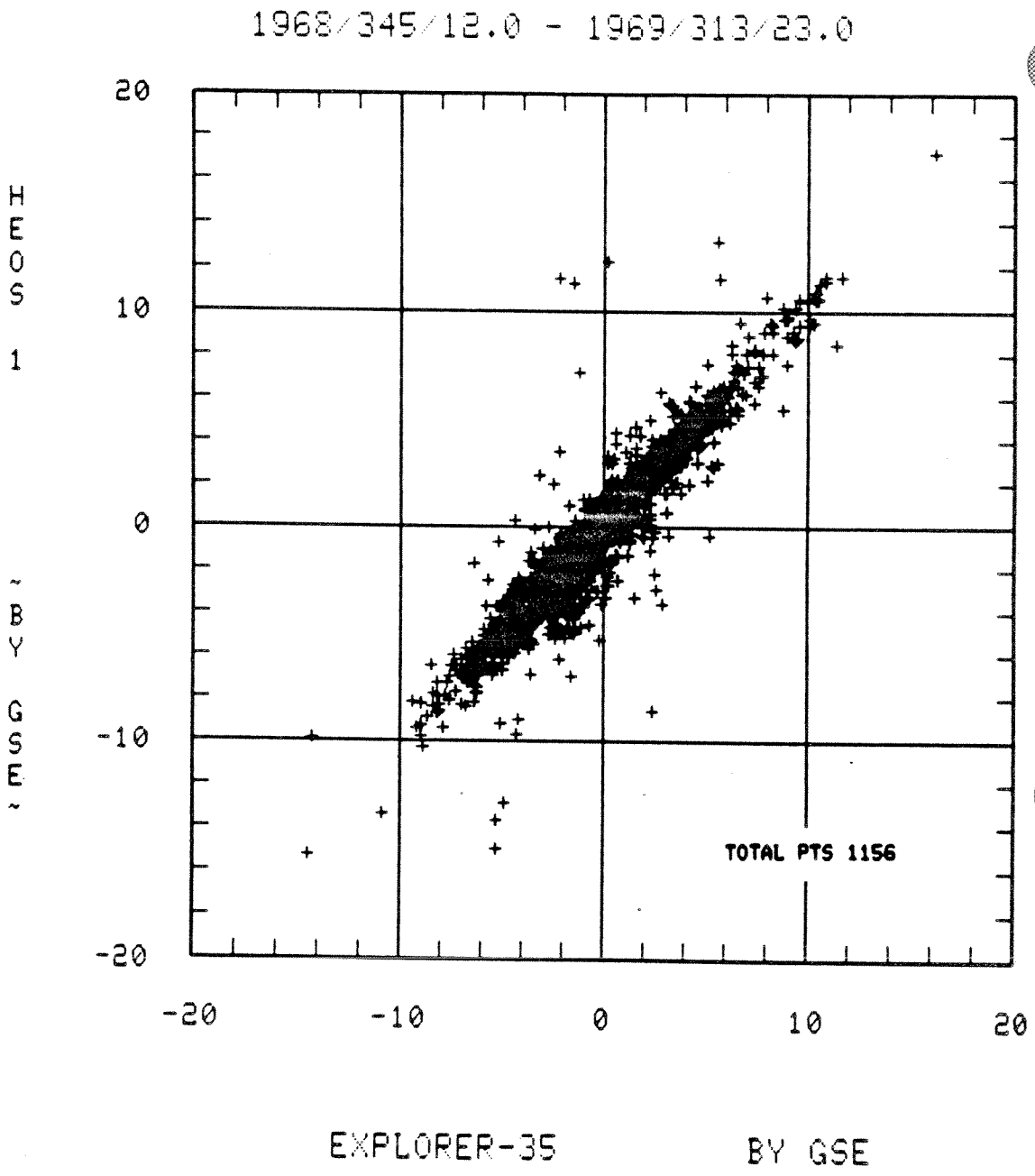

Scatter Plot 20

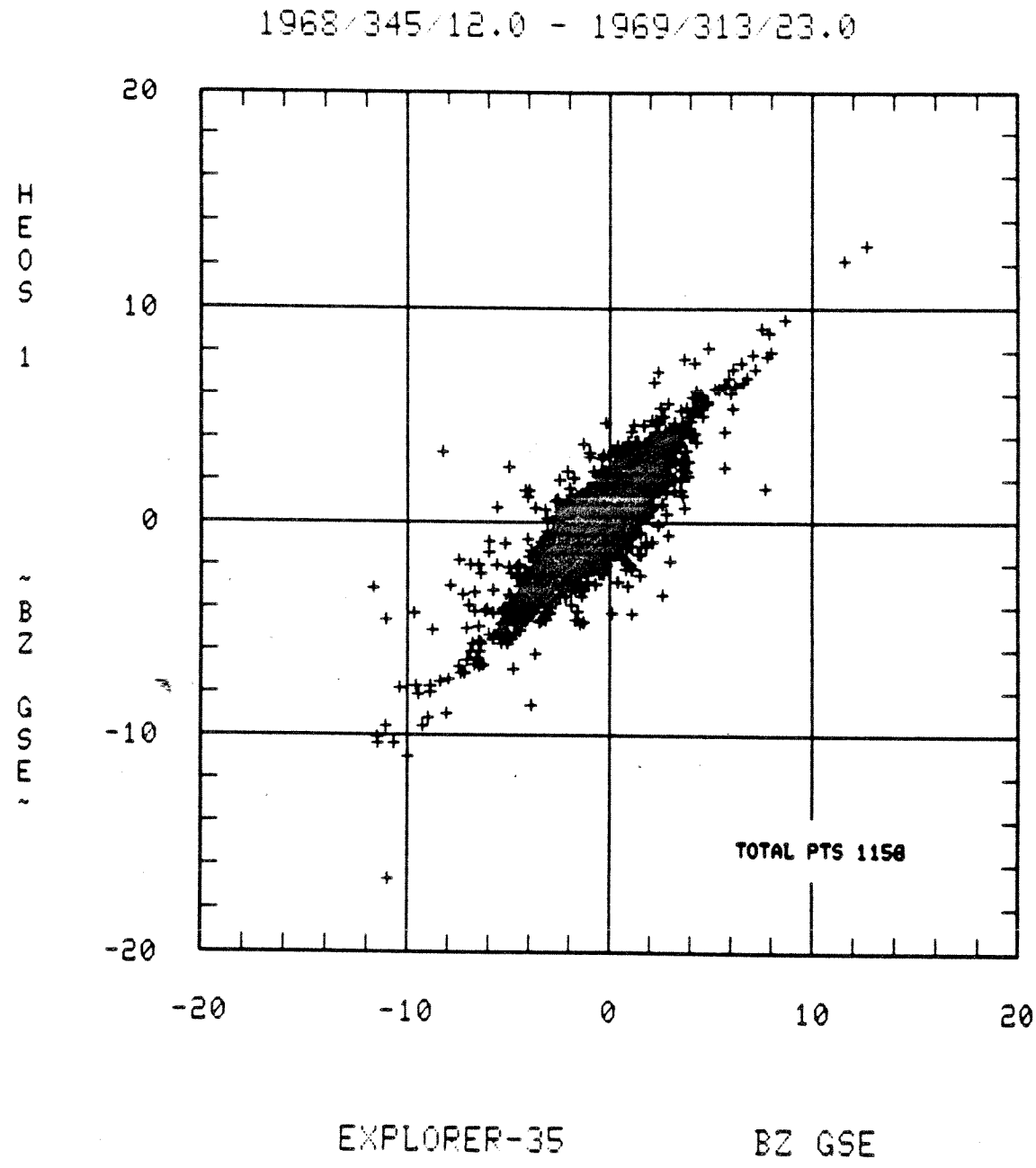

Scatter Plot 21

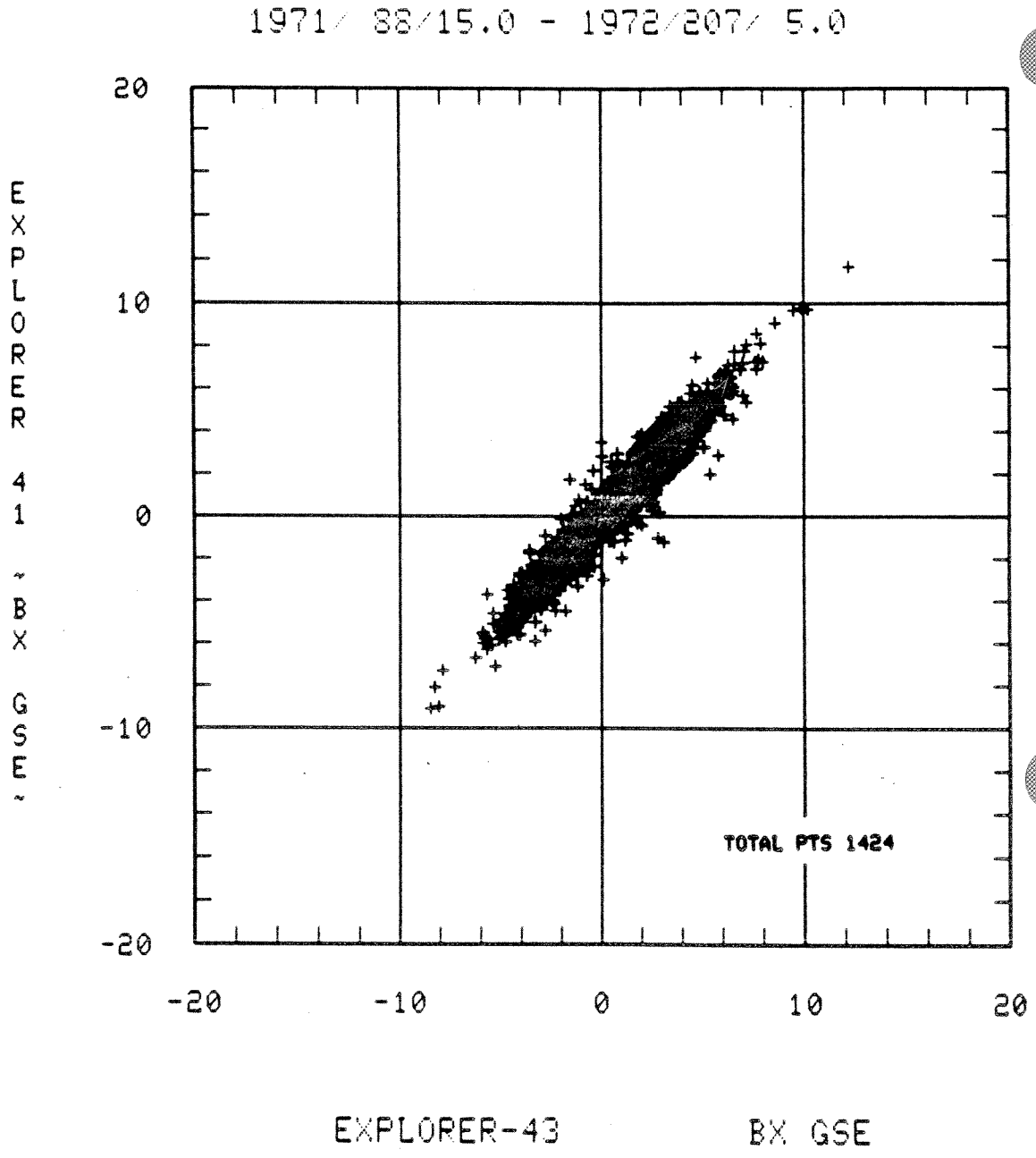

Scatter Plot 22

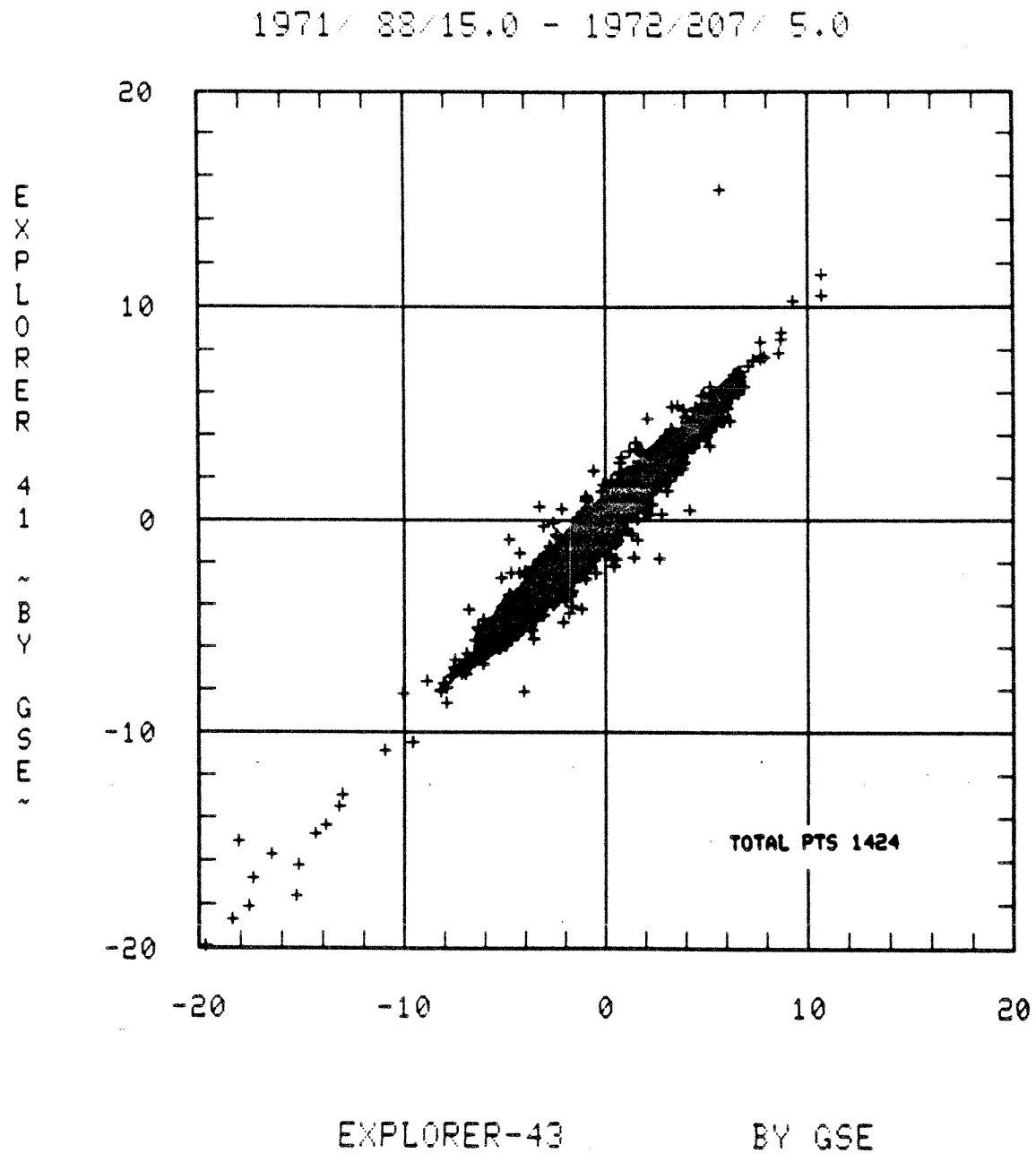

Scatter Plot 23

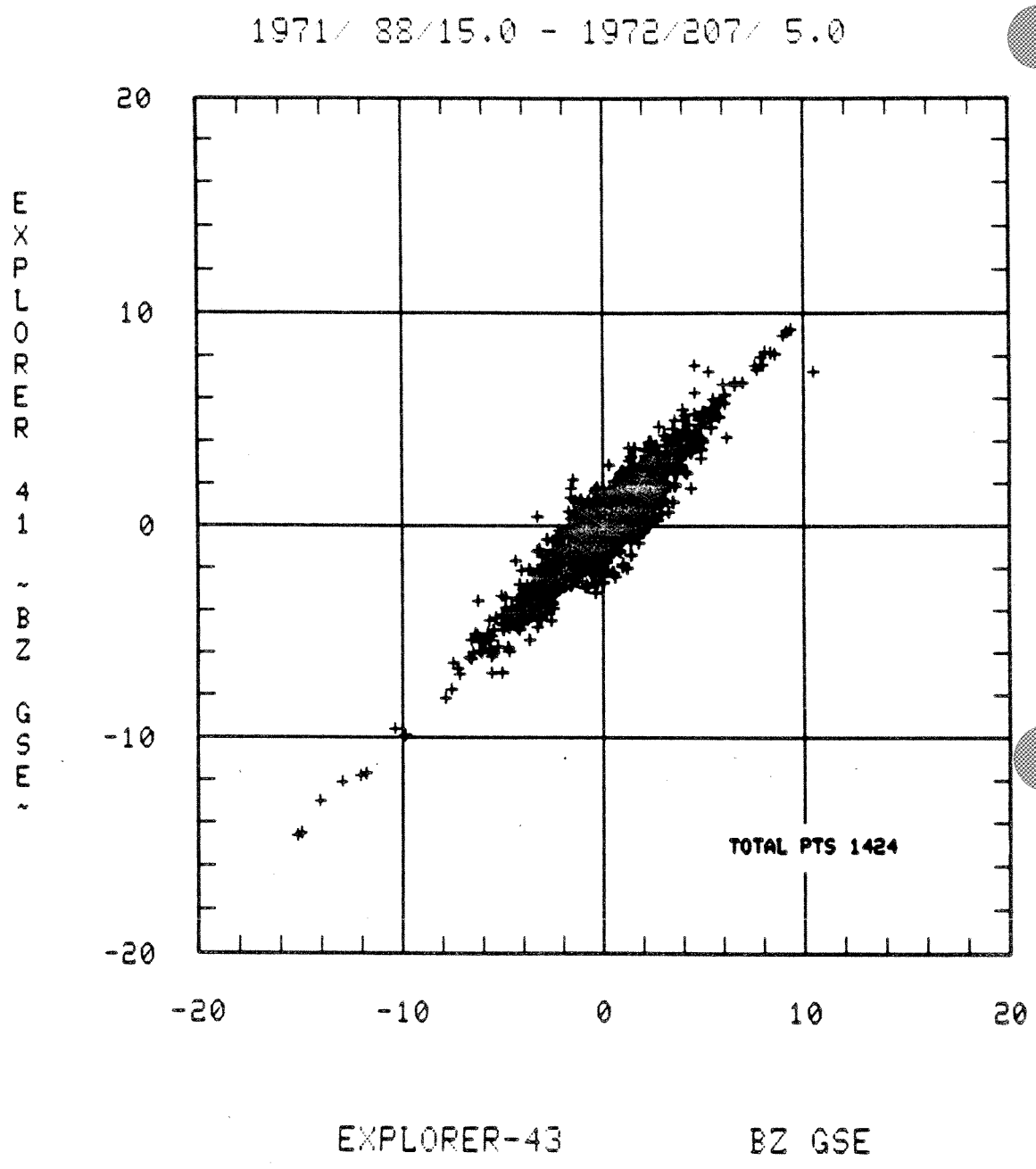

Scatter Plot 24

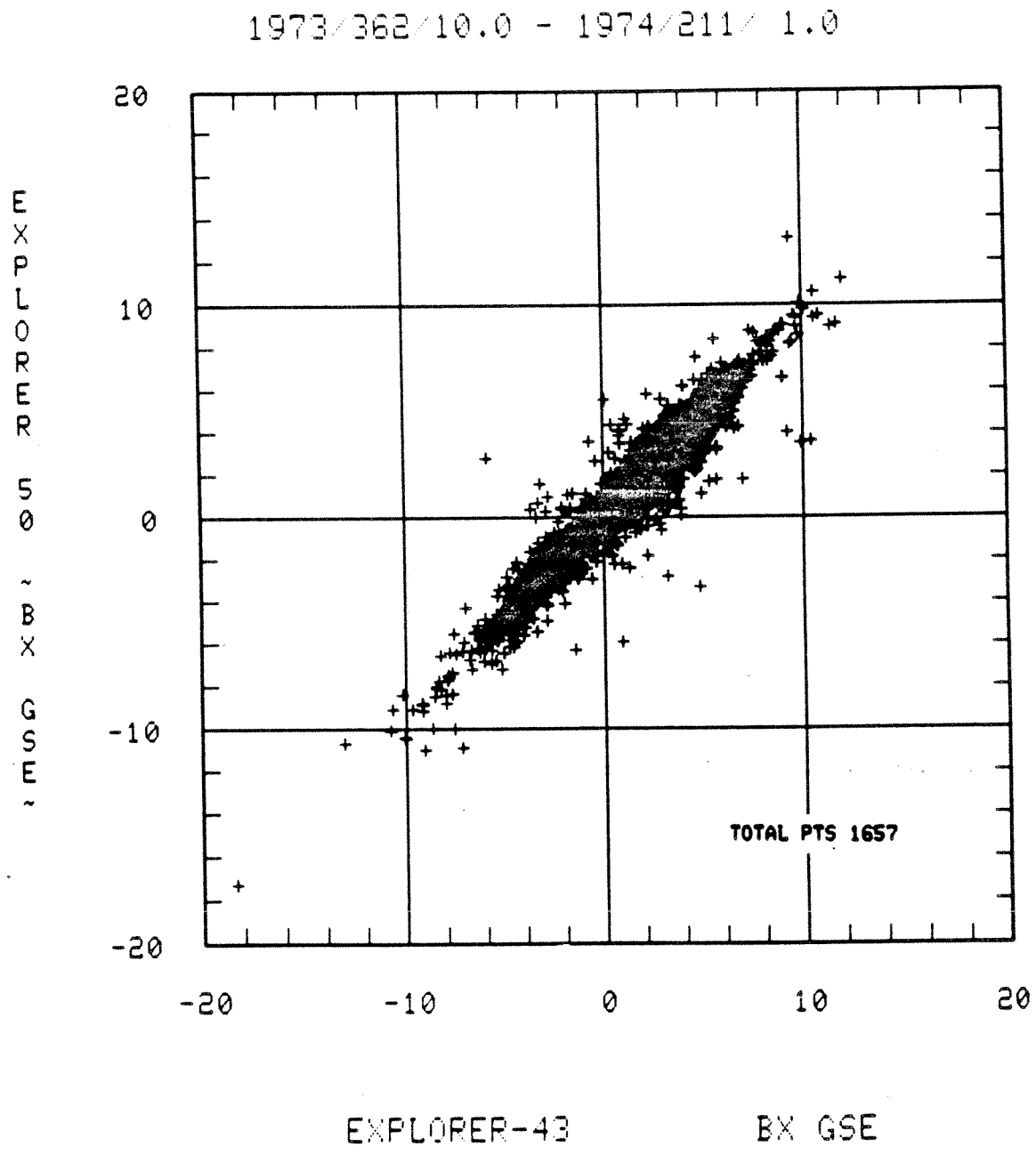

Scatter Plot 25

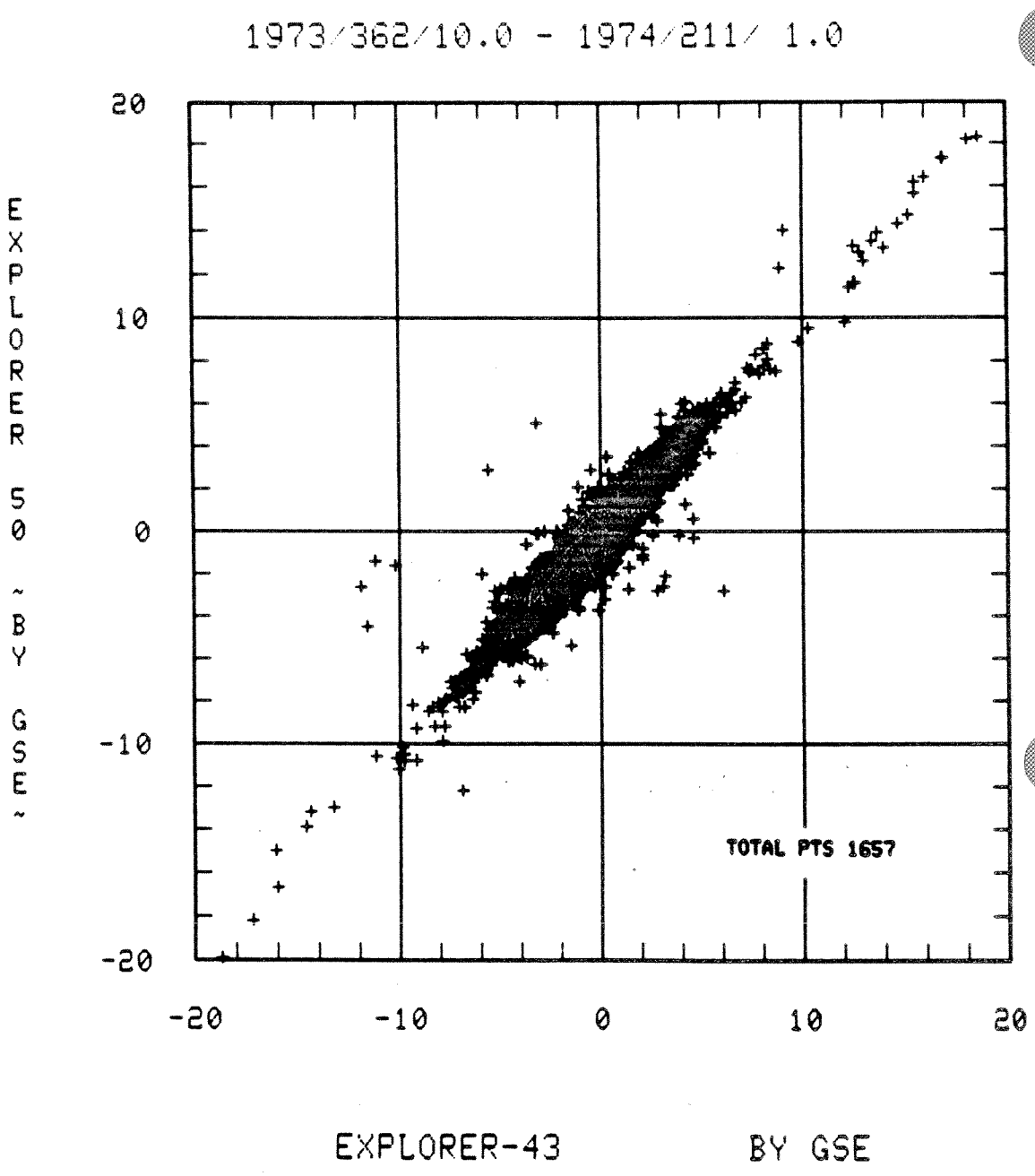

Scatter Plot 26

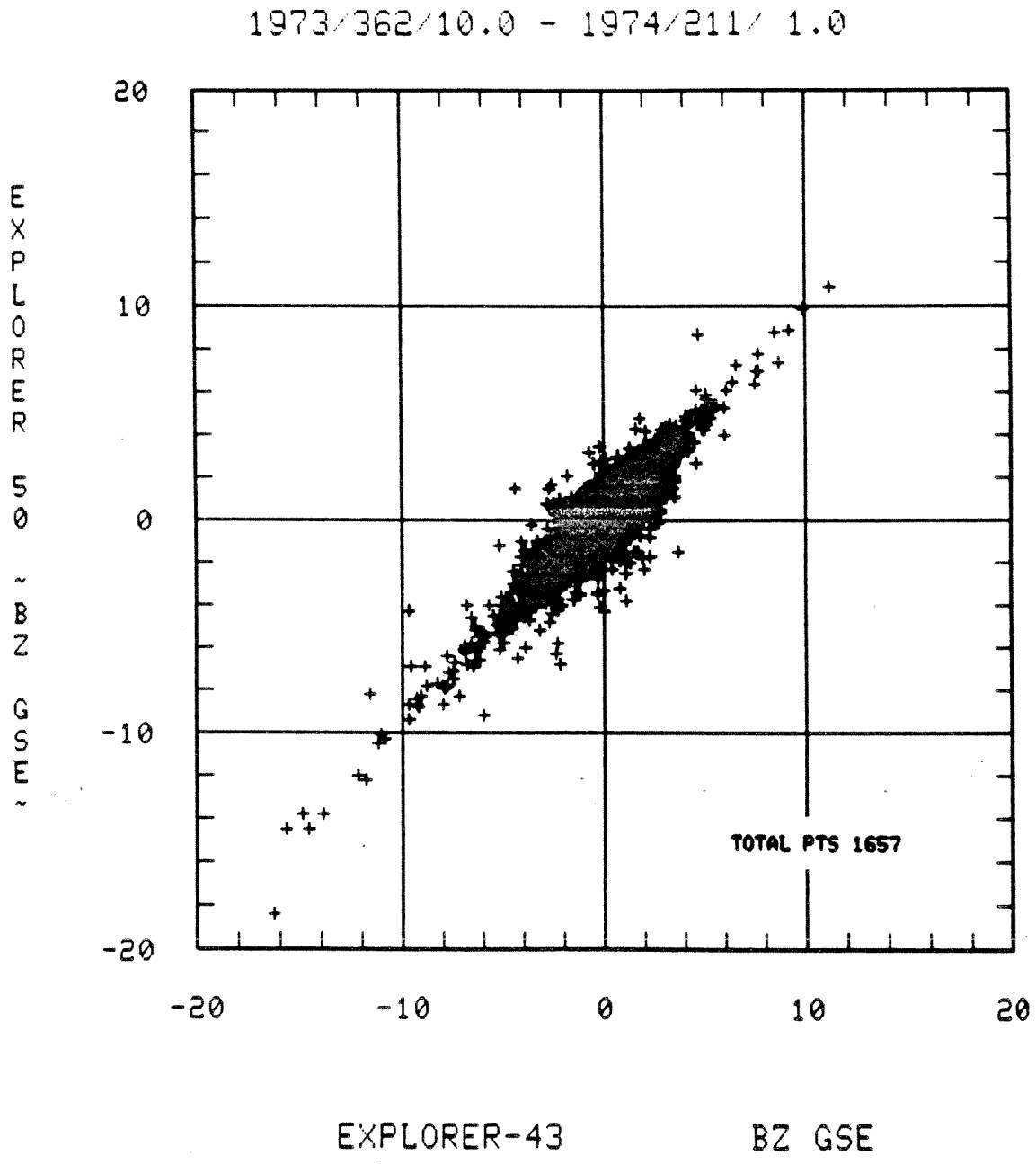

Scatter Plot 27

CONTENTS

TABLES

ILLUSTRATIONS

D-29951
C-19288
11/2/63 - 1/2/64
SM-41A

```
$JOB  13:42:35
$ASS IN MS1
$NOP ********** DUMP OF X-406 **********
$EXEC DPHEX BS
 INPUT TAPE ON MS1
 DATA INPUT    1 1 1
  FILE  1      RECORD   1      LENGTH   28420BYTES
  (    0)  6F040000 00940000 00000005 0000003F 00000131 00000000 000006F7 00000000 00000000 00000000
  (   40)  00000000 00000000 00000000 00000000 00000000 00000000 00000000 00000000 00000000 00000000
  (   80)  00000000 00000000 00000000 00000000 00000000 00000000 00000000 00000000 00000000 00000000
  (  120)  00000000 00000000 00000000 00000000 00000000 00000014 00000004 00000034 00940000 00000005
  (  160)  0000003F 00000131 00000001 000006F7 00000000 00000000 00000000 00000000 00000000 00000000
  (  200)  00000000 00000000 00000000 00000000 00000000 00000000 00000000 00000000 00000000 00000000
  (  240)  00000000 00000000 00000000 00000000 00000000 00000000 00000000 00000000 00000000 00000000
  (  280)  00000000 00000000 00000014 00000004 00000034 00940000 00000005 0000003F 00000131 00000002
  (  320)  000006F7 00000000 00000000 00000000 00000000 00000000 00000000 00000000 00000000 00000000
  (  360)  00000000 00000000 00000000 00000000 00000000 00000000 00000000 00000000 00000000 00000000
  (  400)  00000000 00000000 00000000 00000000 00000000 00000000 00000000 00000000 00000000 00000014
  (  440)  00000004 00000034 00940000 00000005 0000003F 00000131 00000003 000006F7 00000000 00000000
  (  480)  00000000 00000000 00000000 00000000 00000000 00000000 00000000 00000000 00000000 00000000
  (  520)  00000000 00000000 00000000 00000000 00000000 00000000 00000000 00000000 00000000 00000000
  (  560)  00000000 00000000 00000000 00000000 00000000 00000000 00000017 00000004 00000034 00940000
  (  600)  00000005 0000003F 00000131 00000004 000006F7 00000000 00000000 00000000 00000000 00000000
  (  640)  00000000 00000000 00000000 00000000 00000000 00000000 00000000 00000000 00000000 00000000
  (  680)  00000000 00000000 00000000 00000000 00000000 00000000 00000000 00000000 00000000 00000000
  (  720)  00000000 00000000 00000000 00000017 00000004 00000034 00940000 00000005 0000003F 00000131
  (  760)  00000005 000006F7 00000000 00000000 00000000 00000000 00000000 00000000 00000000 00000000
  (  800)  00000000 00000000 00000000 00000000 00000000 00000000 00000000 00000000 00000000 00000000
  (  840)  00000000 00000000 00000000 00000000 00000000 00000000 00000000 00000000 00000000 00000000
  (  880)  00000017 00000004 00000034 00940000 00000005 0000003F 00000131 00000006 000006F7 00000000
  (  920)  00000000 00000000 00000000 00000000 00000000 00000000 00000000 00000000 00000000 00000000
  (  960)  00000000 00000000 00000000 00000000 00000000 00000000 00000000 00000000 00000000 00000000
  ( 1000)  00000000 00000000 00000000 00000000 00000000 00000000 00000000 0000001B 00000004 00000034
  ( 1040)  00940000 00000005 0000003F 00000131 00000007 000006F7 00000000 00000000 00000000 00000000
  ( 1080)  00000000 00000000 00000000 00000000 00000000 00000000 00000000 00000000 00000000 00000000
  ( 1120)  00000000 00000000 00000000 00000000 00000000 00000000 00000000 00000000 00000000 00000000
  ( 1160)  00000000 00000000 00000000 00000000 0000001B 00000004 00000034 00940000 00000005 0000003F
  ( 1200)  00000131 00000008 000006F7 00000000 00000000 00000000 00000000 00000000 00000000 00000000
  ( 1240)  00000000 00000000 00000000 00000000 00000000 00000000 00000000 00000000 00000000 00000000
  ( 1280)  00000000 00000000 00000000 00000000 00000000 00000000 00000000 00000000 00000000 00000000
  ( 1320)  00000000 0000001B 00000004 00000034 00940000 00000005 0000003F 00000131 00000009 000006F7
  ( 1360)  00000000 00000000 00000000 00000000 00000000 00000000 00000000 00000000 00000000 00000000
  ( 1400)  00000000 00000000 00000000 00000000 00000000 00000000 00000000 00000000 00000000 00000000
  ( 1440)  00000000 00000000 00000000 00000000 00000000 00000000 00000000 00000000 0000001B 00000004
  ( 1480)  00000034 00940000 00000005 0000003F 00000131 0000000A 000006F7 00000000 00000000 00000000
  ( 1520)  00000000 00000000 00000000 00000000 00000000 00000000 00000000 00000000 00000000 00000000
  ( 1560)  00000000 00000000 00000000 00000000 00000000 00000000 00000000 00000000 00000000 00000000
  ( 1600)  00000000 00000000 00000000 00000000 00000000 0000001B 00000004 00000034 00940000 00000005
  ( 1640)  0000003F 00000131 0000000B 000006F7 00000000 00000000 00000000 00000000 00000000 00000000
  ( 1680)  00000000 00000000 00000000 00000000 00000000 00000000 00000000 00000000 00000000 00000000
  ( 1720)  00000000 00000000 00000000 00000000 00000000 00000000 00000000 00000000 00000000 00000000
  ( 1760)  00000000 00000000 0000001B 00000004 00000034 00940000 00000005 0000003F 00000131 0000000C
  ( 1800)  000006F7 00000000 00000000 00000000 00000000 00000000 00000000 00000000 00000000 00000000
  ( 1840)  00000000 00000000 00000000 00000000 00000000 00000000 00000000 00000000 00000000 00000000
  ( 1880)  00000000 00000000 00000000 00000000 00000000 00000000 00000000 00000000 00000000 00000017
  ( 1920)  00000004 00000034 00940000 00000005 0000003F 00000131 0000000D 000006F7 00000000 00000000
  ( 1960)  00000000 00000000 00000000 00000000 00000000 00000000 00000000 00000000 00000000 00000000
  ( 2000)  00000000 00000000 00000000 00000000 00000000 00000000 00000000 00000000 00000000 00000000
  ( 2040)  00000000 00000000 00000000 00000000 00000000 00000000 00000017 00000004 00000034 00940000
  ( 2080)  00000005 0000003F 00000131 0000000E 000006F7 00000000 00000000 00000000 00000000 00000000
  ( 2120)  00000000 00000000 00000000 00000000 00000000 00000000 00000000 00000000 00000000 00000000
  ( 2160)  00000000 00000000 00000000 00000000 00000000 00000000 00000000 00000000 00000000 00000000
  ( 2200)  00000000 00000000 00000000 00000017 00000004 00000034 00940000 00000005 0000003F 00000131
```

```
( 21360) 00000000 00000000 00000000 00000000 00000000 00000000 00000000 00000000 00000000 00000000
( 21400) 00000000 00000000 00000000 00000000 00000000 00000000 00000000 00000000 00000000 00000000
( 21440) 00000000 00000000 00000000 0000002B 00000004 00000014 00940000 00000005 0000004C 0000000B
( 21480) 00000001 0000079B 00000000 00000000 00000000 00000000 00000000 00000000 00000000 00000000
( 21520) 00000000 00000000 00000000 00000000 00000000 00000000 00000000 00000000 00000000 00000000
( 21560) 00000000 00000000 00000000 00000000 00000000 00000000 00000000 00000000 00000000 00000000
( 21600) 0000002B 00000004 00000014 00940000 00000005 0000004C 0000000B 00000002 0000079B 00000000
( 21640) 00000000 00000000 00000000 00000000 00000000 00000000 00000000 00000000 00000000 00000000
( 21680) 00000000 00000000 00000000 00000000 00000000 00000000 00000000 00000000 00000000 00000000
( 21720) 00000000 00000000 00000000 00000000 00000000 00000000 0000002B 0000004 00000014 00940000
( 21760) 00000005 0000004C 0000000B 00000003 0000079B 00000000 00000000 00000000 00000000 00000000
( 21800) 00000000 00000000 00000000 00000000 00000000 00000000 00000000 00000000 00000000 00000000
( 21840) 00000000 00000000 00000000 00000000 00000000 00000000 00000000 00000000 00000000 00000000
( 21880) 00000000 00000000 00000000 00000000 00000017 00000004 00000014 00940000 00000005 0000004C
( 21920) 0000000B 00000004 0000079B 00000000 00000000 00000000 00000000 00000000 00000000 00000000
( 21960) 00000000 00000000 00000000 00000000 00000000 00000000 00000000 00000000 00000000 00000000
( 22000) 00000000 00000000 00000000 00000000 00000000 00000000 00000000 00000000 00000000 00000000
( 22040) 00000000 00000017 00000004 00000014 00940000 00000005 0000004C 0000000B 00000005 0000079B
( 22080) 00000000 00000000 00000000 00000000 0000000C 00000000 00000000 00000000 00000000 00000000
( 22120) 00000000 00000000 00000000 00000000 00000000 00000000 00000000 00000000 00000000 00000000
( 22160) 00000000 00000000 00000000 00000000 00000000 00000000 00000000 00000000 00000017 00000004
( 22200) 00000014 00940000 00000005 0000004C 0000000B 00000006 0000079B 00000000 00000000 00000000
( 22240) 00000000 00000000 00000000 00000000 00000000 00000000 00000000 00000000 00000000 00000000
( 22280) 00000000 00000000 00000000 00000000 00000000 00000000 00000000 00000000 00000000 00000000
( 22320) 00000000 00000000 00000000 00000000 00000000 00000017 00000004 00000014 00940000 00000005
( 22360) 0000004C 0000000B 00000007 0000079B 00000000 00000000 00000000 00000000 00000000 00000000
( 22400) 00000000 00000000 00000000 00000000 00000000 00000000 00000000 00000000 00000000 00000000
( 22440) 00000000 00000000 00000000 00000000 00000000 00000000 00000000 00000000 00000000 00000000
( 22480) 00000000 00000000 00000017 00000004 00000014 00940000 00000005 0000004C 0000000B 00000008
( 22520) 0000079B 00000000 00000000 00000000 00000000 00000000 00000000 00000000 00000000 00000000
( 22560) 00000000 00000000 00000000 00000000 00000000 00000000 00000000 00000000 00000000 00000000
( 22600) 00000000 00000000 00000000 00000000 00000000 00000000 00000000 00000000 00000000 00000017
( 22640) 00000004 00000014 00940000 00000005 0000004C 0000000B 00000009 0000079B 00000000 00000000
( 22680) 00000000 00000000 00000000 00000000 00000000 00000000 00000000 00000000 00000000 00000000
( 22720) 00000000 00000000 00000000 00000000 00000000 00000000 00000000 00000000 00000000 00000000
( 22760) 00000000 00000000 00000000 00000000 00000000 00000000 00000017 00000004 00000014 00940000
( 22800) 00000005 0000004C 0000000B 0000000A 0000079B 00000000 00000000 00000000 00000000 00000000
( 22840) 00000000 00000000 00000000 00000000 00000000 00000000 00000000 00000000 00000000 0000000B
( 22880) 00000000 00000000 00000000 00000000 00000000 00000000 00000000 00000000 00000000 00000000
( 22920) 00000000 00000000 00000000 00000017 00000004 00000014 00940000 00000005 0000004C 0000000B
( 22960) 0000000B 0000079B 00000000 00000000 00000000 00000000 00000000 00000000 00000000 00000000
( 23000) 00000000 00000000 00000000 00000000 00000000 00000000 00000000 00000000 00000000 00000000
( 23040) 00000000 00000000 00000000 00000000 00000000 00000000 00000000 00000000 00000000 00000000
( 23080) 00000017 00000004 00000014 00940000 00000005 0000004C 0000000B 0000000C 0000079B 00000000
( 23120) 00000000 00000000 00000000 00000000 00000000 00000000 00000000 00000000 00000000 00000000
( 23160) 00000000 00000000 00000000 00000000 00000000 00000000 00000000 00000000 00000000 00000000
( 23200) 00000000 00000000 00000000 00000000 00000000 00000000 00000000 00000014 00000004 00000014
( 23240) 00940000 00000005 0000004C 0000000B 0000000D 0000079B 00000000 00000000 00000000 00000000
( 23280) 00000000 00000000 00000000 00000000 00000000 00000000 00000000 00000000 00000000 00000000
( 23320) 00000000 00000000 00000000 00000000 00000000 00000000 00000000 00000000 00000000 00000000
( 23360) 00000000 00000000 00000000 00000000 00000014 00000004 00000014 00940000 00000005 0000004C
( 23400) 0000000B 0000000E 0000079B 00000000 00000000 00000000 00000000 00000000 00000000 00000000
( 23440) 00000000 00000000 00000000 00000000 00000000 00000000 00000000 00000000 00000000 00000000
( 23480) 00000000 00000000 00000000 0000000C 00000000 00000000 00000000 00000000 00000000 00000000
( 23520) 00000000 00000014 00000004 00000014 00940000 00000005 0000004C 0000000B 0000000F 0000079B
( 23560) 00000000 00000000 00000000 00000000 00000000 00000000 00000000 00000000 00000000 00000000
( 23600) 00000000 00000000 00000000 00000000 00000000 00000000 00000000 00000000 00000000 00000000
( 23640) 00000000 00000000 00000000 00000000 00000000 00000000 00000000 00000000 0000001B 00000004
( 23680) 00000014 00940000 00000005 0000004C 0000000B 00000010 0000079B 00000000 00000000 00000000
( 23720) 00000000 00000000 00000000 00000000 00000000 00000000 00000000 00000000 00000000 00000000
( 23760) 00000000 00000000 00000000 00000000 00000000 00000000 00000000 00000000 00000000 00000000
( 23800) 00000000 00000000 00000000 00000000 00000000 0000001B 00000004 00000014 00940000 00000005
( 23840) 0000004C 0000000B 00000011 0000079B 00000000 00000000 00000000 00000000 00000000 00000000
( 23880) 00000000 00000000 00000000 00000000 00000000 00000000 00000000 00000000 00000000 00000000
```

```
( 24000)  00000798  00000000  00000000  00000000  00000000  00000000  00000000  00000000  00000000  00000000
( 24040)  00000000  00000000  00000000  00000000  00000000  00000000  00000000  00000000  00000000  00000000
( 24080)  00000000  00000000  00000000  00000000  00000000  00000000  00000000  00000000  00000000  0000001B
( 24120)  00000004  0000014   00940000  00000005  0000004C  0000000B  00000013  00000798  00000000  00000000
( 24160)  00000000  00000000  00000000  00000000  00000000  00000000  00000000  00000000  00000000  00000000
( 24200)  00000000  00000000  00000000  00000000  00000000  00000000  00000000  00000000  00000000  00000000
( 24240)  00000000  00000000  00000000  00000000  00000000  00000000  0000001B  00000004  00000014  00940000
( 24280)  00000005  0000004C  0000000B  00000014  00000798  00000000  00000000  00000000  00000000  00000000
( 24320)  00000000  00000000  00000000  00000000  00000000  00000000  00000000  00000000  00000000  00000000
( 24360)  00000000  00000000  00000000  00000000  00000000  00000000  00000000  00000000  00000000  00000000
( 24400)  00000000  00000000  00000000  0000001B  00000004  00000014  00940000  00000005  0000004C  0000000B
( 24440)  00000015  00000798  00000000  00000000  00000000  00000000  00000000  00000000  00000000  00000000
( 24480)  00000000  00000000  00000000  00000000  00000000  00000000  00000000  00000000  00000000  00000000
( 24520)  00000000  00000000  00000000  00000000  00000000  00000000  00000000  00000000  00000000  00000000
( 24560)  0000001E  00000004  00000014  00940000  00000005  0000004C  0000000B  00000016  00000798  00000000
( 24600)  00000000  00000000  00000000  00000000  00000000  00000000  00000000  00000000  00000000  00000000
( 24640)  00000000  00000000  00000000  00000000  00000000  00000000  00000000  00000000  00000000  00000000
( 24680)  00000000  00000000  00000000  00000000  00000000  00000000  0000001E  00000004  00000014  00940000
( 24720)  00000005  0000004C  0000000B  00000017  00000798  00000000  00000000  00000000  00000000  00000000
( 24760)  00000000  00000000  00000000  00000000  00000000  00000000  00000000  00000000  00000000  00000000
( 24800)  00000000  00000000  00000000  00000000  00000000  00000000  00000000  00000000  00000000  00000000
( 24840)  00000000  00000000  00000000  00000000  0000001E  00000004  00000014

FILE    1      # OF DATA RECORDS   557      # SUCCESSFUL READS  515

        # PERMANENT READ ERRORS   0       # ZERO BYTE ERRORS  46       # SHORT RECORDS   0       # UNDEFINED ERRORS   0

          # OF RECORDS RETRIED   52       TOTAL # OF RETRIES  72
```